Dissertation

PRKDC POLYMORPHISMS AND RADIATION EFFECTS

Submitted by

Kristin Fabre Askin

Graduate Degree Program in Cell and Molecular Biology

In partial fulfillment of the requirements

For the Degree of Doctor of Philosophy

Colorado State University

Fort Collins, Colorado

Fall 2008

COLORADO STATE UNIVERSITY

August 20, 2008

WE HEREBY RECOMMEND THAT THE DISSERTATION PREPARED UNDER OUR SUPERVISION BY KRISTIN FABRE ASKIN ENTITLED *PRKDC* POLYMORPHISMS AND RADIATION EFFECTS BE ACCEPTED AS FULFILLING IN PART THE REQUIREMENTS FOR THE DEGREE OF DOCTOR OF PHILOSOPHY.

Committee on Graduate Work

Edwin H. Goodwin

Susan E. Lana

Joel S. Bedford

Susan M. Bailey

Co-Advisor: Michael M. Weil

Advisor: Robert L. Ullrich

Department Head: Paul J. Laybourn

ABSTRACT OF DISSERTATION

PRKDC POLYMORPHISMS AND RADIATION EFFECTS

The *Prkdc* gene encodes DNA-PKcs which is involved in the immune system, DNA repair and chromosomal integrity. In humans, deficiencies in DNA-PKcs are linked to cancer predisposition. This connection can also be observed in mice models using ionizing radiation as the carcinogenic inducer. In particular, the BALB/c mouse strain is susceptible to mammary cancer after radiation exposure. Subsequent studies have shown that DNA repair is deficient in BALB/c which is attributed to a hypomorphic variant of DNA-PKcs. DNA-PKcs has also been linked to apoptosis because BALB/c is more resistance to ionizing-induced apoptosis in intestinal crypt cells compared to other mouse strains. Furthermore, it has been demonstrated that DNA-PKcs is involved in telomere maintenance. Additional studies have revealed two polymorphisms in $Prkdc^{BALB/c}$ that may be responsible for its DNA-PKcs variant.

The relationship between the targeted effects of ionizing radiation and BALB/c has been characterized, i.e. DNA double-strand break repair. However, little has been done on the non-targeted effects of radiation in BALB/c including the bystander effect. The purpose of this research was to study the bystander effect in BALB/c compared to other mouse strains

with different levels of DNA-PKcs status. I have found that DNA-PKcs is needed to generate a bystander signal, but not necessary for the reception of the signal. These studies were expanded by determining if the lack of a bystander effect was attributed the *Prkdc*$^{BALB/c}$ polymorphism in the kinase domain using the LEWES strain. LEWES has the BALB DNA-PKcs allele in the kinase domain and the common allele downstream of the leucine zipper. These results demonstrate that the SNP in the kinase domain influences DNA-PKcs protein levels and DNA repair, but does not affect bystander signaling capabilities. This would suggest that either the polymorphism downstream of the leucine zipper is responsible for the lack of the bystander effect observed in BALB/c or that additional factors influence its phenotype. Because LEWES has decreased DNA-PKcs levels and DNA-repair (not to the same extent as BALB/c), but is able to induce the bystander effect, we can speculate that the lack of bystander signaling in BALB/c may contribute to BALB/c's sen sitivity to radiation-induced mammary cancer.

Kristin Fabre Askin
Graduate Degree Program in Cell and Molecular Biology
Colorado State University
Fort Collins, Colorado 80523
Fall 2008

ACKNOWLEDGEMENTS

None of the accomplishments I have achieved in my graduate career would be possible without the help and support of so many. I would like to first thank my advisor Dr. Robert Ullrich for taking me under his wing as a graduate student. Bob saw potential in me and with his mentorship, I was able to grow into the scientist that I am today. I will always appreciate his trust and belief in me.

I was fortunate to have two advisors. Dr. Mike Weil is a patient mentor who was always willing to discuss my project even if it meant multiple repeated conversations. I appreciate that his door was always open for me. It was also a bonus that both Bob and Mike share passion with me for Gulf-coast culture which led to several gumbo parties and crawfish boils!

I had a wonderful graduate committee. Every member of my committee, including my advisors, had a very hands-off approach of mentoring and teaching which allowed me to become a self-sufficient and confident scientist. Much of my research involved cytogenetics, a topic foreign to me when I came to CSU. However, with mentorship from Dr. Susan Bailey, Dr. Joel Bedford and Dr. Edwin Goodwin, I was able to master several techniques which became crucial to my graduate career and will be just as important in my post-doctoral experience. Susan always had her door open and was so very passionate about chromosomes and telomeres which made it very pleasurable to talk with her about my research. Conversations with Joel were so insightful and almost every time I left his office, I had a new experiment planned out. Ed was vital in helping me better understand

statistics in the cytogenetic world. Finally, Dr. Susan Lana was wonderful in that she always brought a clinical aspect to my project which is the main purpose as to why we do cancer research.

I would like to give many thanks to a number of others who took the time to teach me a wide array of techniques. Dr. Andy Ray and Dr. Paula Genik taught me the basics of molecular cloning and PCR. Dr. Eli Williams and Dr. Tanner Hagelstrom were great about showing me the wonder that is CO-FISH and FPG.

In science, it is a must to collaborate and I had many wonderful opportunities that taught me how to "play well with others". Tanner and I took the initiative to develop our own experiments in which we ended up with a publication! Abby Williams was also another peer that was involved in these experiments and our work together has led to another potential paper. I also had the pleasure of working with Dr. Ron Carsten. Working with these people has taught me so much about what it means to collaborate in our field and I could not have asked for a better experience.

Of course, I owe so much appreciation and gratitude to ALL of the members of the Ullrich lab. I truly believe that we have all kept each other going when it seemed too hard; to have the support from my lab mates was invaluable. I would especially like to give gratitude to Phuong Le who was always there to help and was so very supportive. Of course, I could not mention lab members without giving my sincere thanks to Chrissy Battaglia. Words can not express how appreciated she is in doing a superb job of running the lab. She really does make a graduate student's life easier.

I would also like to thank the Cell and Molecular Program and administrative persons at CSU. This includes Dr. Mike Fox, Norma Bulera, Dr. Norm Curthoys, Lori Williams, Dr. Paul Laybourn, Julie Asmus and Mary Pridgen.

Last and most importantly, I would like to thank God and family. Getting a doctorate degree is no easy task and it would certainly not be possible without them. My husband Shane gave me the freedom to make the choices I needed to make to get to where I am today. I sincerely thank him for that. It always seemed to amaze me how much confidence my parents Ron and Grace Fabre along with my sister Renee have in me. No matter how much self-doubt and struggles came my way along this experience, they always knew I would overcome them and be better for it. Thank you so much for believing in me.

Tables of Contents

Chapter 1

Introduction

1.1 Cancer/breast cancer statistics

Cancer is the second leading cause of death in Americans, preceded only by heart disease (ACS). Among American women, breast cancer has the second highest frequency in both occurrence and mortality (ACS). It is estimated that 182,460 women will contract this disease, and 40,480 deaths will occur in 2008 (NCI).

Breast cancer research has led to significant improvements in survival rates. Thirty-five years ago, only 75% of women diagnosed with breast cancer survived past five years. Mastectomy was the common surgical method, and use of radiation therapy, chemotherapy and hormone treatments was elementary and limited (NCI). Today, 90% of women diagnosed with breast cancer will survive past five years (NCI). This success is the product of improvements in treatment, more widespread screening and earlier detection.

Identification of the genetic basis for increased risk in certain families has led to a better understanding of potential mechanisms involved in breast cancer development which in turn has provided opportunities for new approaches in treatment and prevention. Research in such high risk families have led to the discovery of several genes linked to predisposition (Thompson, 2002). For example, mutations in *BRCA1* and *BRCA2* are highly penetrance mutations accounting for 80-90% of hereditary breast cancers (Venkitaraman, 2001; Wenham, 2003). Such dominant mutations involved in familial breast cancers are easily identified because these cancers arise in women at an early age and are highly penetrant. Male breast cancers are also associated with *BRCA2* mutations.

However, mutations in these genes occur at a low frequency and account for only 5-10% of the total breast cancers. Recent evidence suggests that 20-40% of the remaining "sporadic" breast cancers are associated with low penetrance, high frequency polymorphisms in genes involved with apoptosis, cell-cycle regulation and DNA repair (Scott, 2004). These low penetrance polymorphisms could potentially be influenced by gene-gene interactions or by gene-environmental interactions (Loeb, 1991; Dempfle, 2008). In gene-gene interaction, a sequence variant in a given gene has no effect. However, additional sequence variants in other genes allow interactions that expose a phenotype. For example, two polymorphisms in genes responsible for alcohol metabolism found in the Japanese population is linked to colorectal cancer. The first polymorphism creates a super-active variant of alcohol dehydrogenase which increases acetaldehyde concentrations. The second polymorphism inactivates aldehyde dehydrogenase which can not break down the acetaldehyde produced. Separately, these mutations would go un-noticed, but together, they increase colorectal cancer risk (Matsuo, 2006).

Gene-environment interactions are another mechanism in which these low penetrance point mutations may express a phenotype. In gene-environment interaction, altered gene function is only detected as a result of environmental insult. For instance, the interaction between aflatoxin and p450 increases the risk for liver carcinogenesis (Eaton, 1994). When peanuts contaminated with fungi *Aspergillus flavus* are ingested, liver cytochrome p450 enzymes metabolize the mold into a number of products including aflatoxin 8,9 epoxide. This particular

compound has carcinogenic potential because it intercalates into DNA, converting guanine to thymine at codon 249 in p53.

Unlike high penetrance mutations that are detected in high risk families, low risk mutations are not as obvious. For example, families with mutations in the BRCA2 gene are easily identifiable because a relatively high number of individuals have similar cancers. Families with low penetrance mutations are more subtle and less likely to stand out, making epidemiological studies problematic (Mahoney, 2007).

1.2 Targeted effects of ionizing radiation

Many years of research have demonstrated that the principle effects of IR are a result of direct energy deposition leading to the production of complex DNA lesions that are difficult to repair (Munro, 1970; Ward, 1981; Cornforth, 1987). IR produces an array of damage including point mutations (via free radicals), single-stranded DNA breaks (SSBs) and double-stranded DNA breaks (DSBs). DSBs, particularly complex forms of DSBs, are believed to be the form of damage that initiates genomic instability, mutation, cell death, mitotic arrest and cancer following IR exposure.

1.3 DNA double-strand break repair

Because of the potentially devastating effects from IR as a result of the induction of DSBs, it is imperative to have mechanisms capable of repairing such lesions to maintain the integrity of the genome. Two pathways are responsible for

repairing DSBs: homologous recombination (HR) and non-homologous end-joining (NHEJ) (Hoeijmakers, 2001).

Homologous recombination

HR (Fig.1A) takes place in S/G2-phase and uses its sister chromatid as a template. Since HR has a template to repair the DSB, it is considered substantially error-free (Helleday, 2003). Initially, the DSB is recognized by the Mre11/Rad50/Nbs1 (MRN) complex to process the ends into a 3' overhang. The single-stranded DNA (ssDNA) is recognized by replication protein A (RPA) which protects the strand and provides access for other HR proteins to the site. The HR proteins BRCA2, XRCC2/3, BRCA1/, RAD52, Rad54, BLM and WRN assist in the removal of RPA and the recruitment/loading of Rad51 onto the ssDNA (Helleday, 2003 and Sung, 2003). RAD54 aides in the RAD51 nucleoprotein filament strand invasion at a homologous region of the sister chromatid to form a D-loop. The second DSB end invades a portion of the D-loop to form a Holliday junction. DNA polymerase is then recruited to the Holliday junction to fill in the missing sequence. The final step is the resolution of the junction by a ligase/resolvase complex.

HR proteins are essential for cell survival and mutations in these genes can greatly increase the risk of carcinogenesis. Mutations in the Ataxia Telangiectasia Mutant (ATM) gene cause the disease Ataxia Telangiectasia. These individuals are susceptible to elevated cancer risk (Thompson, 2002). The most well-known case regarding HR and disease is the discovery of mutations in BRCA1/2 which

has been fundamental in better understanding the link between genetic mutations and elevated breast cancer risk (Venkitaraman, 2001; Wenham, 2003).

Non-homologous end-joining (NHEJ)

Unlike HR, the NHEJ pathway repairs DSB damage throughout the cell cycle and is the primary method for IR-induced DSB repair in mammalian cells (Fig.1B) (Hanakahi, 2000). The nature of how NHEJ rejoins DSBs sometimes creates a loss of sequence, making it more error-prone compared to HR. The DSB is first recognized by the Ku70/Ku80 complex which then recruits DNA-dependent protein kinase catalytic subunit (DNA-PKcs) to damaged site, one on each strand (Fig.1B). Once DNA-PKcs binds to Ku and the DNA, it forms the holoenzyme DNA-PK and becomes activated. In this state, DNA-PKcs is able to autophosphorylate which is imperative for enzymatic function. DNA-PK is responsible for juxtaposition of the DSB ends and recruitment of other NHEJ proteins to the damaged region. The LigaseIV/XRCC4 complex is lastly recruited to the site which ligates the broken DSBs together. Other proteins, Artemis, Cernunnos and Apollo, have been identified to play a role in NHEJ, but are less understood. Artemis is an exonuclease/endonuclease that is thought to process complex DSB ends (Ma, 2002). Studies suggest that Cernunnos stimulates LigaseIV/XRCC4 ligation (Buck, 2006). Apollo is similar to Artemis, but has been shown to be more involved at the telomere (van Overbeek and de Lange, 2006).

Although less characterized than genes associated with HR, such as BRCA1/2 and ATM, numerous recent reports of defects in NHEJ DNA repair genes have been linked to cancer predisposition. Polymorphisms in the LigaseIV, Ku70 and XRCC4 have been shown to correspond to breast cancer risk (Han, 2004; Rafii, 2002; Kuschel, 2002; Roddam, 2002). A more recent study has found specific SNPs in *Prkdc* that are associated with increased risk of breast cancer in Radiation Technologists (Bhatti, 2008).

1.4 DNA-dependent protein kinase catalytic subunit (DNA-PKcs) and the *Prkdc* gene

The *Prkdc* gene encodes the NHEJ protein, DNA-PKcs. DNA-PKcs is a 465kDa serine/threonine protein-specific kinase (Smith, 1999). In mice, the 12,674bp transcript (86 exons) yields a 4128-residue protein product (Boskovic, 2003). In the human genome, the 13, 500bp transcript encodes a 4127aa polypeptide (Connelly, 1996). The complete crystal structure has not been elucidated because of its large size, but configuration models derived from EM imaging and electron crystallography give glimpses of the protein's shape. The models propose three essential regions that constitute DNA-PKcs: the head, the arm and the palm (Boskovic, 2003). The head encloses a cavity that has two openings capable of containing single-stranded and double-stranded DNA. DNA binding induces conformational changes in the protein that can be observed as the arm acting as a hinge to enclose strands of DNA between palm and head.

The bulk of the protein has no homology with most other proteins. However, the kinase domain does share common sequences with the PI3 kinases

(Smith, 1999). This puts DNA-PKcs into the PI3-like family along with ATM and ATR (ATM-related protein). Upon binding to DNA, DNA-PKcs changes the 3-D structure and activates the kinase domain. However, new evidence discovered DNA-PKcs in the cytoplasm and cell membrane, suggesting that DNA-PKcs does not necessarily need DNA to be active (Feng, 2004, Fang, 2007, Dragoi, 2005; Lucero 2003). For example, studies have shown that DNA-PKcs phosphorylates proteins in lipid rafts in a DNA-independent manner and that this phosphorylation is needed for radiation signal transduction (Lucero, 2003).

It has been recently shown that autophosphorylation is necessary for proper DNA-PKcs function (Block, 2004; Douglas, 2007; Cui, 2005). Cells with mutated phosphorylation sites are found to be deficient in DNA repair following radiation and lacked the ability for normal V(D)J recombination. It is noteworthy that these mutated forms of DNA-PKcs result in normal kinase activity and have the ability to phosphorylate substrates *in vitro* similar to wild-type controls (54). The first autophosphorylation cluster is located between the 2609-2647 residues is needed for proper conformational changes of DNA-PKcs and is required for DNA-end processing (Block, 2004). Evidence suggests that phosphorylation at theses sites allow for an "open" conformation of DNA-PKcs which allows access for other NHEJ proteins to the DSB end. This cluster has also been shown to play a role in telomere capping due to the increase of telomere-DSB fusions observed in mutants; but further studies are needed elucidate its specific role at the telomere (Williams, manuscript in preparation). Another autophosphorylation cluster, residues 2023, 2029, 2041, 2053 and 2056, was later identified (Cui, 2005).

Phosphorylation in this cluster promotes a "closed" configuration position and keeps DNA-PKcs from binding to DSB ends. Originally, it was thought these were only substrates for autophosphorylation, but Chen et al. has demonstrated that the 2609aa residue is phosphorylated by ATM (Chen, 2007). This finding not only demonstrates that other proteins can potentially phosphorylate DNA-PKcs, but also that ATM and DNA-PKcs have direct interaction.

Cell and animal models with defective DNA-PKcs have proven to be powerful tools in identifying the function of DNA-PKcs. Utilization of the severe combined immunodeficient (SCID) mouse strain was monumental in studies involving Variable Diversity Joining (V(D)J)) recombination, DSB repair and more recently, telomere maintenance (Blunt, 1996).

DNA-PKcs and Variable diversity joining (V(D)J) recombination

DNA-PKcs plays a crucial role in immunity via V(D)J recombination (Soubeyrand, 2001; Smider, 1997). V(D)J recombination occurs in developing B- and T-lymphocytes to create immunoglobulin variation needed to recognize and respond to the multitude of diverse pathogens. The combination of the variable (V) and diversity (D) gene segments are first joined together, followed by the coupling of the joining (J) gene segment. This complex is produced by introducing DSBs at the specific sites flanking the genes that are recognized by RAG1 and RAG2 (Recombination-Activating Genes), leaving a hairpin substrate. The structure is recognized by the DNA-PKcs/Artemis complex which then accesses the ends and recruits the XRCC4/LigaseIV complex to ligate the DSB.

DNA-PKcs and NHEJ

As previously discussed, DNA-PKcs is also a fundamental component in DSB repair via the NHEJ pathway. The Ku70/Ku80 complex binds to free double-stranded DNA in a nonsequence-specific manner and slides down to allow DNA-PKcs binding. The binding of DNA-PKcs induces conformational changes in the protein that activates kinase activity and autophosphorylation capabilities (Boskovic, 2003; Smith 1999).

Mutants with defective DNA-PKcs exhibit significant decreased DSB repair and V(D)J recombination. Some of these phenotypes are more severe in select mutants than others, depending on the manner of the mutation. For example, SCID mice are null for DNA-PKcs and are completely incapable of V(D)J recombination (Blunt, 1996). The BALB/c mouse strain is also deficient in DNA-PKcs levels; but has some residual protein expression (Okayasu, 2000). These mice are capable of V(D)J recombination, demonstrating that the decreased levels of DNA-PKcs observed in BALB/c were sufficient for V(D)J recombination and that the BALB/c mutation is not as severe as seen in SCID.

Another example of utilizing mutants to study DNA-PKcs involves cells with altered phosphorylation sequence. These mutations have proven a useful tool in examining the role of DNA-PKcs autophosphorylation and NHEJ. Studies have shown that cells with mutant phosphorylation sites, specifically in the 2609-2647aa cluster have a more severe phenotype than kinase dead cells in terms of DSB repair (Block, 2004; Cui, 2005). The current hypothesis suggests that

autophosphorylation is needed for conformational changes in DNA-PKcs that allow access for other DSB repair proteins.

DNA-PKcs and telomere maintenance

More recently, it has been shown that DNA-PKcs is involved in telomere maintenance (Bailey 1999; Bailey 2001; Bailey 2004). Because eukaryotic genomic DNA is linear, it is vital that cells have a capping mechanism to avoid undesired degradation or fusion via the telomere. Mammalian telomeres are tandem TTAGGG-rich repeats (on the leading DNA strand) at the end of chromosomes that allow for replication and protection from chromosomal degradation or fusion (Blackburn, 1984). The relationship between DNA-PKcs and telomeres is not well understood. Chromatin immunoprecipitation (ChIP) assays show that DNA-PKcs is localized at mammalian telomere DNA sequences (Hendrickson, 2005). Studies using mutant or null DNA-PKcs mice reveal conflicting results regarding DNA-PKcs and telomere length which suggests that telomere length maintenance is not its major role. Although much insight has been gained using mouse models to study telomeres, it is important to note that mice are different from humans because they have active telomerase throughout their entire lifespan and has significantly longer telomeres.

There is evidence, however, demonstrating that DNA-PKcs is needed for telomere processing, specifically end-capping (Bailey 1999; Bailey 2001). The end-capping mechanism of telomeres is necessary in order to avoid undesired fusions. Bailey et al. have provided strong evidence to support DNA-PKcs as a

key component in telomere capping, specifically on the leading strand. Mutations in DNA-PKcs lead to increased telomere-to-telomere fusions and IR-induced telomere-DSB fusions which are thought to be due to a lack of proper telomere capping (Bailey 1999; Bailey 2001; Bailey 2004; Williams, manuscript in preparation).

1.5 DNA-PKcs/*Prkdc* in mouse models

DNA-PKcs and SCID mice

Severe compromised immunodeficient (SCID) mice have proven to be a valuable tool to study the function of DNA-PKcs. These mice have a T-cell and B-cell deficiency due to lack of proper V(D)J recombination which aided the discovery of DNA-PKcs. SCID mice have a T → A mutation that converts the 4045aa residue to an early stop codon, truncating the last 88aa of DNA-PKcs (Blunt). This particular strain was vital in our current understanding of DNA-PKcs and its role in NHEJ, V(D)J recombination and telomere maintenance (Blunt, 1996). Investigators have used the SCID strain to examine DNA-PKcs and IR-induced genomic instability (GI) and tumorigenesis compared to other mouse strains. These studies demonstrate that not only are SCID deficient in V(D)J recombination, but also in DSB repair, chromosomal stability and telomere maintenance (Blunt, 1996; van Buul, 1998; Bailey, 2004).

The BALB/c mouse strain

Another strain used to study DNA-PKcs is the BALB/c mouse model. BALB/c expresses a hypomorphic variant of DNA-PKcs and, like SCID, is also susceptible to radiation-induced mammary carcinogenesis (Kallman, 1962). Initial studies demonstrated that BALB/c has increased acute death rates after exposure to low-dose IR compared to other strains (Storer, 1988). Subsequent work has shown a significant induction of both lung and mammary adenocarcinomas after exposure to ^{137}Cs γ-irradiation (Ullrich, 1991). The mechanism behind the observation of IR-induced tumorigenesis in BALB/c is difficult to elucidate because of the long-latency period between exposure of IR to the detection of tumors. Therefore, an approach, pioneered by DeOme et al. to study virally-induced mammary cancer (DeOme, 1978), was developed to quantitatively identify and characterize radiation initiated cells and their progression into a neoplastic phenotype (Ethier, 1982). This assay involves transplanting mammary epithelial cells from donor irradiated mice into the cleared fat-pad of unirradiated mice. Following reconstitution of the mammary gland in recipient mice, IR-induced altered (initiated) cells were quantified as ductal dysplasias and their progression characterized using morphological and molecular approaches (Either, 1982; Either, 1984).

Further studies examined the molecular events associated with the initiation and progression of altered cells. In a series of studies, Selvanayagam et al. characterized initial molecular events in such altered cells as well as events involved in progression (Selvanayagam, 1995). Alterations in *c-myc* and other

mutations, such as cyclin D1, were observed in these mammary adenocarcinomas, as expected based on multiple previous studies on breast cancer. However, early examination of initiated cells revealed multiple p53 mutations found in clonal outgrowths which suggested that these cells were unstable. In light of these data, they hypothesized that IR did not directly induce p53 alterations, but rather these mutations were a result of radiation-induced genomic instability (GI) (Selvanayagam, 1995).

To test this hypothesis, Ponnaiya et al. examined the expression of cytogenetic damage in the progeny of irradiated cells which had not been exposed to IR by measuring chromatid aberrations. Because chromatid aberrations occur only in the previous cell cycle, it was possible to eliminate radiation effects that were a result of direct exposure. These studies found a delayed increase in chromatid aberrations transmitted to the progeny in BALB/c, but not in C57BL/6 (Ponnaiya, 1997). This increase was observed 20 population doublings following radiation exposure. Since these cells were not directly irradiated, they interpreted these results as evidence for radiation-induced GI. A comparison of F1 hybrids (BALB/c X C57BL/6) indicated that sensitivity to IR-induced GI was a recessive genetic trait.

Based on these results, it was then hypothesized that the high levels of chromatid aberrations in BALB/c were due to the cells' inability to properly repair the initial insult produced by IR. To test this, Okayasu et al analyzed repair activity and repair time in the BALB/c compared with other mouse strains including A/J, DBA, C3H, CB6F1 and C57BL/6 (Okayasu, 2000). Primary

kidney fibroblasts from several different mouse strains were examined after exposure to 50Gy of γ-radiation. The A/J, DBA, C3H, CB6F1 and C57BL/6 were effective in repairing DNA damage after radiation exposure. However, the BALB/c and SCID were deficient in DNA repair with SCID displaying a more severe phenotype (Fig.3).

Western blot analysis revealed decreased expression of DNA-PKcs but not Ku70/Ku80 in both SCID and BALB/c compared to C57BL/6 (Fig.3) (Okayasu, 2000). It is interesting to note that tissue from mammary glands of all strains expresses less DNA-PKcs than either spleen or kidney tissue in all mouse strains. Okayasu et al. also examined DNA-PKcs kinase activity in BALB/c (Fig.3). Results revealed a significant decrease in DNA-PKcs kinase activity in both the SCID and BALB/c strains. It was not certain whether the decrease in overall kinase activity was due to a defect in specific activity of the protein or simply due to lower quantities of stable protein in the cell. The virtual lack of DNA-PKcs expression in BALB/c mammary tissue was hypothesized to impart unique vulnerability to the damaging effects of ionizing radiation and to act as an initiator of mammary carcinogenesis. Interestingly, no differences in mRNA levels between BALB/c and C57BL/6 were observed, suggesting a post-translational event (Okayasu, 2000).

The *Prkdc* gene, which encodes DNA-PKcs, was then analyzed to determine if there was a relation between this decreased function and alterations in the genetic sequence (Yu, 2001). In these studies, two separate functional SNPs in the coding regions of *Prkdc* were identified that were specific to BALB/c

compared to other mouse strains, termed *Prkdc*^{BALB}. The first SNP is located downstream of the leucine zipper in a highly-conserved locus. The SNP changes a positive-charged arginine to cysteine and may hinder correct formation of the protein, making it unstable (Yu, 2001). It may also disrupt proper protein interaction, causing a decrease in protein function, including autophosphorylation (Yu, 2001). The second SNP found in the kinase domain of DNA-PKcs is located near the C-terminal domain. This SNP converts a methionine to a valine in a non-conserved region, but still may hinder phosphorylation of other proteins, including DNA-PKcs itself. This implies that the SNPs may affect protein stability or protein interaction. The functional significance of each SNP is not known. It has been further proposed that these two unique SNPs found in the BALB/c *Prkdc* gene are a major factor for this strain's susceptibility to radiation-induced mammary cancer and may play a role in its IR-induced GI.

At about the same time, reports by Bailey et al. demonstrated that the DNA-PKcs null strain SCID was susceptible to telomere-telomere fusions as a result of improper telomere end-capping (Bailey 1999; Bailey 2001; Bailey 2004). Bailey and Ullrich then examined potential defects in telomere maintenance in the BALB/c strain because of its hypomorphic variant of DNA-PKcs (Williams et al., manuscript in progress). While both C57BL/6 and the BALB/c showed a similar increase in chromosome aberrations, mainly dicentric fusions in first cycle cells, an increase in IR-induced telomere-DSB fusions, but not telomere-telomere fusions were observed in BALB/c, and not C57BL/6 (Fig.4). This suggested that the BALB/c defect leads to improperly capped telomeres following IR exposure

to create "sticky" DNA ends which are capable of fusing to IR-induced DNA DSBs. In addition, these telomere-DSB fusions occurred at a higher frequency than dicentric fusions, indicating that the telomere-DSB fusions are a common occurrence in DNA-PKcs deficient mouse strains. Telomere-DSB fusions were also observed after multiple population doublings after IR exposure, demonstrating a delayed response. Therefore, it was hypothesized that these delayed telomere-DSB fusions may contribute to GI and are potentially harmful to the cell.

DNA-PKcs has also been linked with apoptosis. Apoptosis was characterized in BALB/c and compared to STS and C57BL/6 strains (Mori, 1998; Weil, personal correspondence). It has also been reported that BALB/c is more resistant to apoptosis in jejunum and colon crypt cells compared C57BL/6 and STS. Further studies involving the CcS recombinant congenic set (derived from BALB/c and STS/A progenitors) have identified three polymorphisms that were linked to BALB/c's resistance to apoptosis in crypt cells, one of which maps to the same locus as *Prkdc* (Mori, 1998). Based on these studies, it is tempting to hypothesize that the BALB/c apoptotic phenotype may be linked to expression of persistent GI.

LEWES strain

While $Prkdc^{BALB}$ is unique to this strain, it has been shown that the LEWES has the BALB/c-like SNP in the kinase domain but the common allele downstream of the leucine zipper (Chapter 3). The LEWES strain has interesting

origins being derived from a wild mouse captured in Lewes, Delaware. This raises interesting genealogical questions regarding its origin and relationship to BALB/c. Regardless of its origin, this strain can be utilized as a tool to specifically study the impact of this BALB/c SNP in the kinase domain on radiation sensitivity using a variety of end-points.

1.6 DNA-PKcs/*Prkdc* and human studies

SNPs in the *Prkdc* gene are not limited to inbred mouse strains. Recent reports have demonstrated a link between susceptibility to both lung and breast cancer and defective *Prkdc* in the human population (Auckley, 2001; Bhatti; 2008). Auckley et al. examined a population with lung cancer and found that patients with lung cancer showed a significant decrease in DNA-PKcs enzymatic activity compared to a control population. (Auckley, 2001) More recently, Bhatti et al studied radiation exposure and cancer risk in a group of radiologic technologists and breast cancer risk. This group found an elevated risk for those who have specific SNPs in *Prkdc* (Bhatti, 2008). These studies provide support that defective DNA-PKcs or mutations in *Prkdc* are associated with cancer, but it does not provide direct evidence.

1.7 Non-targeted effects of IR/the bystander effect

Direct, or targeted, effects of IR are well established. However, more recent investigations have identified effects in neighboring non-irradiated cells which has been termed the radiation-induced bystander effect (BSE). The BSE

was first described in 1992 by Nagasawa and Little who showed that sister chromatid exchange (SCE) frequency in CHO cells was significantly higher than expected following exposure to low fluences of alpha particles that transversed only a small fraction of CHO cells in culture (Nagasawa, 1992). Subsequent investigations explored the BSE further by using a number of different end-points including cytogenetic aberrations, clonogenic survival, mutation frequency and apoptosis (Prise, 2003). Most, if not all, of these studies are confirmatory of the existence of the BSE, but little is known the mechanism. Currently, extensive efforts are underway to better understand the processes that underlie the BSE. Several independent investigations suggest that cytokines, reactive oxygen species (ROS) and/or nitric oxygen species (NOS) are generated in irradiated cells and may induce a bystander response through signaling processes (Kashino, 2007; Shao, 2006; Banaz-Yasar, 2007).

Arguments can certainly be made that the BSE may result in increased cancer risk. Conversely, research has also provided evidence for potential beneficial effects (Belyakov, 2003; Belyakov, 2002; Mothersill and Seymour, 2004; Prise, 2003; Goldberg, 2002). If the BSE is beneficial, then it would promote a radioprotective response. Conversely, if the BSE is harmful, then a larger target size would be impacted compared to what was originally believed following exposure to IR.

Additional evidence has demonstrated a link between the BSE and GI (another nontargeted effect) (Goldberg, 2002). Evidence for IR affecting unirradiated cells was first observed in plasma from irradiated patients. Plasma

from these individuals had clastogenic activity which produced chromosome breakage in non-irradiated peripheral blood lymphocytes which can contribute to GI (Morgan, 2003; Goldberg, 2002). Later investigations have observed cytogenetic instability in the progeny of unirradiated cells, a hallmark of GI (Goldberg, 2002; Clutton, 1996). Considering the numerous reports that imply GI as an initiating event in IR-induced carcinogenesis, then it would be reasonable to hypothesize that a BSE-induced GI may play a role in radiation carcinogenesis.

1.8 Specific Aims

It has been shown that BALB/c is sensitive to IR-induced mammary carcinogenesis and that this phenotype has been linked to a hypomorphic variant of the DNA-repair protein, DNA-PKcs. Studies have also shown that the defective DNA-PKcs is responsible for deficiencies in DSB repair and telomere maintenance. This deficiency has been linked to two functional SNPs identified in the coding region of *Prkdc* that may be responsible for the BALB/c radiosensitive phenotype. However, the specific role of the individual SNPs has not yet been identified. As previously mentioned, the SNP downstream of the leucine zipper is in a highly conserved region, suggesting that it may be at a crucial site. In addition, the SNP is surrounded by autophosphorylation clusters that have been established to be critical for DNA-PKcs function. It is therefore reasonable to hypothesize that this SNP may affect autophosphorylation which may disrupt protein activity. Conversely, the SNP in the kinase domain may be responsible for deficient kinase activity and would explain the observed

phenotypes in BALB/c. And because we know that DNA-PKcs protein levels are less in BALB/c, it is possible that one of these SNPs affects protein stability. In addition to these uncertainties, it is also possible that both SNPs work together to produce to the BALB/c phenotype. Insight into these mechanisms will provide clues to help identify sensitive subpopulations in human that are sensitive to IR-induced breast cancer risk.

The purpose of this research is to determine the functional significance of the BALB/c SNPs. Such studies provide an important first step that directly links GI to radiation-induced mammary carcinogenesis in the BALB/c strain. These studies have three specific aims: 1. examine the impact the SNPs have on cell-to-cell communication via the bystander effect; 2. Characterize the consequence of the BALB-like SNP in the kinase domain by using the LEWES mouse strain; 3. Generate knock-in mice which will allow for detailed studies on the relevance of each SNP on the BALB/c phenotype.

Figures

Figure 1: DSB Repair

A. Homologous Recombination

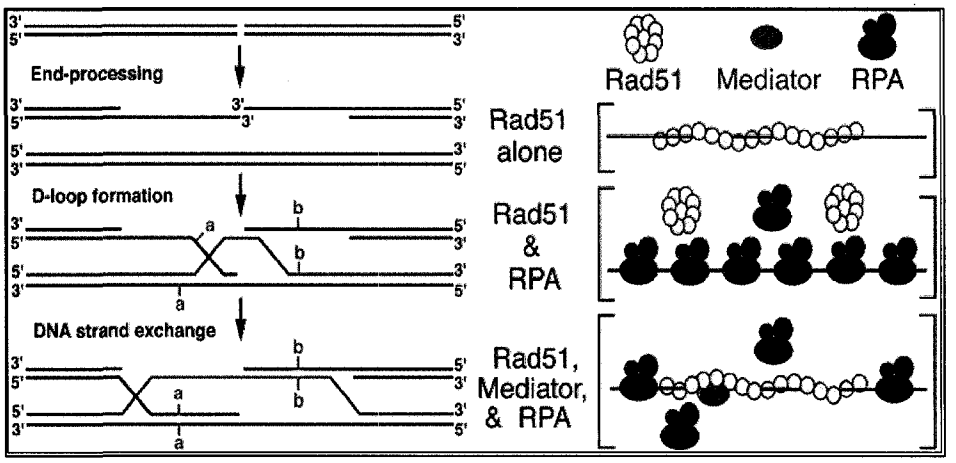

Sung P et al, The Journal of Biological Chemistry, Vol 278, NO 44, 2003

B. Non-homologous Recombination

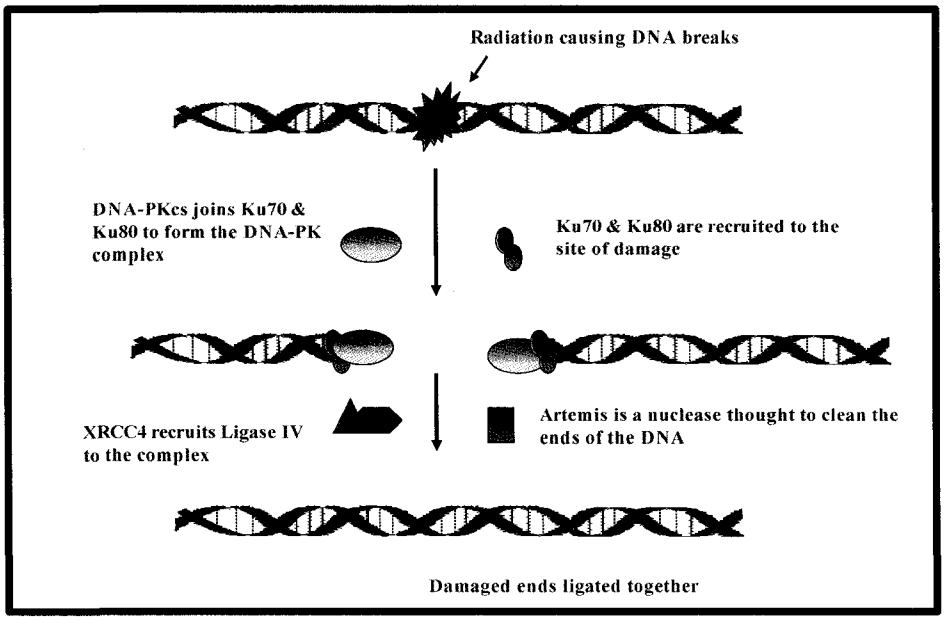

Figure 1: DSB Repair The pathways are involved in DSB repair in mammalian cells. **A.** HR occurs in dividing cells. HR proteins (BRCA1/2, RPA, Rad54 and XRCC2/3) assist in RAD51 strand invasion which forms a Holliday junction. DNA polymerase fills in the damaged region and the junctions are resolved. **B.** NHEJ is the main pathway in IR-induced DSB repair. The DNA-PK holoenzyme (Ku70/80 and DNA-PKcs) bind to free DSB ends and recruit the XRCC4/ligaseIV complex to ligate the broken ends. Other less-understood NHEJ proteins, like Artemis, have roles in processing complex DSBs.

Figure 2: The *Prkdc* gene

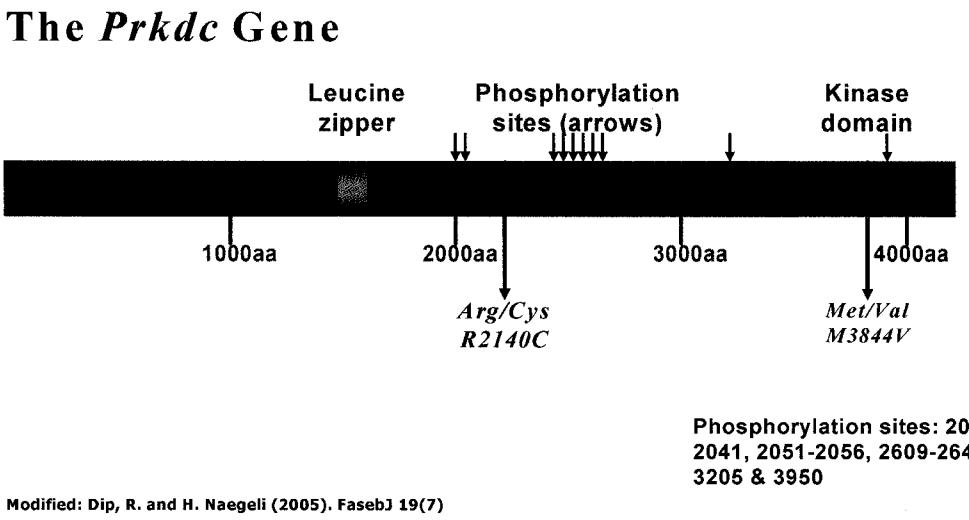

Figure 2: The Prkdc gene The Prkdc gene encodes DNA-PKcs. The leucine zipper domain can potentially interact with other proteins or DNA. The kinase domain is located near the C-terminal domain and phosphorylates proteins on serine/threonine residues. There are several sites along the gene that are substrates for autophosphorylation, which is crucial for enzymatic function. In the BALB/c strain, there are 2 functional SNPs that may be responsible for its radiosensitivity. One is located downstream of the leucine zipper and the other located in the kinase domain.

Figure 3: BALB/c and DNA-PKcs

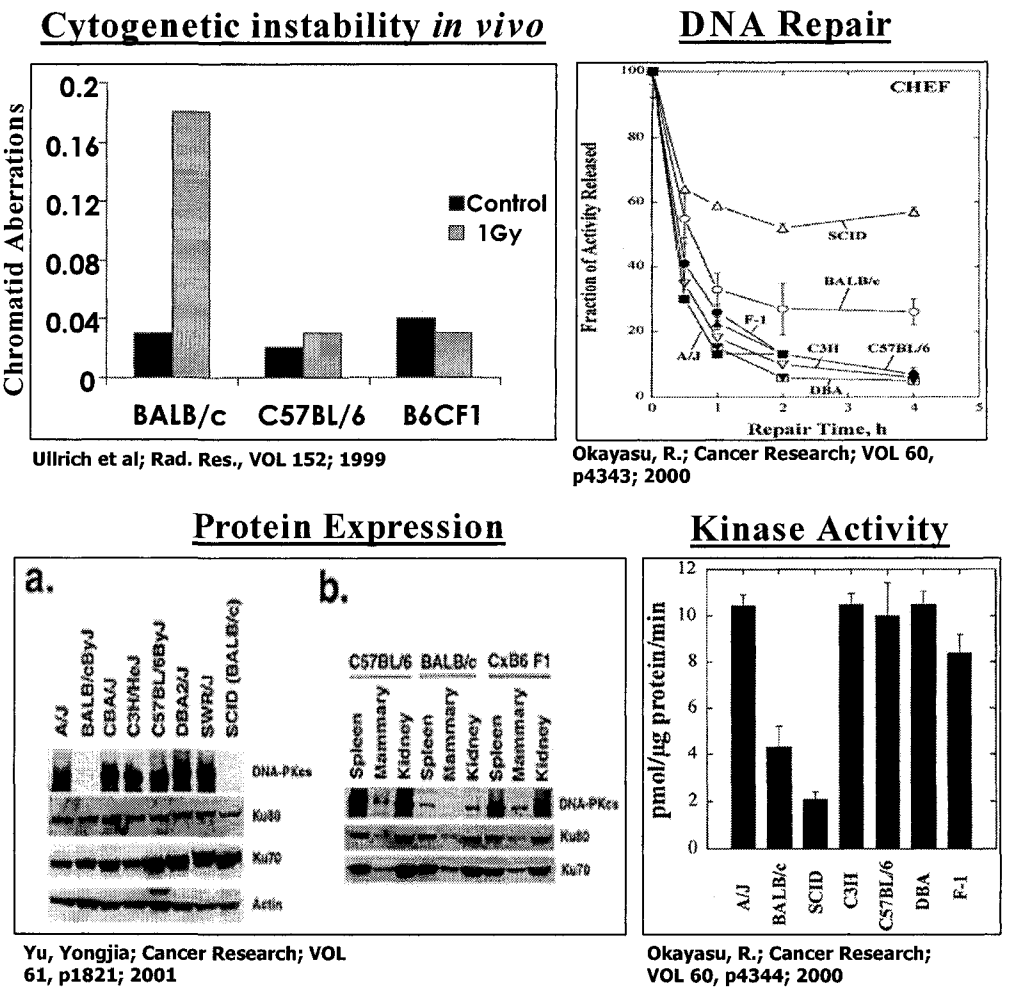

Figure 3: BALB/c and DNA-PKcs BALB/c has significantly more IR-induced chromatid-type aberrations than C57BL/6, suggesting that it is susceptible to IR-induced GI. BALB/c and SCID are deficient in DSB repair, with SCID demonstrating a more severe phenotype. DNA-PKcs protein levels are deficient in BALB/c and more so in SCID. Kinase activity was measured and showed decreased enzymatic activity in BALB/c and SCID.

Figure 4: DNA-PKcs and telomeres

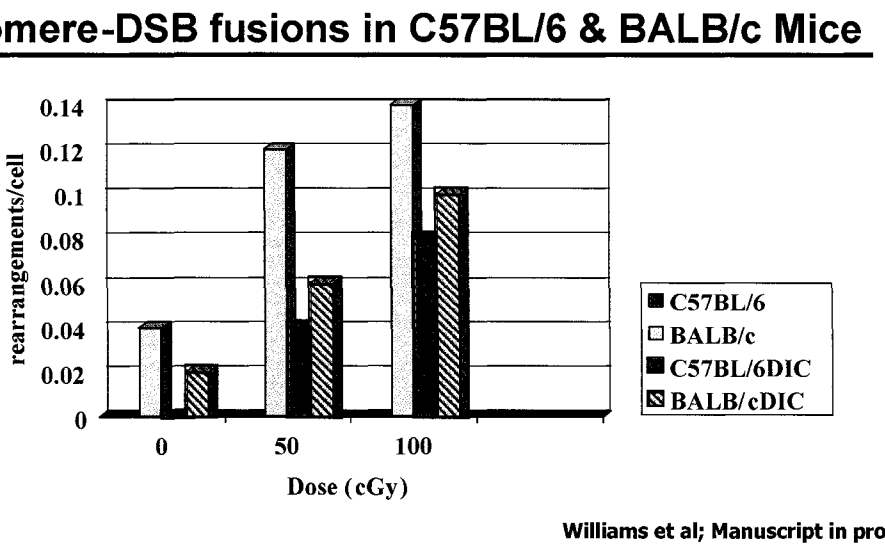

Figure 4: DNA-PKcs and telomeres Dicentric aberrations and telomere-DSB fusions were examined in BALB/c and C57BL/6. BALB/c showed a slight background of telomere-DBS fusions, but increased significantly after IR exposure. It was found that these events occurred at a higher frequency than dicentrics, suggesting this is a frequent event in BALB/c. C57BL/6 showed no telomere-DSB fusions in either case.

References

1. Allen-Brady, K., et al., A role for XRCC4 in age at diagnosis and breast cancer risk.
2. Cancer Epidemiol Biomarkers Prev, 2006. 15(7): p. 1306-10.
3. American Cancer Society (ACS) database http://www.cancer.org
4. Auckley DH, Crowell RE, Heaphy ER, Stidley CA, Lechner JF, Gilliland FD and Belinsky SA; Reduced DNA-dependent protein kinase activity is associated with lung cancer, Carcinogenesis, 22, NO 5, 723-727, 2001
5. Bailey SM, Goodwin; DNA and telomeres: beginnings and endings. Cytogenet Genome Res. 2004;104(1-4):109-15.
6. Bailey SM, Cornforth MN, Kurimasa A, Chen DJ and Goodwin EH . Strand-specific fluorescence in situ hybridization: the CO-FISH family (2004) Cytogenet Genome Res 2004;107:14-17
7. Bailey SM, Brenneman MA, Halbrook J, Nickoloff JA, Ullrich RL and Goodwin EH. (2004). *DNA Repair (Amst)*, 3, 225-33.
8. Bailey SM, Cornforth MN, Kurimasa A, Chen DJ and Goodwin EH. (2001). *Science*, 293, 2462-5.
9. Bailey SM, Meyne J, Chen DJ, Kurimasa A, Li GC, Lehnert BE and Goodwin EH. (1999). *Proc Natl Acad Sci U S A*, 96, 14899-904
10. Banaz-Yasar, F., Lennartz, K., Winterhager, E. and Gellhaus, A. (2007) Radiation-induced bystander effects in malignant trophoblast cells are independent from gap junctional communication. *J Cell Biochem.*
11. Bhatti, P., et al., Polymorphisms in DNA repair genes, ionizing radiation exposure and risk of breast cancer in U.S. Radiologic technologists. Int J Cancer, 2008. 122(1): p. 177-82.
12. Blackburn, EH; Telomeres: Do the ends justify the means, Cell, 37, 1984, 7-8
13. Block, W.; Yu, Y.; Merkle, D.; Gifford, J.; Ding, Q.; Meek, K. and Lees-Miller, S. Autophosphorylation-dependent protein kinase catalytic subunit regulates ligation of DNA ends, Nucleic Acids Research, 32, No. 14, 4351-4357, 2004
14. Blunt T, Gell D, Fox M, Taccioli GE, Lehmann AR, Jackson SP, Jeggo PA. Identification of a nonsense mutation in the carboxyl-terminal region of DNA-dependent protein kinase catalytic subunit in the scid mouse. Proc Natl Acad Sci U S A. 1996 Sep 17;93(19):10285-90.
15. Boskovic, J.; Rivera-Calzada, A.; Maman, J.; Chacon, P.; Willison, K.; Pearl, L. and Llorca, O. Visualization of DNA-induced conformational changes in the DNA repair kinase DNA-PKcs, EMBO, 22, No. 21, 5875-5882, 2003
16. Buck D, Malivert L, de Chasseval R, Barraud A, Fondanèche MC, Sanal O, Plebani A, Stéphan JL, Hufnagel M, le Deist F, Fischer A, Durandy A, de Villartay JP, Revy P.; Cernunnos, a novel nonhomologous end-joining factor, is mutated in human immunodeficiency with microcephaly. Cell. 2006 Jan 27;124(2):287-99
17. Chen BPC, Uematsu N, Kobayashi J, Lerenthal Y, Krempler A, Yajima H, Chen DJ; ATM is essential for DNA-PKcs phosphorylation at the Thr-2609 cluster upon DNA DSB; Journal of Biological Chemistry; 282, NO 9, 2007, 6582-6587

18. Connelly MA, Zhang H, Kieleczawa J, Anderson CW. The promoters for human DNA-PKcs (PRKDC) and MCM4: divergently transcribed genes located at chromosome 8 band q11. Genomics. 1998 Jan 1;47(1):71-83.
19. Cornforth MN, Bedford JS; A quantitative comparison of potentially lethal damage repair and rejoining of interphase chromosome breaks in low passage normal human fibroblasts; Radiat Res, 111, 385-405, 1987
20. Cui X, Yu Y, Gupta S, Cho YM, Lees-Miller SP, Meek K.; Autophosphorylation of DNA-dependent protein kinase regulates DNA end processing and may also alter double-strand break repair pathway choice. Mol Cell Biol. 2005 Dec;25(24):10842-52.
21. Dempfle A, Scherag A, Hein R, Beckmann L, Chang-Claude J, Schäfer H; Gene-environment interactions for complex traits: definitions, methodological requirements and challenges; Eur J Hum Genet; 2008 Jun 4
22. DeOme KB, Miyamoto MJ, Osborn RC, Guzman RC, Lum K. Detection of inapparent nodule-transformed cells in the mammary gland tissues of virgin female BALB/cfC3H mice. Cancer Res. 1978 Jul;38(7):2103-11.
23. Douglas P, Cui X, Block WD, Yu Y, Gupta S, Ding Q, Ye R, Morrice N, Lees-Miller SP, Meek K.; The DNA-dependent protein kinase catalytic subunit is phosphorylated in vivo on threonine 3950, a highly conserved amino acid in the protein kinase domain.Mol Cell Biol. 2007 Mar;27(5):1581-91. Epub 2006 Dec 11.
24. Dragoi, A.M., et al., DNA-PKcs, but not TLR9, is required for activation of Akt by CpGDNA.Embo J, 2005. **24**(4): p. 779-89.
25. Eaton LD and Gallhager EP; Mechanism of aflatoxin carcinogenesis, Annu Rev Pharmacol Toxicol, 34, 1994, 135-172
26. Ethier SP, Ullrich RL. Detection of ductal dysplasia in mammary outgrowths derived from carcinogen-treated virgin female BALB/c mice. Cancer Res. 1982 May;42(5):1753-60.
27. Ethier SP, Adams LM, Ullrich RL. Morphological and histological characteristics of mammary dysplasias occurring in cell dissociation-derived murine mammary outgrowths. Cancer Res. 1984 Oct;44(10):4517-22.
28. Fang, L., et al., Cell polarity protein Par3 complexes with DNA-PK via Ku70 and regulates DNA double-strand break repair. Cell Res, 2007. **17**(6): p. 572-574.
29. Feng, J., et al., Identification of a PKB/Akt hydrophobic motif Ser-473 kinase as DNA dependent protein kinase. J Biol Chem, 2004.
30. Fu, Y.P., et al., Breast cancer risk associated with genotypic polymorphism of the nonhomologous end-joining genes: a multigenic study on cancer susceptibility. Cancer Res, 2003. 63(10): p. 2440-6.
31. Gofman, J. Confirmation that ionizing radiation can induce genomic instability, ONLINE, www.ratical.com/radiation/CNR/GenomicInst.html, 1998
32. Han, J., et al., Polymorphisms in DNA double-strand break repair genes and breast cancer risk in the Nurses' Health Study. Carcinogenesis, 2004. 25(2): p. 189-95.
33. Hanakahi, Les A.; Bartlet-Jones, Michael; Chappell, Claire; Pappin, Darryl and West, Stephen C. Binding of inositol phosphate to DNA-PKcs and repair stimulation of DSB repair, Cell, 102, 721-729, September 15, 2000

34. Hartley, K.; Gell, D.; Smith, G.; Zhang, H.; Divecha, N.; Connelly, M; Admon, A.; Lees-Miller, S.; Anderson, C. and Jackson, S. DNA-dependent protein kinase catalytic subunit: a relative of PI3-kinase and the ATM gene product, Cell, 82, 849-856, September 8, 1995
35. Helleday, T; Pathways for mitotic homologous recombination in mammalian cells. Mutation Research, 532, 2003, 103-115
36. Hendrickson, E. A. , Huffman, J. and Tainer, J. A. Structural aspects of Ku and the DNA dependent protein kinase complex. (2005) In: DNA Damage Recognition. W. Seide, Y. W. Kow and and P. W. Doetsch, Eds., Marcel-Dekker, Inc., New York, NY, in press. (Review)
37. Hoeijmakers, J. Genome maintenance mechanisms for preventing cancer, Nature, 411, 366-374, May 17, 2001
38. Kallman, RF; The effect of dose rate on mode of acute radiation death of C57BL/6 and BALB/c mice. Radiat Res., 16, 1962, 796-810
39. Kashino, G., Prise, K.M., Suzuki, K., Matsuda, N., Kodama, S., Suzuki, et al. (2007) Effective suppression of bystander effects by DMSO treatment of irradiated CHO cells. *J Radiat Res (Tokyo)*, 48, 327-333.
40. Kuschel, B., et al., Variants in DNA double-strand break repair genes and breast cancer susceptibility. Hum Mol Genet, 2002. 11(12): p. 1399-407.
41. Lehnert, B.E., Goodwin, E.H. and Deshpande, A. (1997) Extracellular factor(s) following exposure to alpha particles can cause sister chromatid exchanges in normal human cells. *Cancer Res*, 57, 2164-2171.
42. Loeb, LA; Mutator phenotype may be required for multistage carcinogenesis; Cancer Research, 51, 1991, 3075-3079
43. Lucero H, Gae D and Taccioli G; Novel localization of the DNA-PK complex in lipid rafts, The Journal of Biological Chemistry, 278, NO 24, Issue June 13th, 2003, 22136-22143
44. Ma, Y.; Pannicke, U.; Schwartz, K. and Lieber, M. Hairpin opening and overhang processing by an Artemis/DNA-dependent protein kinase complex in nonhomologous end joining and V(D)J recombination, Cell, 108, 781-794, March 22, 2002
45. Martin C. Mahoney, MD, PhD, FAAFP Genetic Polymorphisms and Disease Prevention; Pediatr Blood Cancer 2007;48:742–747
46. Matsuo K, Wakai K, Hirose K, Ito H, Saito T, Suzuki T, Kato T, Hirai T and Tajima K; A gene-gene interaction between ALDH2 Glu487Lys and ADH2 His47Arg polymorphisms regarding the risk of colorectal cancer in Japan, Carcinogenesis, 27, NO 5, 2006, 1018-1023
47. Morgan WF. Is there a common mechanism underlying genomic instability, bystander effects and other nontargeted effects of exposure to ionizing radiation? Oncogene. 2003 Oct 13;22(45):7094-9. Review.
48. Mori N, van Wezel T, van der Valk M, Yamate J, Sakuma S, Okumoto M, Demant P. Genetics of susceptibility to radiation-induced apoptosis in colon: two loci on chromosomes 9 and 16. Mamm Genome. 1998 May;9(5):377-80
49. Mothersill, C. and Seymour, C.B. (1998) Cell-cell contact during gamma irradiation is not required to induce a bystander effect in normal human

keratinocytes: evidence for release during irradiation of a signal controlling survival into the medium. *Radiat Res*, 149, 256-262.
50. Munro TR; The relative radiosensitivity of the nucleus and cytoplasm of the Chinese hamster fibroblasts; Radiat Res, 42, 451-470, 1970
51. Nagasawa, H. and Little, J.B. (1992) Induction of sister chromatid exchanges by extremely low doses of alpha-particles. *Cancer Res*, 52, 6394-6396.
52. Nagasawa, H., Peng, Y., Wilson, P.F., Lio, Y.C., Chen, D.J., Bedford, J.S., et al. (2005) Role of homologous recombination in the alpha-particle-induced bystander effect for sister chromatid exchanges and chromosomal aberrations. *Radiat Res*, 164, 141-147.
53. National Cancer Institute (NCI) database http://www.cancer.gov
54. Okayasu, R.; Suetomi, K.; Yu, Y.; Silver, A.; Bedford, J, Cox, R. and Ullrich, R.L. A deficiency in DNA repair and DNA-PKcs expression in the radiosensitive BALB/c mouse, Cancer Research, 60, 4342-4345, August 15, 2000
55. Ponnaiya, B.; Cornforth, M.N. and Ullrich, R.L. Radiation-induced chromosomal instabililty is as clear as black and white, Radiation Research, 147, 121-125, 1997
56. Prise KM, Folkard M, Michael BD. A review of the bystander effect and its implications for low-dose exposure. Radiat Prot Dosimetry. 2003;104(4):347-55. Review.
57. Rafii, S., et al., A potential role for the XRCC2 R188H polymorphic site in DNA-damage repair and breast cancer. Hum Mol Genet, 2002. 11(12): p. 1433-8.
58. Roddam, P.L., et al., Genetic variants of NHEJ DNA ligase IV can affect the risk of developing multiple myeloma, a tumour characterised by aberrant class switch recombination. J Med Genet, 2002. 39(12): p. 900-5.
59. Scott, D Chromosomal radiosensitivity and low penetrance predisposition to cancer, Cytogenetics Genome Research, 104, 365-370, 2004
60. Selvanayagam CS, Davis CM, Cornforth MN, Ullrich RLCancer Res. Latent expression of p53 mutations and radiation-induced mammary cancer.1995 Aug 1;55(15):3310-7.
61. Shao, C., Lyng, F.M., Folkard, M. and Prise, K.M. (2006) Calcium fluxes modulate the radiation-induced bystander responses in targeted glioma and fibroblast cells. *Radiat Res*, 166, 479-487.
62. Smider, V and Chu, G. The end-joining reaction in V(D)J recombination, Immunology, 9 187-197, 1997
63. Smith, G.; and Jackson, S. The DNA-dependent protein kinase (Review), Genes and Development, 13, 916-934, 1999
64. Sonoda E, Sasaki MS, Buerstedde JM, Bezzubova O, Shinohara A, Ogawa H, Takata M, Yamaguchi-Iwai Y, Takeda S. Rad51-deficient vertebrate cells accumulate chromosomal breaks prior to cell death. EMBO J. 1998 Jan 15;17(2):598-608.
65. Soubeyrand, S.; Torrance, H.; Giffin, W.; Gong, W., Schild-Poulter, C. and Hache, R. Activation and autoregulation of DNA-PK from structured single-stranded DNA and coding end hairpins, PNAS, 98, No. 17, 9605-9610, August 14, 2001

66. Storer JB, Mitchell TJ, Fry RJ. Extrapolation of the relative risk of radiogenic neoplasms across mouse strains and to man. Radiat Res. 1988 May;114(2):331-53. Erratum in: Radiat Res 1989 Feb;117(2):362.
67. Sung, P., Krejci, L. VanKomen, S. and Sehorn, MG., Rad51 Recombinase and recombination mediators, The Journal of Biological Chemistry, 278, NO. 44, 2003, 42729-42732
68. Thompson, LH. and Schild, D; Recombinational DNA repair and human disease, Mutation Research, 509, 2002, 49-78
69. Ullrich, R.L. Cellular and Molecular changes in mammary epithelium following irradiation, Radiation Research, 128, S136-S140, 1991
70. Ullrich R.L. and Ponnaiya, B. Radiation-induced instability and its relation to radiation carcinogenesis, INT. J. RADIAT. BIOL, 74, No. 6, 747-754, 1998
71. van Buul, P.P L. Abramsson-Zetterberg, I.M. Zandman and A. van Buul, P.P., Abramsson-Zetterberg, L. Zandman . I.M and van Duyn-Goedhart A., Further characterization of the radiosensitivity of the scid mouse. Int. J. Radiat. Biol. **74** (1998), p. 35.
72. van Overbeek M, de Lange T; Apollo, an Artemis-related nuclease, interacts with TRF2 and protects human telomeres in S phase, Curr Biol. 2006 Jul 25;16(14):R544-6
73. Venkitaraman, A. Functions of BRCA1 and BRCA2 in the biological response to DNA damage, Journal of Cell Science, 114, 3591-3598, 2001
74. Ward JF; DNA damage produced by ionizing radiation in mammalian cells, Prog Nucleic Acis Res Mol Biol, 35, 95-125, 1988
75. Wenham, R.; Schildkraut, J.; McLean, K.; Calingaert, B.; Bentley, R.; Marks, J. and Berchuck, A. Polymorphisms in BRCA1 and BRCA2 and risk of epithelial ovarian cancer, Clinical Cancer Research, 9, 4396-4403, 2003
76. Yu, Y.; Okayasu, R.; Weil, M.; Silver, A.; McCarthy, M. Zabriskie, R.; Long, S.; Cox, R. and Ullrich, R.L. Elevated breast cancer risk in irradiated BALB/c mice associates with unique functional polymorphisms of the Prkdc gene, Cancer Research, 61, 1820-1824, March 1, 2001
77. Zhang, Y., Zhou, J., Cao, X., Zhang, Q., Lim, C.U., Ullrich, R.L., et al. (2007) Partial deficiency of DNA-PKcs increases ionizing radiation-induced mutagenesis and telomere instability in human cells. *Cancer Lett*, 250, 63-73

Chapter 2

DNA-PKcs and ATM influence generation of ionizing radiation-induced bystander signals

Abstract. The phenomenon by which irradiated cells influence non-irradiated neighboring cells, referred to as the bystander effect (BSE), is not well understood in terms of the underlying pathways involved. We sought to enlighten connections between DNA damage repair and the BSE. Utilizing sister chromatid exchange (SCE) frequencies as a marker of the BSE, we performed cell transfer strategies that enabled us to distinguish between generation versus reception of a bystander signal. We find that DNA-dependent Protein Kinase catalytic subunit (DNA-PKcs) and Ataxia Telangectasia Mutated (ATM) are necessary for the generation of such a bystander signal in normal human cells following gamma (γ)-ray exposure, but are not required for its reception. Importantly, we also show that directly irradiated human cells do not respond to receipt of a bystander signal, helping to explain why the BSE is a low dose phenomenon. These studies provide the first evidence for a role of the DNA damage response proteins DNA-PKcs and ATM specifically in the generation of a bystander signal and inter-cellular signaling.

Introduction

Newly emerging insight into the mechanistic basis of carcinogenesis supports the concept that the genetic effects of low-dose radiation cancer risks are considerably more complex than one might imagine based on linear no-threshold extrapolations from the high-dose radiation received by Japanese atomic-bomb survivors. The observation of a low dose ionizing radiation (IR) induced bystander effect (BSE), i.e., irradiated cells signaling their distress to, and stimulating a response in, non-irradiated neighbors and inducing an effect is a case in point.

The BSE occurs when a directly irradiated cell generates and transmits a signal, such as reactive oxygen species (ROS) (Kashino et al., 2007), nitric oxide species (NOS) (Shao et al., 2006), or cytokines (Banaz-Yasar et al., 2007) either through gap junctions (Azzam et al., 1998; Azzam et al., 2001) or through media (Lehnert et al., 1997; Mothersill and Seymour, 1998) to a neighboring non-irradiated cell. Given that the multiple markers that have been used to study the BSE, i.e., micronuclei formation (Yang et al., 2007), clonogenic survival (O'Neill-Mehlenbacher et al., 2007), apoptosis (Grifalconi et al., 2007), and sister chromatid exchange (SCE) (Nagasawa et al., 2005) (Figure 1), are themselves considered to be detrimental, it has been assumed that the BSE is harmful to neighboring cells. However, it has also been proposed that the BSE may actually be beneficial at a tissue level; cells exposed to a bystander signal are more radioresistant to subsequent IR-induced damage indicative of an adaptive response (Iyer and Lehnert, 2002). It is also noteworthy that of these markers,

only SCE frequency is not significantly influenced by direct low LET (e.g., gamma-ray) radiation exposure (Ardito et al., 1980), making SCE an attractive marker of the BSE.

Given numerous studies demonstrating the importance of DNA repair proteins in directly irradiated cells, we sought to examine what, if any, role they might play in the BSE. We focused on the repair proteins DNA-PKcs (DNA-dependent Protein Kinase catalytic subunit) and ATM (Ataxia Telangectasia Mutated). DNA-PK is a primary component of the Non-Homologous End-Joining (NHEJ) DSB repair pathway, consisting of the Ku 70/80 hetero-dimer and DNA-PKcs (Collis et al., 2005). DNA-PK is critical for DSB repair and for V(D)J recombination (Jackson and Jeggo, 1995). It has also been shown that DNA-PK is important for the protection of mammalian telomeres by helping to maintain effective end-capping and preventing inappropriate fusions (Bailey et al., 2004; Bailey et al., 2001; Bailey et al., 1999). Like DNA-PKcs, ATM is a member of the phosphoinositide 3-kinase-like kinase (PIKK) family. ATM plays a critical role in the early detection of IR-induced DSBs (Barzilai et al., 2002) and is responsible for phosphorylation of numerous proteins involved in cell-cycle control, apoptosis and DNA repair (Lavin and Kozlov, 2007).

Previous studies investigating how DNA repair status influences the BSE include several by Nagasawa et al., who demonstrated that cells deficient in DNA repair proteins tend to exhibit large bystander responses following alpha-particle irradiation (Nagasawa et al., 2005). These authors speculated that cells experiencing defective repair of DNA damage induced by direct irradiation,

display an increased bystander response likely due to increased production of ROS (Nagasawa and Little, 2002). These early experiments were not capable of determining whether the role of these proteins was in the generation or in the reception of the bystander signal. Later, media transfer experiments revisited the role of several DNA repair proteins in generation of the bystander signal; here it was concluded that these proteins played no role in the BSE (Mothersill et al., 2004). However, media transfer experiments inherently limit the role of short-lived ROS, which many believe to be a crucial contributor to the BSE.

In the current study, we designed cell transfer strategies to assess the role of DNA-PKcs and ATM in the generation and/or reception of the IR-induced BSE following γ-ray exposure. Cells were divided into two groups, donors (irradiated) and recipients (non-irradiated). The donor cells were either un-irradiated (control) or exposed to 1 Gy of ^{137}Cesium γ-rays (treated), rinsed and then co-cultured with the recipient cells at a dilution of either 1:100 or 1:1000. Cells were harvested after two cell cycles in the presence of bromodeoxyuridine (BrdU) in order to facilitate visualization and analyses of SCE frequencies in unirradiated recipient cells as a marker of the BSE. Utilizing both mouse and human cell lines deficient in either DNA-PKcs or ATM and normal human fibroblasts, and by altering which was the donor, we assessed how DNA-PKcs and ATM influence the generation and/or reception of bystander signals.

Results

SCE frequencies in primary normal human dermal fibroblasts (5C HDF), both with and without exposure to 1Gy of direct γ-irradiation (^{137}Cs), were determined. It has been reported previously that direct low LET IR exposure does not significantly enhance SCE frequency (Ardito et al., 1980), which we confirmed here. 5C HDF's did not display elevated SCE frequencies subsequent to direct γ-irradiation as compared to the 0 Gy controls; SCE frequencies were 3.76 SCE/ metaphase (0 Gy) and 3.4 SCE/ metaphase (1 Gy) (Figure 2A), with no statistically significant difference between sample means.

We designed a cell transfer approach that utilizes SCE frequencies as a marker of the IR-induced BSE, and importantly facilitates discrimination between generation versus receipt of bystander signals. A small number of irradiated cells (donors) were added to a non-irradiated cell population (recipients). Immediately following IR exposure (1 Gy ^{137}Cs γ-rays), human fibroblast (5C HDF) donor cells were pelleted and rinsed in PBS to remove any remaining media. Donor cells were then diluted either 1:100 or 1:1000 and added to non-irradiated recipient cells (5C HDF). The co-culture was collected following two rounds of replication in the presence of BrdU and scored for SCE (vast majority were non-irradiated recipient cells). Our results revealed a significant elevation in SCE frequency in the samples whose donor cells were irradiated compared to the control samples whose donors were not irradiated (Figure 2A). The 1:100 dilutions displayed a frequency of 3.14 SCE/ metaphase (0 Gy) and 5.28 SCE/ metaphase (1 Gy). The 1:1000 dilutions displayed a frequency of 3.68 SCE/

metaphase (0 Gy) and 5.48 SCE/ metaphase (1 Gy). Frequency histograms (Figure 2B) illustrate that this is a general increase, rather than being limited to a subset of cells. It is also interesting to note that there was a similar increase in SCE frequency for both the 1:100 and 1:1000 dilutions, which is consistent with previous reports that the BSE appears to operate by an "on/off" mechanism (Deshpande et al., 1996; Hu et al., 2006; Nagasawa and Little, 1992). Therefore, only the 1:100 dilution cell transfer method was utilized in subsequent experiments.

We confirmed that direct IR (γ-ray) exposure did not elevate SCE frequencies in our experimental system. These results imply that directly irradiated cells are refractory to the bystander signal. To test this hypothesis, we repeated the experiments outlined above, with addition of irradiated recipient cells (5C HDF) to the protocol (Figure 3). As seen previously, SCE frequencies did not increase in directly irradiated cells; 4.2 SCE/ metaphase (0 Gy) and 4.03 SCE/ metaphase (1 Gy) (Figure 3A). Also as expected, an increase in SCE frequency was observed when irradiated donor cells were added to non-irradiated recipient cells; 3.9 SCE/ metaphase (0 Gy) and 5.03 SCE/ metaphase (1 Gy) (Figure 3A.) However, there was no significant increase in SCE when irradiated donor cells were added to irradiated recipient cells; 4.08 SCE/ metaphase (0 Gy) and 3.88 SCE/ metaphase (1 Gy). This result supports the hypothesis that directly irradiated cells are refractory to the BSE, i.e., they are unable to either receive or respond to a bystander signal once they have activated the mechanism to generate bystander signals.

We recognized the unavoidable reality that some, although very few, directly irradiated cells were scored as bystander cells in our cell transfer approach. Although we repeatedly determined that SCE frequencies do not increase in directly irradiated 5C HDFs (Fig 2A and 3A), we sought to further ensure that only bystander, non-hit cells were scored for SCE. Therefore, mouse cells, whose chromosome morphology is clearly distinguishable from human, were used as the irradiated donor cells and 5C HDFs were used as the non-irradiated recipient cells. Wild-type C57BL/6 mouse donor cells were irradiated and cultured with non-irradiated 5C HDF recipient cells. A significant increase in SCE frequency was observed in the 5C HDF recipients; 3.72 SCE/ metaphase (0 Gy) and 5.33 SCE/ metaphase (1Gy) ($p < 0.05$) (Figure 4A).

To examine the role of DNA-PKcs in the generation and/or reception of bystander signals in our system, we utilized BALB/c primary mouse kidney fibroblasts, which contain a hypomorphic variant of DNA-PKcs that results in reduced expression and kinase activity (Okayasu et al., 2000). Irradiated BALB/c donor cells were added to non-irradiated 5C HDF recipient cells. No significant increase in SCE frequency was observed in the 5C HDF recipient cells; 3.70 SCE/ metaphase (0Gy) and 3.86 SCE/ metaphase (1Gy) (Figure 4A), suggesting that DNA-PKcs is required for generation of the bystander signal. While background frequencies varied slightly (common with SCE), all trends were consistent (see supplementary Table 1 for additional SCE data demonstrating consistent trends).

Next, we utilized severe combined immunodeficiency (SCID) primary mouse kidney fibroblasts. SCID mice have a truncated version of DNA-PKcs and

are essentially null for activity (Blunt et al., 1996). Again, no significant increase in SCE was seen when irradiated SCID donor cells were added to non-irradiated 5C HDF recipient cells; 4.18 SCE/ metaphase (0 Gy) and 4.36 SCE/ metaphase (1 Gy) (Figure 4A).

To further define a role for DNA-PKcs in the generation of bystander signals, additional transfer experiments were performed using a congenic mouse model recently created in our laboratory (manuscript in preparation). B6.C-*Prkdc*^{BALB} mice have a C57BL/6 wild type genetic background with the BALB/c variant allele of the *Prkdc* gene, while C.B6-*Prkdc* mice have a BALB/c genetic background with the C57BL/6 wild type *Prkdc* gene. Consistent with our C57BL/6 results, SCE frequencies were significantly increased when irradiated C.B6 donor cells (wild type *Prkdc*) were added to the 5C HDF recipient cells; 3.88 SCE/ metaphase (0Gy) and 5.19 SCE/ metaphase (1Gy) (Figure 4A). SCE frequencies were also evaluated in 5C HDF recipient cells using the B6.C strain (*Prkdc*^{BALB}) as the irradiated donor cells. Consistent with our BALB/c results, no significant increase in SCE frequency was observed; 4.29 SCE/ metaphase (0 Gy) and 4.13 SCE/ metaphase (1 Gy). Our results utilizing these unique congenic mouse strains add additional mechanistic support for DNA-PKcs being involved in generation of bystander signals.

Reverse experiments were also preformed in which irradiated or non-irradiated 5C HDF's were added to non-irradiated mouse cells. Both the recipient C57BL/6 and BALB/c mouse cells displayed significant increases in SCE frequencies after the addition of irradiated human donor cells (5C HDF). The

C57BL/6 mouse cells displayed a SCE frequency of 0.106 SCE/chromosome (0 Gy) and 0.148 SCE/ chromosome (1 Gy) (Figure 4B). The BALB/c mouse cells displayed frequencies of 0.108 SCE/chromosome (0 Gy) and 0.154 SCE/chromosome (1 Gy) (Figure 4B). Note that SCE frequencies for mouse cells were calculated on a per chromosome basis as they do not have stable karyotypes (aneuploid). The somewhat lower number of mouse metaphases analyzed for SCE reflects the difficulty these cells seemed to experience in co-culture with human cells. However, results are statistically significant and represent a significant number of chromosomes scored. Others have also reported similar results in that DNA-PK is not necessary for the reception of the bystander signal (Kanasugi et al., 2007; Mothersill et al., 2004). Taken together, our results demonstrate that while DNA-PKcs is needed for the generation of bystander signals, it is not necessary for the receipt of such signals.

Our focus then turned to ATM, another DNA repair and signaling protein in the same PI3K family as DNA-PKcs. A human dermal fibroblast line (AG04450) derived from an Ataxia Telangectasia patient was used to determine if ATM also plays a role in the bystander response. Similar to other 5C HDF controls, the 5C HDF cells did not show an increase in SCE frequency when directly exposed to γ-radiation; 4.2 SCE/ metaphase (0 Gy) and 4.03 SCE/ metaphase (1 Gy) (Figure 5A). There was also no significant increase in SCE frequency when ATM-/- donor cells were irradiated and added to the non-irradiated 5C HDF recipient cells; 4.76 SCE/ metaphase (0 Gy) and 4.24 SCE/ metaphase (1 Gy) (Figure 5A). The reverse experiment, adding irradiated 5C

HDF donor cells to ATM-/- non-irradiated recipient cells, revealed a highly significant increase in SCE frequencies; 3.9 SCE/ metaphase (0 Gy) and 5.92 SCE/ metaphase (1 Gy) (Figure 5B). Like the 5C HDF, directly irradiated ATM-/- human fibroblasts did not show a change in SCE frequency; 4.34 SCE/ metaphase (0 Gy) and 4.22 SCE/ metaphase (1 Gy) (Figure 5B). These data suggest that ATM, like DNA-PKcs, is necessary for generation of the bystander signal, but is not required for receiving such signals. Note all numbers are organized in Tables 1 (Figures 2 and 3) and 2 (Figures 4 and 5) demonstrating averages and statistical significance.

Discussion

DNA-PKcs and ATM are members of the PI3K family and each participates in multiple cellular processes. DNA-PKcs, the catalytic subunit of DNA-PK, orchestrates NHEJ in response to DSBs. It is also critical in V(D)J recombination, and is essential for effective mammalian telomeric end-capping function (Bailey et al., 1999; Dudley et al., 2005; Lieber, 1999; Meek et al., 2004; Weinstock and Jasin, 2006; Zhang et al., 2007). Activation of ATM is an early event in response to IR-induced DSBs, and once activated ATM mediates downstream damage response pathways that include DNA repair, cell-cycle control, and apoptosis (Lavin and Kozlov, 2007). ATM is reported to play a role in telomere maintenance as well (Denchi and de Lange, 2007; Pandita, 2002). In addition to DNA-PKcs and ATM's well-established roles in repair and intra-cellular signaling, (Collis et al., 2005; Lavin and Kozlov, 2007; Nagasawa et al., 2003; Nagasawa et al., 2005), our findings indicate a role for these proteins in inter-cellular signaling of the radiation-induced BSE.

We designed a cell transfer strategy that enables us to differentiate between the generation versus the reception of bystander signals. In our system, donor cells are irradiated (1 Gy γ-rays) and seeded at a very low concentration (1:100 or 1:1000) onto non-irradiated normal human fibroblast recipient cells. Using a low concentration of donor cells and ensuring that recipient cells were at low confluency, we reduced and/or eliminated any possibility of a bystander response transmitted via gap junctions. We then measured SCE frequencies in the normal human fibroblast recipient cells as an indicator of IR-induced BSE.

To validate our approach, we tested normal human fibroblasts (5C HDF) as both the donor and recipient cells to be assured that they were able to both generate and receive a bystander signal. Cultures were at low-passage (non-transformed) to circumvent any problem of decreased BSE with increasing passage. When directly irradiated, 5C HDFs do not display an increase in SCE frequency, in agreement with previous reports showing that direct low-LET IR does not influence SCE levels (Ardito et al., 1980). Our cell transfer strategy also demonstrated that 5C HDFs can generate a bystander signal, inducing significant increases in SCE frequencies in recipient cells. The observation that the irradiated donor cells at both dilutions were able to increase SCE levels in the non-irradiated recipient cells by approximately the same amount is consistent with previous data suggesting that the BSE operates through an "on/off" switch-like mechanism (Deshpande et al., 1996).

The data demonstrating that directly irradiated cells do not display elevated SCE frequencies suggest that directly irradiated cells are themselves refractory to bystander signals. To test this, we used our cell transfer assay to again show that directly irradiated cells do not show elevated levels of SCE (Figure 3A). Also in agreement with our other results, we show that by seeding irradiated donor cells with non-irradiated recipient cells, an elevation in SCE frequency in the non-irradiated recipient cells occurs (Figure 3A). However, when the reverse is done and *recipient* cells are irradiated (1 Gy γ-rays) before irradiated donor cells are added, there is no elevation in SCE frequency observed in the recipient population. This supports the hypothesis that once irradiated,

"hit" cells become refractory to either *receiving* or responding to a bystander signal.

We sought to determine whether the repair protein DNA-PKcs plays a role in the BSE. The BALB/c mouse strain contains two single nucleotide polymorphisms in the *Prkdc* gene, which produces a hypomorphic version of DNA-PKcs (Yu et al., 2001). We compared the wild type C57BL/6 mouse strain to the BALB/c strain for the ability to generate and/or receive bystander signals. Our results show that wild type C57BL/6 mouse cells are able to generate a bystander signal in response to IR. The irradiated C57BL/6 donor cells increased SCE frequency in the 5C HDF recipient cells by over 40% compared to the 0 Gy controls when seeded at a 1:100 dilution (Figure 4A). Similar results were observed when the C57BL/6 donor cells were seeded at 1:1000 (supplementary data). However, irradiated BALB/c donor cells were not able to influence SCE frequencies in the 5C HDF recipient cells, demonstrating that DNA-PKcs-deficient BALB/c mouse cells are unable to generate a bystander signal following γ-ray exposure. The reverse experiments revealed that DNA-PKcs is not necessary for receipt of and response to bystander signals (Figure 4B). We conclude that DNA-PKcs is necessary for the generation, but not the reception, of bystander signals.

To confirm that DNA-PKcs deficiency, rather than a coincidental mutation in BALB/c mice, is responsible for abolishing the bystander response, we utilized congenic mouse strains generated in our laboratory. The B6.C-*Prkdc*^{BALB} strain has a C57BL/6 background with the BALB/c variant of the *Prkdc* gene, while the

C.B6-*Prkdc* has the BALB/c background with the C57BL/6 *Prkdc* gene. Interestingly, the C.B6-*Prkdc* showed a significant increase in SCE frequency, thus was able to generate a bystander response; however, the B6.C-$Prkdc^{BALB}$ was not able to significantly influence SCE levels. These results provide additional support for DNA-PKcs playing a critical role in generation of a bystander response.

Next we examined the role of the closely related protein ATM, in generating and/or receiving bystander signals. Again, we found no significant increase in SCE frequencies following direct irradiation of human ATM-/- cells. By irradiating ATM-/- cells (donors) and using our cell transfer approach, we found no significant increase in SCE frequencies in the 5C HDF recipient cells. However, when the reverse cell transfer was performed, the irradiated 5C HDF donor cells were in fact able to generate a response in the ATM-/- cells, implying that ATM -/- recipient cells can receive and respond to a bystander signal, but they cannot generate one. Therefore, like DNA-PKcs, ATM is necessary for the generation, but not the reception of bystander signals.

The role of DNA repair proteins in the generation of bystander signals may involve DNA-PKcs and ATM's capabilities as DNA damage sensors in signaling pathways. Such a damage response may initiate as yet undefined pathways that ultimately lead to the generation of a BSE in non-irradiated cells, and hints at a tissue-level response to radiation injury moderated by some of the same proteins that orchestrate the inter-cellular response to DNA damage. While an intra-cellular IR-induced signaling response has been demonstrated (Wu et al.,

1999), it has also been shown that ATM and DNA-PKcs signaling activates NF-kB via the p53-independent MEK/ERK/p90rsk/IKK signaling pathway in an anti-apoptotic response to DNA damage (Panta et al., 2004). In addition, DNA-PKcs is required for the activation of the stress kinases SAPK/JNK (Fritz and Kaina, 2006). It has also been shown that DNA-PKcs activation can be induced by exposure to nitric oxide (Xu et al., 2000), which has been suggested as a possible bystander signal. Taken together, these data support the idea that ATM and DNA-PKcs may regulate, or be regulated by, other kinds of signaling events, such as the BSE (Figure 6). This model suggests that the BSE is an active process in response to IR exposure, rather than a passive response to DNA damage.

While this model is currently speculative, our data do suggest previously unrecognized roles for the repair proteins DNA-PKcs and ATM in generation, but not receipt, of bystander signals. It should be noted that a previous study concluded that DNA repair proteins were not involved in generation of the bystander signal (Mothersill et al., 2004). Our conflicting results may reflect differences in experimental design including: cells used (primary fibroblasts versus various cell lines), endpoints examined (SCE versus clonogenic survival), and methods used (cell transfer versus media transfer). For example, the media transfer experiments limit the role of short-lived ROS, whereas in our cell transfer approach, the likelihood for continued ROS generation and interaction remains.

A better understanding of the underlying pathways involved in bystander signal generation and reception is an essential step to better understanding of the BSE. Moreover, because predominately low biologically/environmentally

relevant doses of radiation elicit a bystander response (Morgan, 2003; Nagasawa and Little, 1992; Seymour and Mothersill, 2000), increased knowledge about this phenomena holds important implications for individual radiosensitivity and susceptibility to radiation carcinogenesis caused by inadequate DNA repair capacity, a condition relevant to human populations and health.

Some degree of exposure to radiation above the natural background level is an unavoidable consequence of living in the modern world. A better understanding of the radiation-induced BSE and its influence on radiation carcinogenesis will aid regulators as they seek to protect human health while avoiding undue economic hardship.

Materials and Methods

Cell Lines and Cell Culture. Kidney tissue from 8–12 week old female C57 BL/6, BALB/c, SCID, or congenic mice were minced, and digested in 199 medium containing collagenase (Worthington Type III; 200 units/ml) at 37°C for 3–5 h with gentle agitation. Disaggregated cells were washed 6x in phosphate buffered saline (PBS) containing 0.5% fetal bovine serum (FBS) and cultured in α-MEM medium (15% FBS, penicillin/streptomycin). Media was changed after 3 days of incubation. Low passage neonatal Human Dermal Fibroblasts (HDF C-004-5C; Cascade Biologics) were grown in α-MEM supplemented with 10% fetal bovine serum and antibiotics. Cells were counted using a Coulter Counter (Coulter Beckman, Fullerton, CA) and 4 X 10^5 human fibroblasts were plated into T-75 flasks, then co-cultured with 1:100 dilutions of either 0 Gy or 1 Gy γ-irradiated, exponentially growing donor cells. Donor cells were not allowed to near confluency and included human ATM-/- (AG04450), DNA-PKcs deficient (BALB/c mouse), wild-type DNA-PKcs (C57BL/6 mouse), or congenic DNA-PKcs (manuscript in preparation). Irradiations were performed using a sealed-source Mark I ^{137}Cs γ-irradiator (J.L. Shepherd and Associates). 5'-bromo-2'-deoxyuridine (BrdU; Sigma) was added to cultures at a final concentration of 2 X 10^{-5}M and cells were allowed to grow for two rounds of cell division. Colcemid (Invitrogen) was added at a final concentration of 0.2 μg/ml and cells were harvested approximately 2-3 hours later. Cells were trypsinized, centrifuged, then resuspended in 0.075M KCl for 15 minutes at room temperature and then fixed with 3:1 methanol: acetic acid.

C.B6-*Prkdc*$_a$ and B6.C-*Prkdc*^{BALB} congenic mouse strains. Two strains congenic for the common allele (C57BL/6) and BALB/c variant allele of *Prkdc* were generated (manuscript in preparation) using the parental strains C57BL/6J (B6) and BALB/cByJ (C) (both obtained from Jackson Laboratory). For the congenic strain C.B6-*Prkdc*$_a$, B6CByF1 females were mated with C.B6 males to produce the N2 generation. Subsequent generations N2 – N10 were repeatedly backcrossed to BALB/cByJ mice. For congenic strain B6.C-*Prkdc*^{BALB}, CByB6F1 females were mated with B6 males to produce the N2 generation. Subsequent generations N2 – N10 were repeatedly backcrossed to C57BL/6J mice. In both congenic strains, progeny were selected for backcross mating if they carried donor *Prkdc* sequence as determined by PCR/RFPL (Yu et al., 2001). Additionally, a marker-directed breeding strategy (speed congenics) was adopted at backcross generations N8 – N12 which selected against progeny carrying background donor genome (Weil et al., 1997). Microsatellite markers polymorphic between B6.C and C.B6 were used to select backcross progeny whose genome contained the least donor sequence at loci other than *Prkdc*. Mice at backcross N10 or later were intercrossed and progeny homozygous for the donor *Prkdc* allele were selected for inbreeding. Mouse colonies were maintained at the Colorado State University Painter Center.

SCE Staining and Analysis. Slides of metaphase chromosomes were prepared using standard cytogenetic techniques, then stained using the Fluorescence Plus Giemsa technique (Wolff and Perry, 1975) in order to obtain harlequin staining

and to visualize SCE. Briefly, slides were stained with Hoescht 33258 (Thermo Sci Acros Organics) for 15 minutes at room temperature, rinsed with distilled water and exposed to UV light (365nm; Stratalinker) for 25 minutes. Slides are then soaked in 2x SSC at 60°C for 30 minutes. Following thorough rinses with distilled water, slides are allowed to air dry, and then stained with 2% Giemsa for 10 minutes. Images were analyzed and captured using a Zeiss Axioskop2 Plus microscope equipped with a Photometrics Coolsnap ES2 camera and Metavue 7.1 software.

Statistical Analysis. Slides were blinded and scored by independent investigators for SCE. Standard deviations were calculated and used to determine the standard error of the mean (SEM) to generate error bars. A student's T-test was calculated to determine statistical significance. All conditions were repeated at least twice, and each experiment was scored by at least two individuals. If results were not significantly different, data was pooled. Results from additional experiments are provided as supplemental data (table).

Acknowledgements. The authors would like to thank Dakim Gaines for technical assistance. Support for this research is gratefully acknowledged from the NIH/NCI, grants CA-09236-30 (RLU) and CA-043322-20 (RLU and SMB), the U.S. Department of Energy (DOE), grant DE-FG02-01ER63239 (RLU and SMB), and from the National Aeronautics and Space Administration (NASA), grant NNJ04HD83G (SMB).

References

Ardito, G., Lamberti, L., Piccotti, F. and Poggio, G. (1980) Analysis of chromosome aberrations after exposure to ionizing radiation in "in vitro" cultures of human lymphocytes by means of BrdU incorporation. *Boll Soc Ital Biol Sper*, 56, 719-724.

Azzam, E.I., de Toledo, S.M., Gooding, T. and Little, J.B. (1998) Intercellular communication is involved in the bystander regulation of gene expression in human cells exposed to very low fluences of alpha particles. *Radiat Res*, 150, 497-504.

Azzam, E.I., de Toledo, S.M. and Little, J.B. (2001) Direct evidence for the participation of gap junction-mediated intercellular communication in the transmission of damage signals from alpha -particle irradiated to nonirradiated cells. *Proc Natl Acad Sci U S A*, 98, 473-478.

Bailey, S.M., Brenneman, M.A., Halbrook, J., Nickoloff, J.A., Ullrich, R.L. and Goodwin, E.H. (2004) The kinase activity of DNA-PK is required to protect mammalian telomeres. *DNA Repair (Amst)*, 3, 225-233.

Bailey, S.M., Cornforth, M.N., Kurimasa, A., Chen, D.J. and Goodwin, E.H. (2001) Strand-specific postreplicative processing of mammalian telomeres. *Science*, 293, 2462-2465.

Bailey, S.M., Meyne, J., Chen, D.J., Kurimasa, A., Li, G.C., Lehnert, B.E. and Goodwin, E.H. (1999) DNA double-strand break repair proteins are required to cap the ends of mammalian chromosomes. *Proc Natl Acad Sci U S A*, 96, 14899-14904.

Banaz-Yasar, F., Lennartz, K., Winterhager, E. and Gellhaus, A. (2007) Radiation-induced bystander effects in malignant trophoblast cells are independent from gap junctional communication. *J Cell Biochem.*

Barzilai, A., Rotman, G. and Shiloh, Y. (2002) ATM deficiency and oxidative stress: a new dimension of defective response to DNA damage. *DNA Repair (Amst)*, 1, 3-25.

Blunt, T., Gell, D., Fox, M., Taccioli, G.E., Lehmann, A.R., Jackson, S.P. and Jeggo, P.A. (1996) Identification of a nonsense mutation in the carboxyl-terminal region of DNA-dependent protein kinase catalytic subunit in the scid mouse. *Proc Natl Acad Sci U S A*, 93, 10285-10290.

Collis, S.J., DeWeese, T.L., Jeggo, P.A. and Parker, A.R. (2005) The life and death of DNA-PK. *Oncogene*, 24, 949-961.

Denchi, E.L. and de Lange, T. (2007) Protection of telomeres through independent control of ATM and ATR by TRF2 and POT1. *Nature.*

Deshpande, A., Goodwin, E.H., Bailey, S.M., Marrone, B.L. and Lehnert, B.E. (1996) Alpha-particle-induced sister chromatid exchange in normal human lung fibroblasts: evidence for an extranuclear target. *Radiat Res*, 145, 260-267.

Dudley, D.D., Chaudhuri, J., Bassing, C.H. and Alt, F.W. (2005) Mechanism and control of V(D)J recombination versus class switch recombination: similarities and differences. *Adv Immunol*, 86, 43-112.

Fritz, G. and Kaina, B. (2006) Late activation of stress kinases (SAPK/JNK) by genotoxins requires the DNA repair proteins DNA-PKcs and CSB. *Mol Biol Cell*, 17, 851-861.

Grifalconi, M., Celotti, L. and Mognato, M. (2007) Bystander response in human lymphoblastoid TK6 cells. *Mutat Res*, 625, 102-111.

Hu, B., Wu, L., Han, W., Zhang, L., Chen, S., Xu, et al. (2006) The time and spatial effects of bystander response in mammalian cells induced by low dose radiation. *Carcinogenesis*, 27, 245-251.

Iyer, R. and Lehnert, B.E. (2002) Alpha-particle-induced increases in the radioresistance of normal human bystander cells. *Radiat Res*, 157, 3-7.

Jackson, S.P. and Jeggo, P.A. (1995) DNA double-strand break repair and V(D)J recombination: involvement of DNA-PK. *Trends Biochem Sci*, 20, 412-415.

Kanasugi, Y., Hamada, N., Wada, S., Funayama, T., Sakashita, T., Kakizaki, T., Kobayashi, Y. and Takakura, K. (2007) Role of DNA-PKcs in the bystander effect after low- or high-LET irradiation. *Int J Radiat Biol*, 83, 73-80.

Kashino, G., Prise, K.M., Suzuki, K., Matsuda, N., Kodama, S., Suzuki, et al. (2007) Effective suppression of bystander effects by DMSO treatment of irradiated CHO cells. *J Radiat Res (Tokyo)*, 48, 327-333.

Lavin, M.F. and Kozlov, S. (2007) ATM activation and DNA damage response. *Cell Cycle*, 6, 931-942.

Lehnert, B.E., Goodwin, E.H. and Deshpande, A. (1997) Extracellular factor(s) following exposure to alpha particles can cause sister chromatid exchanges in normal human cells. *Cancer Res*, 57, 2164-2171.

Lieber, M.R. (1999) The biochemistry and biological significance of nonhomologous DNA end joining: an essential repair process in multicellular eukaryotes. *Genes Cells*, 4, 77-85.

Meek, K., Gupta, S., Ramsden, D.A. and Lees-Miller, S.P. (2004) The DNA-dependent protein kinase: the director at the end. *Immunol Rev*, 200, 132-141.

Morgan, W.F. (2003) Is there a common mechanism underlying genomic instability, bystander effects and other nontargeted effects of exposure to ionizing radiation? *Oncogene*, 22, 7094-7099.

Mothersill, C. and Seymour, C.B. (1998) Cell-cell contact during gamma irradiation is not required to induce a bystander effect in normal human keratinocytes: evidence for release during irradiation of a signal controlling survival into the medium. *Radiat Res*, 149, 256-262.

Mothersill, C., Seymour, R.J. and Seymour, C.B. (2004) Bystander effects in repair-deficient cell lines. *Radiat Res*, 161, 256-263.

Nagasawa, H., Huo, L. and Little, J.B. (2003) Increased bystander mutagenic effect in DNA double-strand break repair-deficient mammalian cells. *Int J Radiat Biol*, 79, 35-41.

Nagasawa, H. and Little, J.B. (1992) Induction of sister chromatid exchanges by extremely low doses of alpha-particles. *Cancer Res*, 52, 6394-6396.

Nagasawa, H. and Little, J.B. (2002) Bystander effect for chromosomal aberrations induced in wild-type and repair deficient CHO cells by low fluences of alpha particles. *Mutat Res*, 508, 121-129.

Nagasawa, H., Peng, Y., Wilson, P.F., Lio, Y.C., Chen, D.J., Bedford, J.S., et al. (2005) Role of homologous recombination in the alpha-particle-induced bystander effect for sister chromatid exchanges and chromosomal aberrations. *Radiat Res*, 164, 141-147.

O'Neill-Mehlenbacher, A., Kilemade, M., Elliott, A., Mothersill, C. and Seymour, C. (2007) Comparison of direct and bystander effects induced by ionizing radiation in eight fish cell lines. *Int J Radiat Biol*, 83, 593-602.

Okayasu, R., Suetomi, K., Yu, Y., Silver, A., Bedford, J.S., Cox, R. , et al. (2000) A deficiency in DNA repair and DNA-PKcs expression in the radiosensitive BALB/c mouse. *Cancer Res*, 60, 4342-4345.

Pandita, T.K. (2002) ATM function and telomere stability. *Oncogene*, 21, 611-618.

Panta, G.R., Kaur, S., Cavin, L.G., Cortes, M.L., Mercurio, F., Lothstein, L., et al. (2004) ATM and the catalytic subunit of DNA-dependent protein kinase activate NF-kappaB through a common MEK/extracellular signal-regulated kinase/p90(rsk) signaling pathway in response to distinct forms of DNA damage. *Mol Cell Biol*, 24, 1823-1835.

Seymour, C.B. and Mothersill, C. (2000) Relative contribution of bystander and targeted cell killing to the low-dose region of the radiation dose-response curve. *Radiat Res*, 153, 508-511.

Shao, C., Lyng, F.M., Folkard, M. and Prise, K.M. (2006) Calcium fluxes modulate the radiation-induced bystander responses in targeted glioma and fibroblast cells. *Radiat Res*, 166, 479-487.

Weil, M.M., Brown, B.W. and Serachitopol, D.M. (1997) Genotype selection to rapidly breed congenic strains. *Genetics*, 146, 1061-1069.

Weinstock, D.M. and Jasin, M. (2006) Alternative pathways for the repair of RAG-induced DNA breaks. *Mol Cell Biol*, 26, 131-139.

Wolff, S.H. and Perry, P. (1975) Insights on chromosome structure from sister chromatid exchange ratios and the lack of both isolabelling and heterolabelling as determined by the FPG technique. *Exp Cell Res*, 93, 23-30.

Wu, L.J., Randers-Pehrson, G., Xu, A., Waldren, C.A., Geard, C.R., Yu, Z., et al. (1999) Targeted cytoplasmic irradiation with alpha particles induces mutations in mammalian cells. *Proc Natl Acad Sci U S A*, 96, 4959-4964.

Xu, W., Liu, L., Smith, G.C. and Charles, G. (2000) Nitric oxide upregulates expression of DNA-PKcs to protect cells from DNA-damaging anti-tumour agents. *Nat Cell Biol*, 2, 339-345.

Yang, H., Anzenberg, V. and Held, K.D. (2007) The time dependence of bystander responses induced by iron-ion radiation in normal human skin fibroblasts. *Radiat Res*, 168, 292-298.

Yu, Y., Okayasu, R., Weil, M.M., Silver, A., McCarthy, M., Zabriskie, R., et al. (2001) Elevated breast cancer risk in irradiated BALB/c mice associates with unique functional polymorphism of the Prkdc (DNA-dependent protein kinase catalytic subunit) gene. *Cancer Res*, 61, 1820-1824.

Zhang, Y., Zhou, J., Cao, X., Zhang, Q., Lim, C.U., Ullrich, R.L., et al. (2007) Partial deficiency of DNA-PKcs increases ionizing radiation-induced mutagenesis and telomere instability in human cells. *Cancer Lett*, 250, 63-73.

FIGURES

Figure 1:

Figure 2:

A.

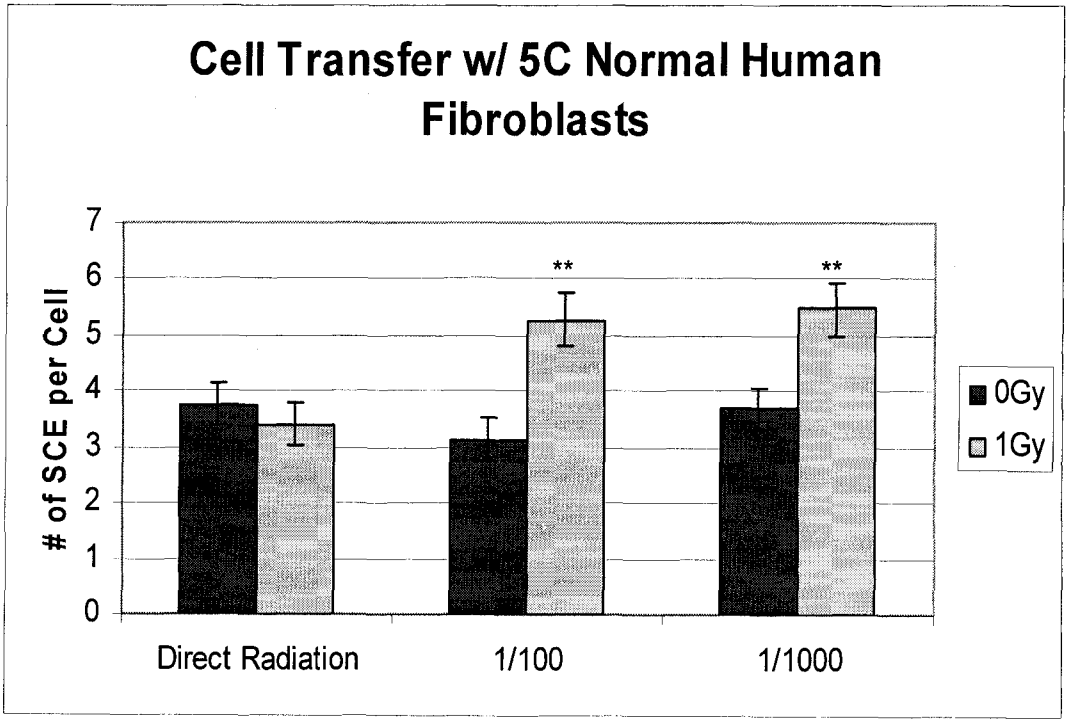
Cell Transfer w/ 5C Normal Human Fibroblasts
# of SCE per Cell
0
1
2
3
4
5
6
7
**
**
Direct Radiation
1/100
1/1000
0Gy
1Gy

B.

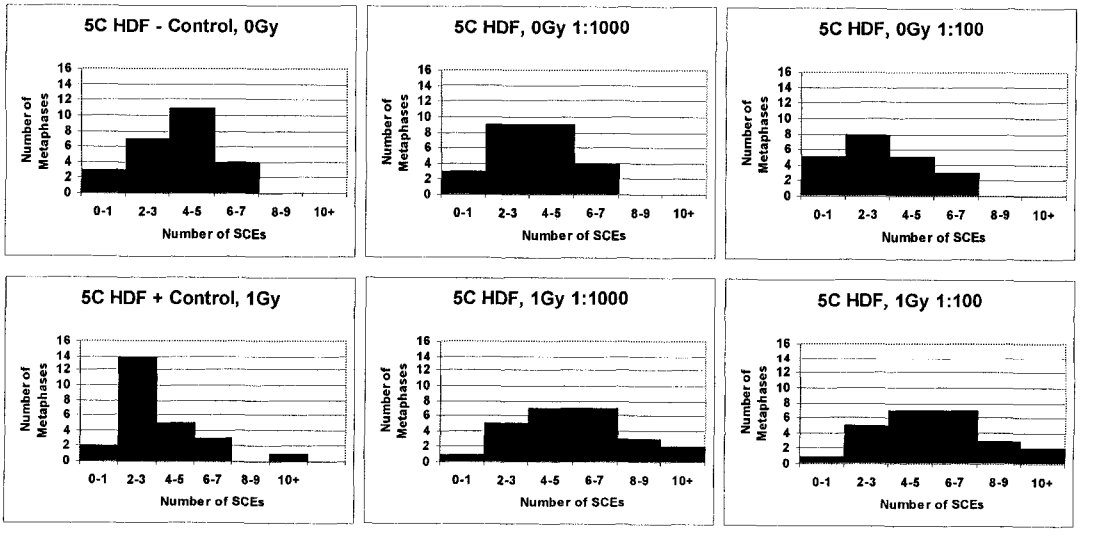
5C HDF - Control, 0Gy
5C HDF, 0Gy 1:1000
5C HDF, 0Gy 1:100
5C HDF + Control, 1Gy
5C HDF, 1Gy 1:1000
5C HDF, 1Gy 1:100
Number of Metaphases
Number of SCEs
0-1
2-3
4-5
6-7
8-9
10+

Figure 3:

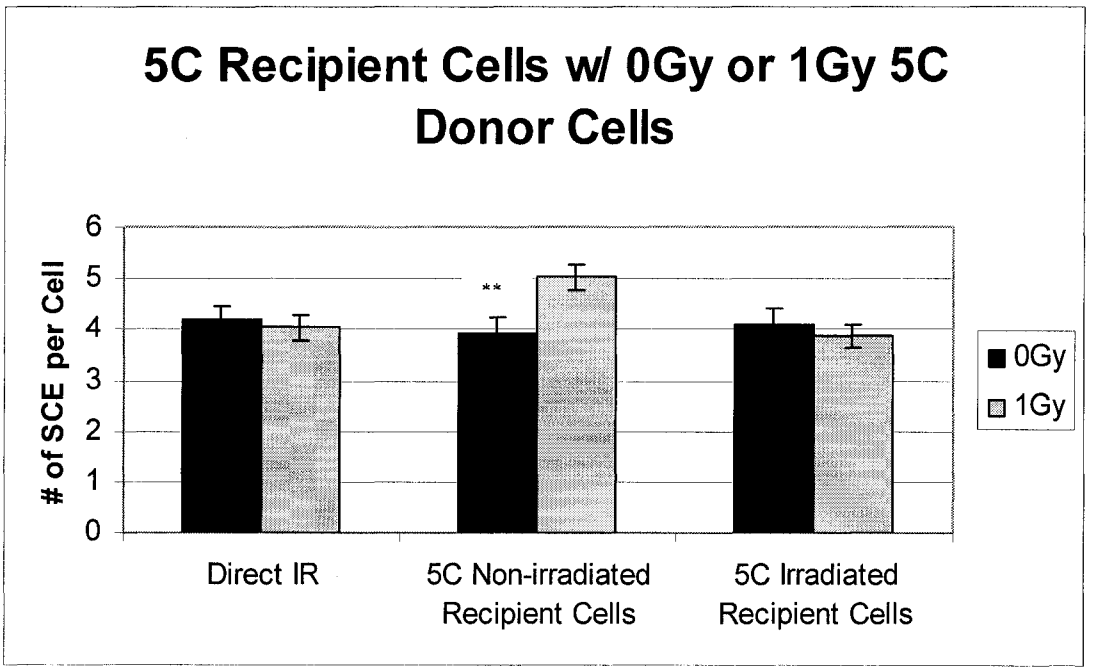
5C Recipient Cells w/ 0Gy or 1Gy 5C Donor Cells
# of SCE per Cell
6
5
4
3
2
1
0
**
Direct IR
5C Non-irradiated Recipient Cells
5C Irradiated Recipient Cells
0Gy
1Gy

Figure 4:

A.

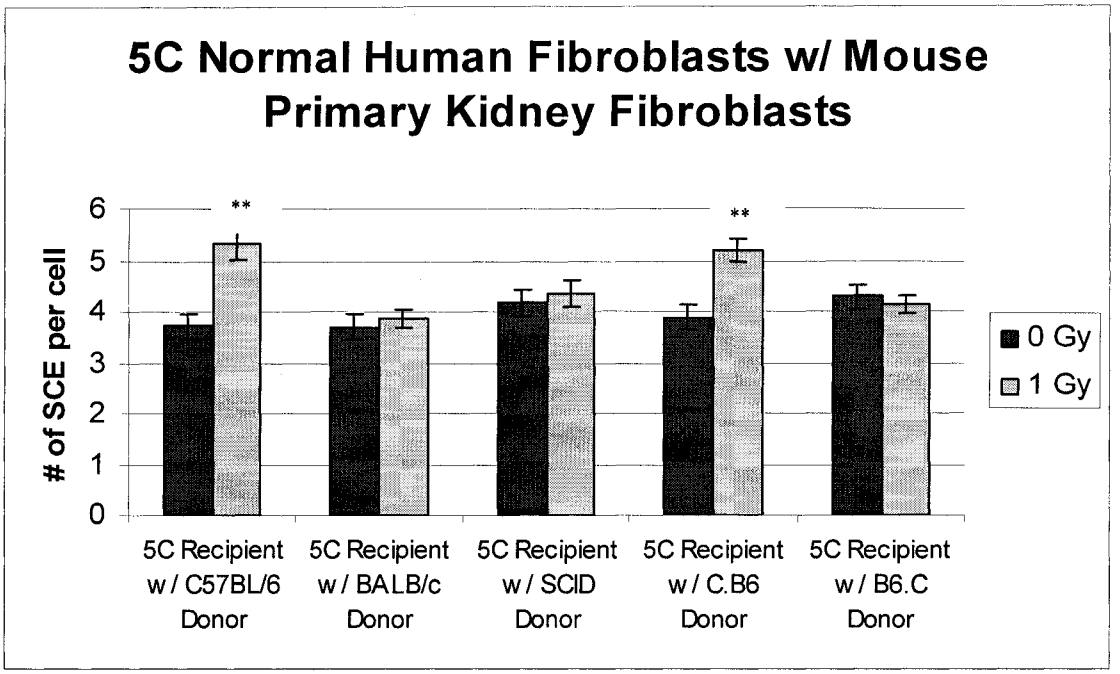
5C Normal Human Fibroblasts w/ Mouse Primary Kidney Fibroblasts
# of SCE per cell
6
5
4
3
2
1
0
**
**
0 Gy
1 Gy
5C Recipient w / C57BL/6 Donor
5C Recipient w / BALB/c Donor
5C Recipient w / SCID Donor
5C Recipient w / C.B6 Donor
5C Recipient w / B6.C Donor

B.

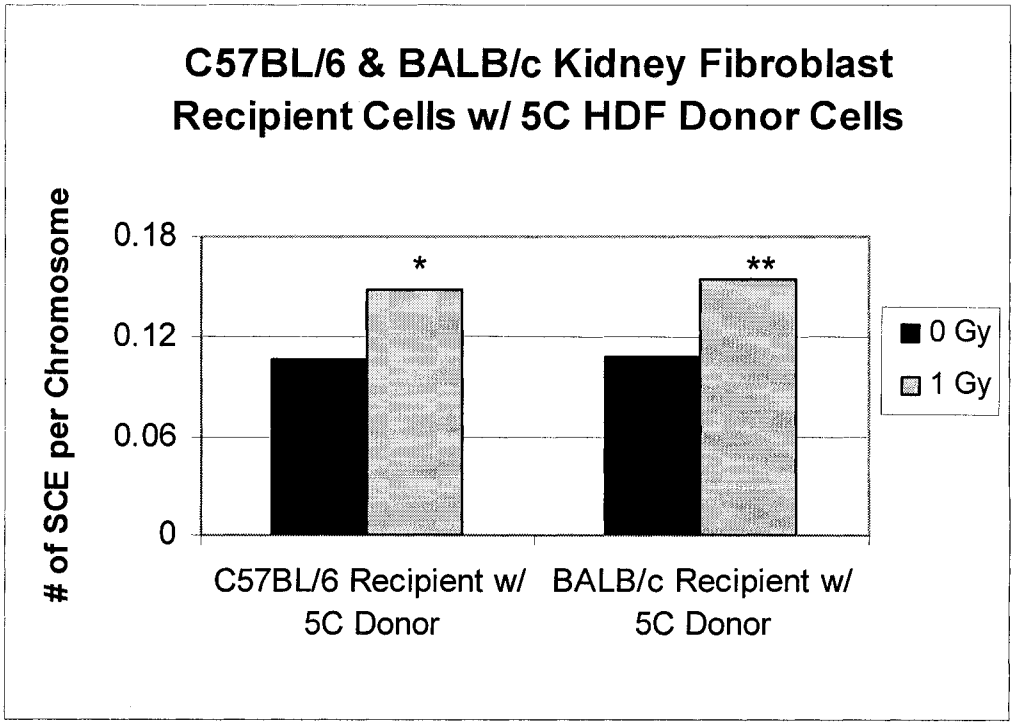
C57BL/6 & BALB/c Kidney Fibroblast Recipient Cells w/ 5C HDF Donor Cells
# of SCE per Chromosome
0.18
0.12
0.06
0
*
**
0 Gy
1 Gy
C57BL/6 Recipient w/ 5C Donor
BALB/c Recipient w/ 5C Donor

Figure 5:

A.

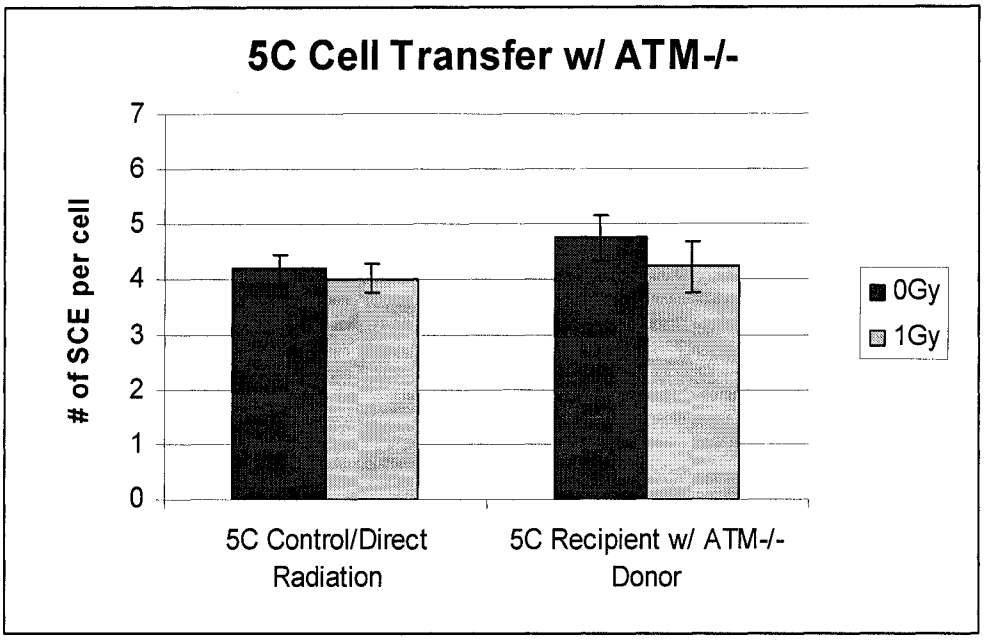
5C Cell Transfer w/ ATM-/-
# of SCE per cell
7
6
5
4
3
2
1
0
5C Control/Direct Radiation
5C Recipient w/ ATM-/- Donor
0Gy
1Gy

B.

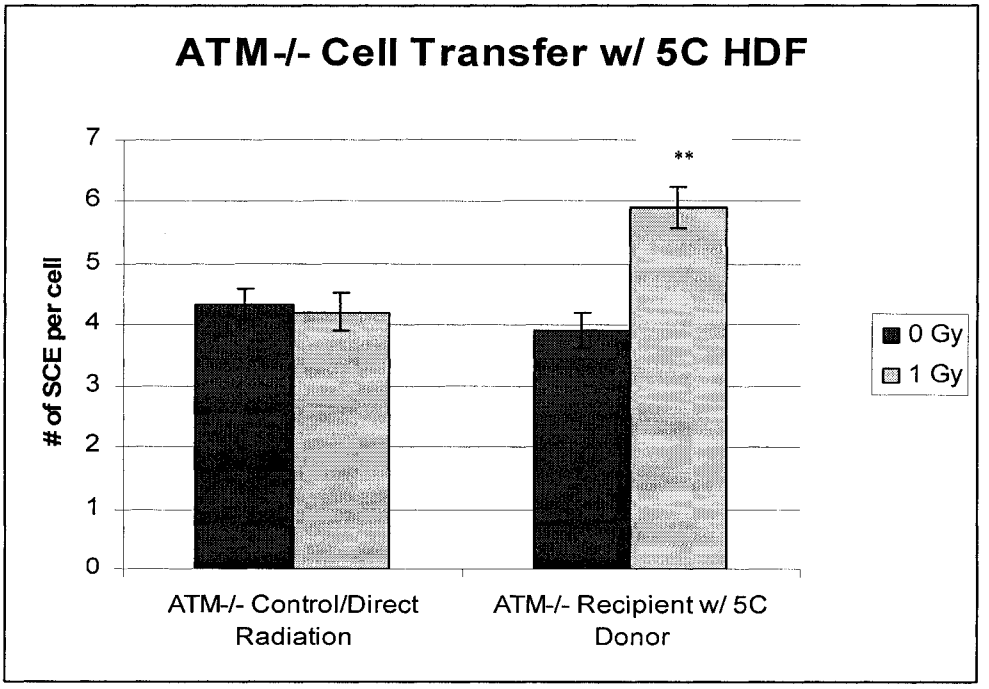
ATM-/- Cell Transfer w/ 5C HDF
# of SCE per cell
7
6
5
4
3
2
1
0
**
ATM-/- Control/Direct Radiation
ATM-/- Recipient w/ 5C Donor
0 Gy
1 Gy

Figure 6:

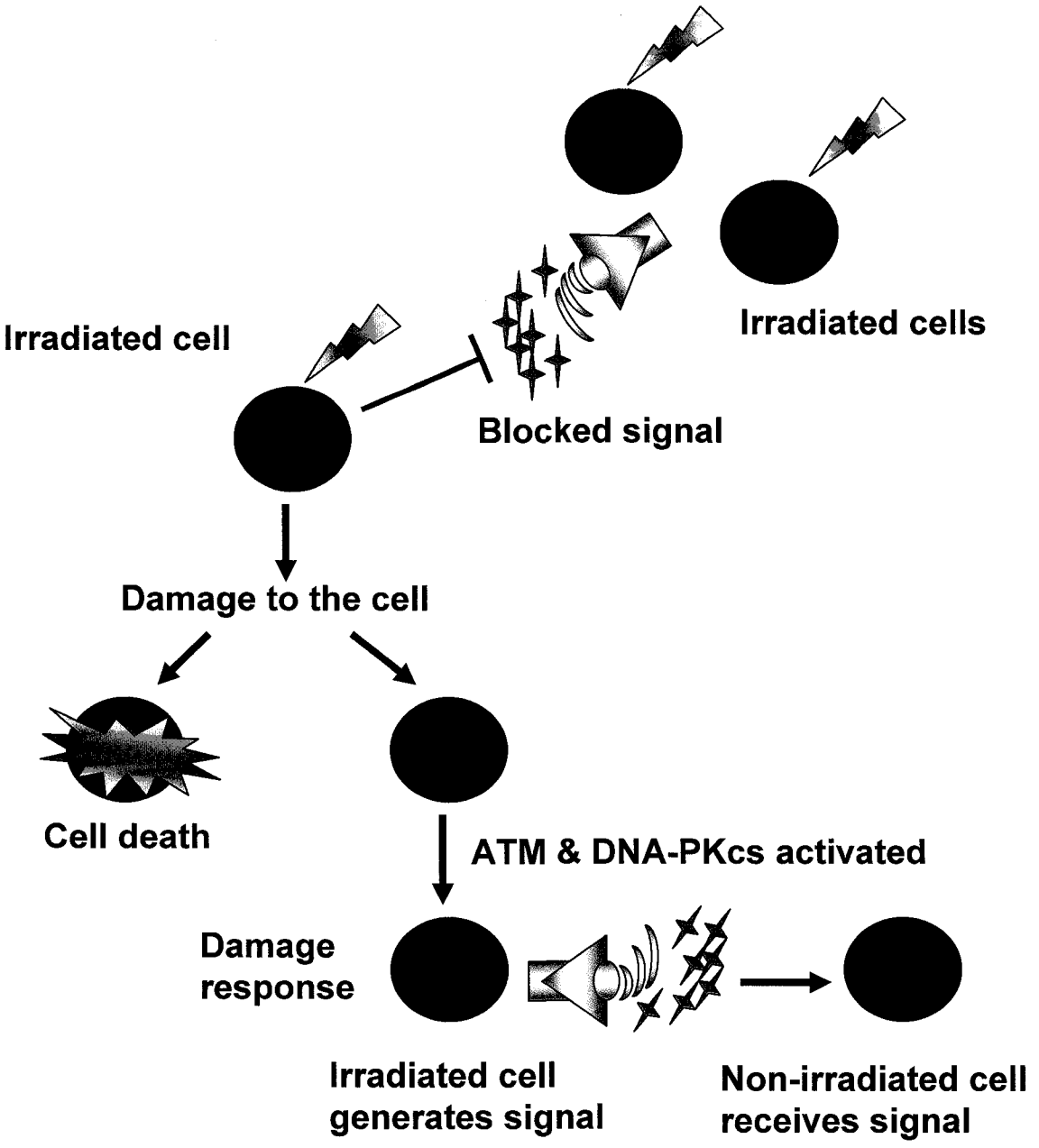
Irradiated cell
Irradiated cells
Blocked signal
Damage to the cell
Cell death
ATM & DNA-PKcs activated
Damage response
Irradiated cell generates signal
Non-irradiated cell receives signal

Table 1:

Summary Table for Figures 2 & 3

Cell Sample	Mean Frequency/Cell		p-value		Cells Scored	
	0Gy	1Gy			0Gy	1Gy
Figure 2:						
5C HDF						
Control	3.76	3.4	.532	NS	25	25
1:100	3.14	5.28	.0054	**	21	25
1:1000	3.68	5.48	.0018	**	25	25
Figure 3:						
5C HDF						
Control	4.2	4.03	.641	NS	40	40
0Gy Recipients (1:100)	3.9	5.03	.009	*	40	40
1Gy Recipients (1:100)	4.08	3.88	.614	NS	25	50

NS: Not significant
*: >95% confidence level
**: >99% confidence level

Table 2:

Summary Table for Figures 4 & 5

Cell Sample	Mean Frequency/Cell		p-value		Cells Scored	
	0Gy	1Gy			0Gy	1Gy
Figure 4:						
5C HDF with C57BL/6 MPF	3.72	5.33	.0001	**	50	30
5C HDF with BALB/c MPF	3.7	3.86	.6085	NS	70	78
5C HDF with SCID MPF	4.18	4.36	.6325	NS	50	50
5C HDF with C.B6 MPF	3.88	5.19	.0002	*	50	67
5C HDF with B6.C MPF	4.29	4.13	.5904	NS	65	76
C57BL/6 with 5C[a]	0.106	0.148	< 0.05	*	20	10
BALB/c with 5C[a]	0.108	0.154	< 0.005	**	30	20
Figure 5:						
ATM-/- HDF Control	4.34	4.22	.7568	NS	50	50
5C HDF with AT	4.76	4.24	.412	NS	50	50
AT-/-HDF with 5C HDF	3.9	5.92	.0018	**	25	25

NS: Not significant
*: >95% confidence level
**: >99% confidence level
[a]: SCE/chromosome

Figure Legends

Figure 1. Sister Chromatid Exchange (SCE). Partial human fibroblast (5C HDF) metaphase chromosome spread illustrating FPG harlequin staining (100x). A "color switch" (arrows) indicates an SCE has occurred.

Figure 2A. Direct Irradiation versus BSE. Following γ-ray direct irradiation (no cell transfer), human fibroblasts (5C HDF) show no significant increase in SCE frequency. Using 5C HDFs as both donor (1 Gy), and recipient (0 Gy) bystander cells at 1:100 and 1:1000 dilutions, significant, and similar, increases in SCE levels were observed. **B.** The distributions of SCE number per metaphase illustrate an overall increase in SCE levels. * ≥ 95% confidence, ** ≥ 99% confidence.

Figure 3A. Irradiated cells are refractory to bystander signals. Direct irradiation does not increase SCE levels. Irradiated donor cells (5C HDF) induce an increase in SCE frequency in non-irradiated recipient cells (5C HDF). When recipient cells were irradiated (1 Gy), they were no longer able to respond to the bystander signal.

Figure 4A. Role of DNA-PKcs in generation, but not reception of bystander signals. Gamma-ray irradiation of both mouse C57BL/6 and congenic C.B6 (wild type Prkdc) cells produced a significant increase in SCE frequencies in bystander cells (5C HDF), while BALB/c and B6.C ($Prkdc^{BALB}$) did not. **B.** Reverse

experiments demonstrate that DNA-PKcs is not necessary for the receipt of bystander signals. Both C57BL/6 and BALB/c show significant increase in SCE when irradiated 5C HDF are added. (* ≥ 95% confidence, ** ≥ 99% confidence).

Figure 5A. Role of ATM in generation, but not reception of bystander signals. No increase in SCE frequency was observed following direct irradiation of 5C human fibroblasts. Irradiated donor ATM-/- cells added to non-irradiated 5C HDF recipient cells, produced no significant change in SCE frequency. **B.** The reverse experiment revealed a significant increase in SCE in non-irradiated ATM-/- (recipients) when irradiated 5C HDF donor cells were added, while no significant change was seen in the direct irradiation of ATM-/- human fibroblasts. (* ≥ 95% confidence, ** ≥ 99% confidence).

Figure 6. Proposed model for the function of DNA-PKcs and ATM in the generation of radiation-induced bystander signals.

Table 1. Summary of figures 2 and 3 SCE frequencies and statistical outcomes for all cell transfer experiments. (* ≥ 95% confidence, ** ≥ 99% confidence).

Table 2. Summary of figures 4 and 5 SCE frequencies and statistical outcomes for all cell transfer experiments. (* ≥ 95% confidence, ** ≥ 99% confidence).

Chapter 3

Mouse Embryonic Fibroblasts Fail to Generate a Radiation-Induced Bystander Response

Abstract

The bystander effect (BSE) is the process by which directly irradiated cells communicate with and impose an effect on neighboring non-irradiated cells. Despite strenuous efforts to elucidate the mechanism, much is still unknown about the BSE, including specifics on bystander signals, pathways and the purpose of the bystander effect. To complicate matters, it has been shown that a variety of primary cells and established cell lines can be either capable or incapable of producing a bystander effect. Here, we extend the study of the BSE by comparing mouse primary fibroblasts versus mouse embryonic fibroblasts (MEFs). We designed a cell transfer method in which γ-irradiated adult mouse fibroblasts or MEFs (donors) are co-cultured with unirradiated normal 5C human fibroblasts (recipients). Sister chromatid exchange frequencies were evaluated in the human cells as a marker of the BSE. Our results show that adult mouse fibroblasts are capable of producing a BSE, whereas MEFs of the same genotype are unable to generate a bystander signal. This is the first report that MEFs are incapable of producing a bystander signal.

Introduction

Ionizing radiation (IR) is a well known carcinogen that interacts with DNA to produce multiple forms of damage including base damage, single-strand breaks (SSBs) and double-strand breaks (DSBs), which can lead to initiation of cellular transformation (1-4). Nontargeted effects from IR such as the bystander effect (BSE), have also been examined over the past few decades and have greatly impacted the field of radiation biology (5-9). The impact these secondary effects have in biological systems is currently unknown. Some would suggest that these effects are another mechanism through which radiation is detrimental to the cell and can potentially lead to carcinogenesis. This would indeed make sense, specifically if one considers the end-points used to study the BSE, i.e. clonogenic survival, micronuclei, apoptosis, etc. Another possibility is that these effects may have some benefit for the biological system as a whole (36), such as promoting death of damaged cells and/or cells surrounding the area of insult to avoid possible future problems.

The BSE occurs when an irradiated cell imposes an effect on a non-irradiated cell, which can be measured by a variety of endpoints including SCE frequency, micronuclei formation, clonogenic survival, and apoptosis (10-13). Currently, two models are accepted as methods for bystander signaling. One requires cell-to-cell contact and utilizes gap junctions as a means to transport intercellular signals (14, 15). Media transfer experiments suggest another possible mechanism in that signals are released from irradiated cells and are free-flowing in the media and able to interact with non-irradiated cells (16, 17).

Proposed BSE factors consist of reactive oxygen species (ROS), nitric oxygen species (NOS), and cytokines (18-20). These observations suggest that the target for radiation response is likely greater than the actual volume of cells or tissues directly irradiated and, thus warrant further study.

Previous work has shown that not all cell types can generate a bystander response and that not all cell types respond to a bystander signal (8, 21, 22). For example, Chinese hamster ovary (CHO) cells deficient in the homologous recombination (HR) proteins Rad51C, Rad51D, XRCC2, XRCC3 and BRCA2 were incapable of producing a bystander effect (23). In addition, we have previously shown that the DNA repair proteins DNA-PKcs and ATM are necessary to produce a bystander signal, but not receive one (Hagelstrom et al., Oncogene 2008 in press). Here, we used a cell transfer method involving normal human cells, ATM-/- deficient human cells and mouse primary kidney fibroblasts. SCE frequencies were measured in the non-irradiated cells to determine a bystander response. We furthered our studies by utilizing MEFs in addition to adult mouse primary kidney/dermal fibroblasts.

The purpose of this study was to utilize the cell transfer method that allows for the co-culture of directly irradiated MEFs or corresponding primary "adult" mouse cells (donors) with non-irradiated normal human fibroblasts (recipients). Control or irradiated primary mouse fibroblasts (dermal or kidney) were plated at a 1:100 dilution with 5C normal human fibroblasts. The cell mixture was then cultured for 2 population doublings in the presence of 5'-bromo-2'-deoxyuridine (BrdU; Sigma) and then analyzed for SCE levels as a measure of

the BSE. Despite genotypic variety in the MEFs used, none were able to induce a change in SCE levels in normal human fibroblast recipients, while their corresponding primary adult mouse cells were effective in producing a significant bystander response in normal human fibroblasts, as seen by increased SCE frequencies.

Results

We designed a cell transfer approach that utilizes SCE frequencies as a marker of the IR-induced BSE, and importantly facilitates discrimination between the generation versus the reception of bystander signals. Immediately following IR exposure (1 Gy ^{137}Cs γ-rays), mouse irradiated (donor) cells were pelleted and rinsed in PBS to remove any remaining media. The irradiated donor cells were added to human (recipient) cells at a 1:100 dilution and co-cultured for two rounds of replication in the presence of BrdU. The cells where then harvested and scored for SCE frequency in human cells only.

Consistent with our previous work, irradiated adult C57BL/6 mouse cells induced a bystander response in normal human fibroblasts as measured by a significant increase in SCE numbers compared to non-irradiated donor C57BL/6 cells (Figure 1A). SCE frequencies in 5C HDF with adult C57BL/6 primary donor fibroblasts were 4.28 SCE/metaphase (0Gy donor) and 5.76 (1Gy donor), demonstrating a statistically significant increase in SCE levels. In contrast, when normal MEFs derived from C57BL/6 mice (C57MEF and MEF286) were used as the donor cells, no significant increase in SCEs was observed. The frequencies for the C57MEFs were 4.67 SCE/metaphase (0Gy donor) and 4.77 SCE/metaphase (1Gy donor); MEF286 frequencies were 4.38 SCE/metaphase (0Gy donor) and 3.96 SCE/metaphase (1Gy donor) (Figure 1A). Distribution graphs (Figure 1B) illustrate that this is an overall increase, rather than a few cells with many SCE skewing the data.

To further explore the hypothesis that MEFs are incapable of generating a bystander signal, we sought to compare these results to other sets of mouse cells to determine if only C57BL/6 mouse strain failed or if it is a general phenomenon in mice. We obtained Artemis+/+ or Artemis-/- adult mouse dermal fibroblasts and their MEF counterparts from Dr. JoAnn Sekiguchi's laboratory (Rooney, 2005). These cells are on a 129SvEvTac /C57BL/6 mixed background. Results demonstrate a significant increase in SCE numbers in normal 5C HDF recipient cells when either Art+/+ or Art-/- mouse adult dermal fibroblasts were irradiated and co-cultured (Figure 2A and 2C). The adult Art+/+ frequencies were 3.60 SCE/metaphase (0Gy) and 4.86 SCE/metaphase (1Gy), and the adult Art-/- frequencies were 3.64 SCE/metaphase (0Gy) and 4.92 SCE/metaphase (1Gy). Again, the MEFs could not generate a bystander signal. No significant increase in SCEs was observed when irradiated Art+/+ or Art-/- MEFs were co-cultured with 5C HDF recipient cells (Figure 2A and 2C). Art+/+ MEF frequencies were 4.08 SCE/metaphase (0Gy) and 4.30 SCE/metaphase (1Gy), and the Art-/- MEF frequencies were 4.28 SCE/frequency (0Gy) and 4.34 SCE/frequency (1Gy). Figure 2B and 2D show SCE distribution for both adult and MEF Art+/+ and Art-/- cells. These results display two concepts: 1.) The DNA repair protein Artemis is not needed to generate a bystander signal; 2.) MEFs derived from C57BL/6 mice and C57BL/6 X 129SvEvTac F1 hybrid mice are incapable of generating a bystander response.

We extended this study by examining the outbred strain, CF-1. Adult kidney CF-1 fibroblasts were either sham irradiated or exposed to 1Gy γ-radiation

and added to normal 5C HDF recipient cells. SCE frequency in the 5C HDF for the 0Gy sample was 3.87, which significantly increased to 5.05 when irradiated CF-1 adult donor cells were added (Figure 3A).

CF-1 MEFs were also utilized as donor cells in the BSE experiments. Consistent with previous observations, the irradiated MEFs were incapable of significantly increasing SCE levels in 5C HDF (Figure 3A). Frequencies were 3.16 for the 0Gy samples and 3.44 for the 1Gy samples. Distributions for both experiments showed a general trend and were not skewed by a small outlying population (Figure 3B).

*Note all data are presented in Table 1, and averages and statistical significance were also shown.

Discussion

Despite numerous, often contradictory, reports of the BSE, mechanistic details remain elusive. The present work is the first to demonstrate a significant difference in the induction of a bystander response in adult mouse cells versus their MEF counterpart. We have shown that wild-type C57BL/6, Artemis+/+, Artemis -/-, and outbred CF-1 adult mouse fibroblasts are capable of generating a bystander response in normal human fibroblasts as measured by SCE, but their corresponding MEFs do not. These studies also reveal that the DNA end-processing repair protein Artemis is not necessary for the generation of a bystander signal, as irradiated adult mouse Artemis-/- cells elevate SCE frequencies in normal human fibroblasts.

MEFs have been widely used in a variety of studies; only a few of which note differences as compared to adult mouse cells. Several studies utilizing MEFs to examine cellular signaling report no differences compared to adult cells (24-27). In addition, no differences in apoptosis were observed in MEFs compared to mouse adult fibroblasts (28, 29). MEFs were used to study the BSE (clonogenic survival) in one media transfer study and in contrast to our observations, they observed a bystander response (30). However, one investigation reported that wild-type MEFs, as well as MEFs with mutated Ku80, do not display an adaptive response (31). The adaptive response, like the BSE, is a non-targeted effect of IR, so in that sense, these results are consistent with our findings.

We have recently shown that the DNA repair proteins DNA-PKcs and ATM are required for IR-induced bystander signaling (Hagelstrom and Askin,

Oncogene 2008). It has also been recently reported that DNA-PKcs levels are reduced in mouse embryonic stem (ES) cells compared to MEFs (32). Although MEFs are not the same as ES cells, MEFs do exhibit some epigenetic marks that are similar to ES cells, suggesting impartial commitment to differentiated lineage (personal correspondence, Schemanti JI). If in fact MEFs do have decreased levels of DNA-PKcs compared to mouse adult fibroblasts, this may provide an explanation for their inability to generate bystander signals.

Although it is not readily apparent why MEFs would not exhibit a bystander response, we speculate that this may be beneficial to a developing organism. A cell directly hit by IR promotes several types of damage to surrounding non-targeted cells. In a developing embryo, damage to and/or death of even one cell may be especially detrimental because a defect or deformity may arise in the anatomical structure to which the dead or damaged cell would have contributed. Therefore, it may be more beneficial for the developing embryo to suppress a bystander response in order to keep the actual number of damaged cells to an absolute minimum.

Future directions

Our results highlight the need to better characterize MEFs and so warrant further study to define mechanisms. We have used the cell transfer assay previously in adult cells to examine DNA repair protein involvement in the BSE (Hagelstrom et al., Oncogene 2008, in press). Bystander studies in MEFs will be expanded to include additional end-points such as micronuclei, clonogenic

survival and p53/p21 expression. It will also be important to establish DNA-PKcs protein levels in MEFs versus mouse adult fibroblasts, as well as to initiate DNA repair studies of γ-H2AX foci induction and kinetics. It may also be possible that seeding (with or without IR) at such low densities (4,000 in a T-75cm^2 flask) is not conducive to the production of a bystander signal. For example, if these cells are dying, then it would be reasonable to suspect that bystander signals are not being produced. Therefore, we plan on determining plating efficiency of MEFs (with and without IR) at low cell densities to resolve this uncertainty. If the cells do survive, then genome-based analysis will be utilized (with focus on DNA-repair, cell signaling and oxidative response genes) using microarrays with MEFs versus mouse adult fibroblasts (in collaboration with Dr. M. Story). Results of such studies would be extremely informative and provide possible insight into mechanistic explanations for our findings.

Materials and Methods

Cell Lines and Cell Culture. Kidney tissue from 8–12 week old female C57BL/6 (Jackson Laboratories) and CF-1 (Charles River Laboratories) mice were minced, and digested in 199 medium containing collagenase (Worthington Type III; 200 units/ml) at 37°C for 3–5 h with gentle agitation. Disaggregated cells were washed 6x in phosphate buffered saline (PBS) containing 0.5% fetal bovine serum (FBS) and cultured in α-MEM medium (15% FBS, penicillin/streptomycin). Media was changed after 3 days of incubation.

Adult Artemis +/+ and Artemis -/- (129Sv1/C57BL/6 background) mouse tail snips and corresponding MEFs were obtained from Dr. JoAnn Sekiguchi's laboratory (University of Michigan). Tails were minced, placed into media and grown for two weeks before passaging. Artemis +/+ and Artemis -/- MEFs and low passage neonatal Human Dermal Fibroblasts (HDF C-004-5C; Cascade Biologics) were grown in α-MEM supplemented with 10% fetal bovine serum and antibiotics. The 5C HDF cells were counted using a Coulter Counter (Coulter Beckman, Fullerton, CA) and 4 X 10^5 human fibroblasts were plated into T-75 flasks, then co-cultured with 1:100 dilutions of either 0 Gy or 1 Gy γ-irradiated, exponentially growing mouse donor cells. Donor cells included wild-type MEF C57BL/6 (ATCC, #SCRC-1008; (33)), C57BL/6 primary kidney fibroblasts, Artemis+/+ & Artemis -/- primary dermal fibroblasts (34), Artemis+/+ & Artemis -/-MEF (34), CF-1 primary kidney fibroblasts, and CF-1 MEFs (ATCC, SCRC #1040).

Irradiations were performed using a sealed-source Mark I ^{137}Cs γ-irradiator (J.L. Shepherd and Associates). 5'-bromo-2'-deoxyuridine (BrdU; Sigma) was added to cultures at a final concentration of 2 X 10^{-5}M and cells were allowed to grow for two rounds of cell division. Colcemid (Gibco) was added at a final concentration of 0.2 μg/ml and cells were harvested approximately 2-3 hours later. Cells were trypsinized, centrifuged, then resuspended in 0.075M KCl for 15 minutes at room temperature and then fixed with 3:1 methanol: acetic acid.

SCE Staining and Analysis. Slides were prepared using standard cytogenetic techniques and then stained via Fluorescence Plus Giemsa (FPG; (35)). Briefly, cells are grown for two replication rounds in the presence of BrdU. Slides are stained with Hoescht dye 33258 for 15 minutes at room temperature, rinsed with distilled water and exposed to UV light at 365nm for 25 minutes. Immediately slides are then soaked in 2x SSC for 30 minutes in a 60°C water bath. Following thorough rinses with distilled water, slides are allowed to air dry, then stained with 5% Giemsa for 10 mintues. Images were analyzed using a Zeiss Axioskop2 Plus microscope with a Photometrics Coolsnap ES2 camera and Metavue 7.1 software.

Statistical Analysis. Twenty five metaphases were scored for genomic SCE per sample and slides were blind to the viewer. All experiments were performed a minimum of two times. Error bars represent standard error of the mean (SEM)

and a student's T-test was used to calculate statistical significance. Data was pooled if not significantly different.

Acknowledgements

The authors wish to thank Dr. Edwin Goodwin for his critical reading of the manuscript, Dr. Phillip Smiraldo (University of Texas Southwestern Medical Center) and Dr. Douglas Pittman (University of South Carolina) for the Rad51D MEFs, Dr. Penny Jeggo (Genome Damage and Stability Centre, University of Sussex, East Sussex, UK Funding sources as per bystander paper) for the LigIV MEFs, and Dr. JoAnn Sekiguchi (University of Michigan) for all Artemis mouse cells used. This work was supported by funds from ____.

Figure Legends

Figure 1. C57BL/6 mouse donor cells added to normal human fibroblast recipient cells. **A.** A significant increase in SCE is seen in recipient human cells when irradiated adult mouse fibroblasts are the donors, but no effect is seen when MEFs are the donors. **B.** The distribution of SCE number per metaphase illustrates an overall increase in SCE levels.

* ≥ 95% confidence, ** ≥ 99% confidence

Figure 2. Murine Artemis donor cells added to human recipient cells. **A.** An increase in SCE frequency was seen in human cells with irradiated adult Art+/+ donor cells, but not with MEF Art+/+ donor cells. **B.** The distribution of SCE number per metaphase illustrates an overall increase in SCE levels. **C.** An increase in SCE frequency was observed in human cells with irradiated adult Art-/- donors, but no increase is seen with MEF Art-/- donor cells. **D.** Distribution graphs again illustrate an overall increase in SCE for the adult mouse Art-/- donor cells.

* ≥ 95% confidence, ** ≥ 99% confidence

Figure 3. Both CF-1 adult and MEF donor cells were added to normal human 5C recipient cells. **A.** An increase in SCE frequency was observed in the human recipient cells when irradiated adult CF-1 mouse cells were added. The MEFs could not generate a response in that no significant increase was noted when

irradiated cells were added. **B**. The distribution of SCE number per metaphase illustrates an overall increase in SCE levels

* ≥ 95% confidence, ** ≥ 99% confidence

Table 1. Summary of SCE frequencies and statistical outcomes for all cell transfer experiments. (**≥ 99% confidence).

Figures

Figure 1A

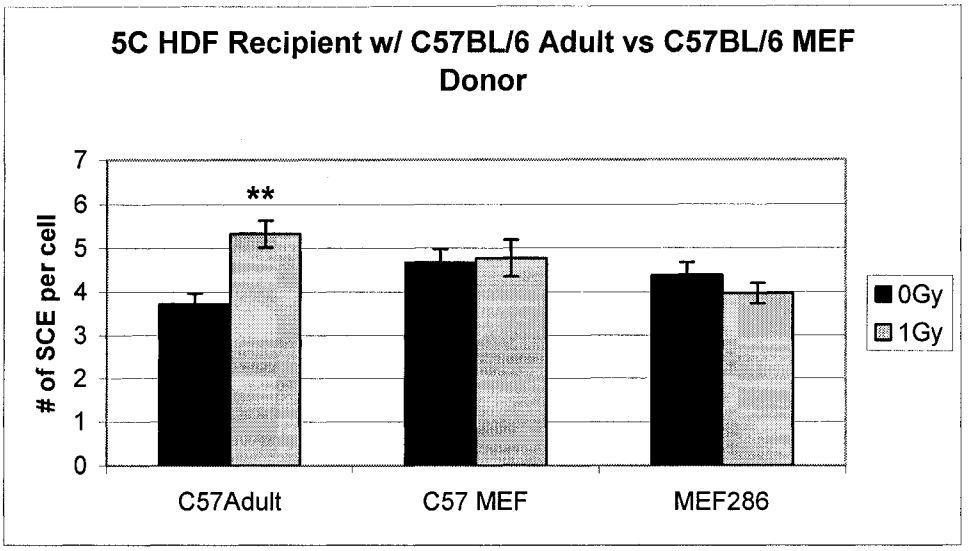

Figure 1B

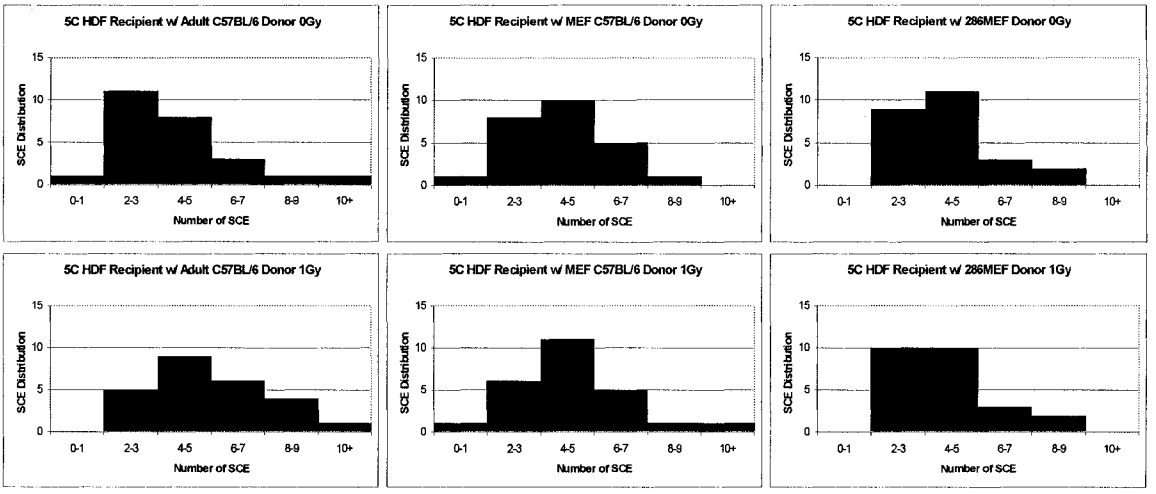

Figure 2A

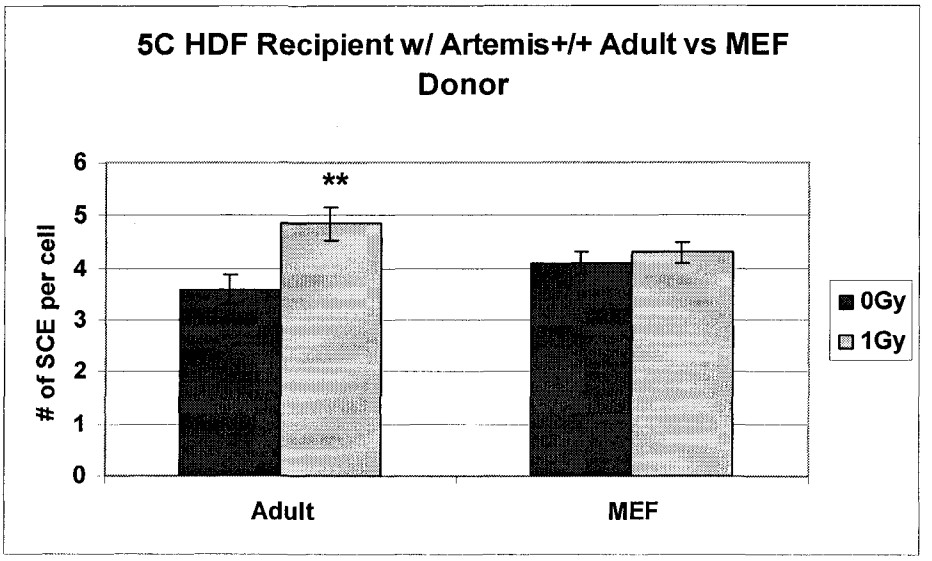

Figure 2B

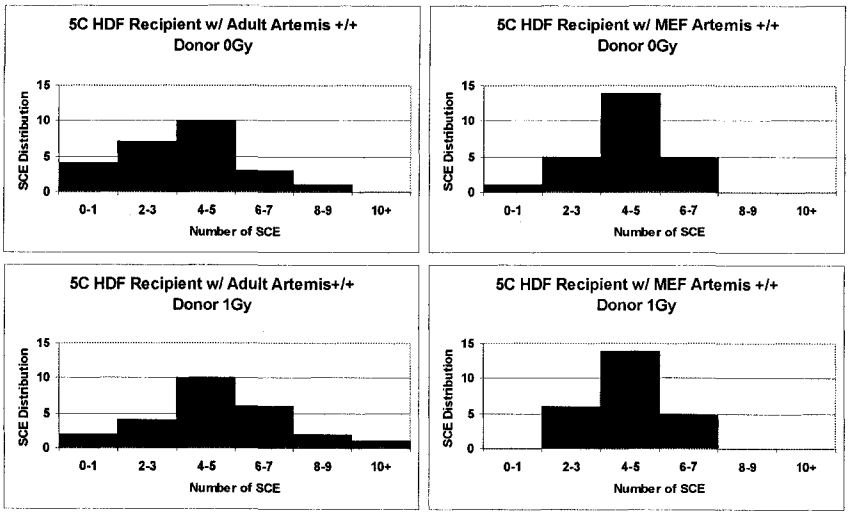

Figure 2C

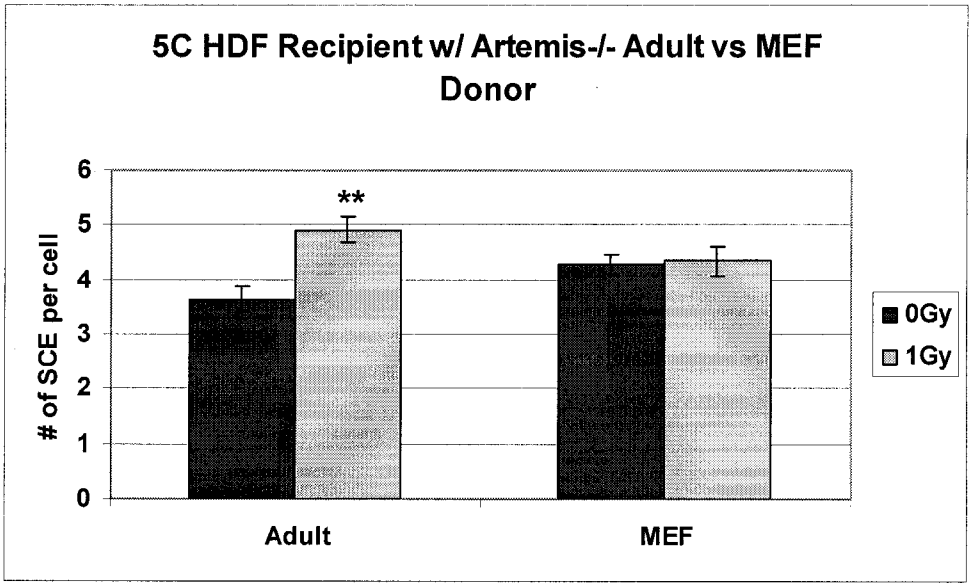

Figure 2D

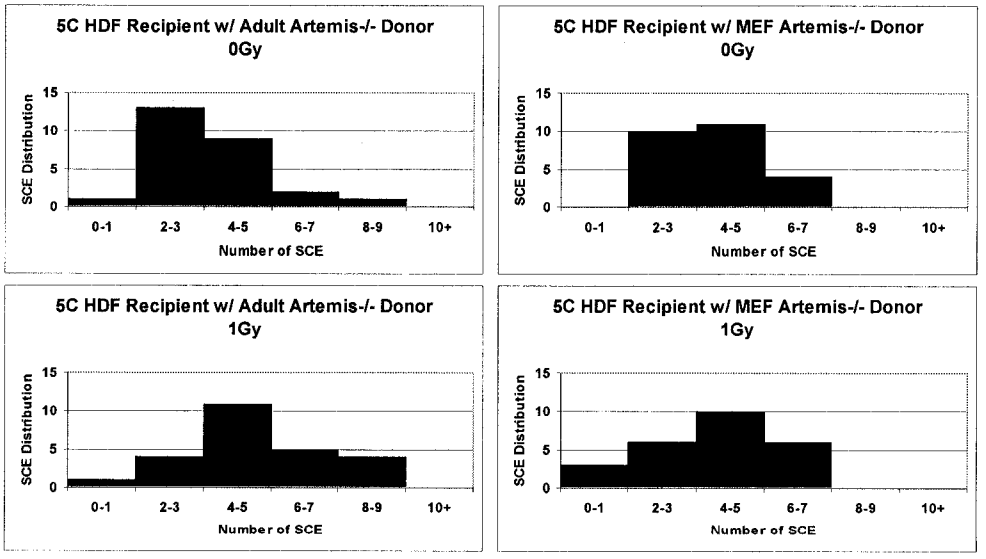

Figure 3A

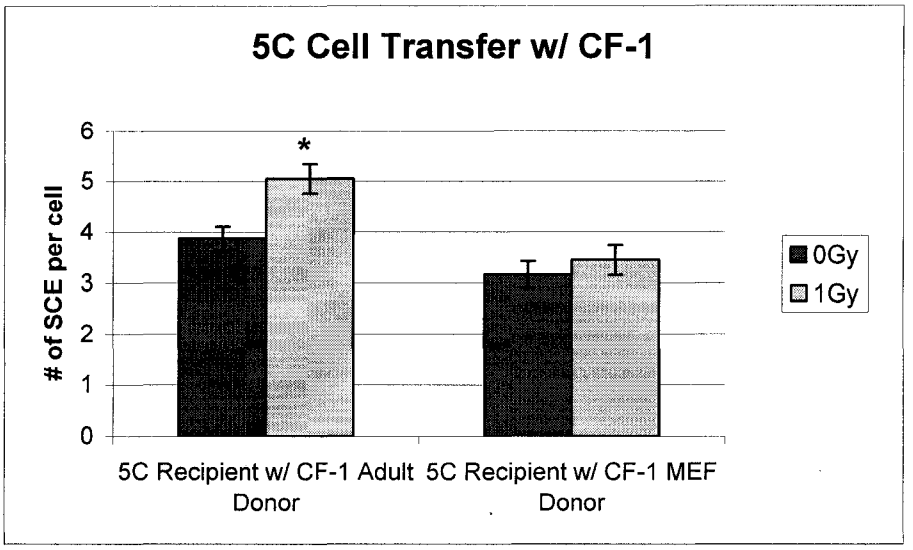

Figure 3B

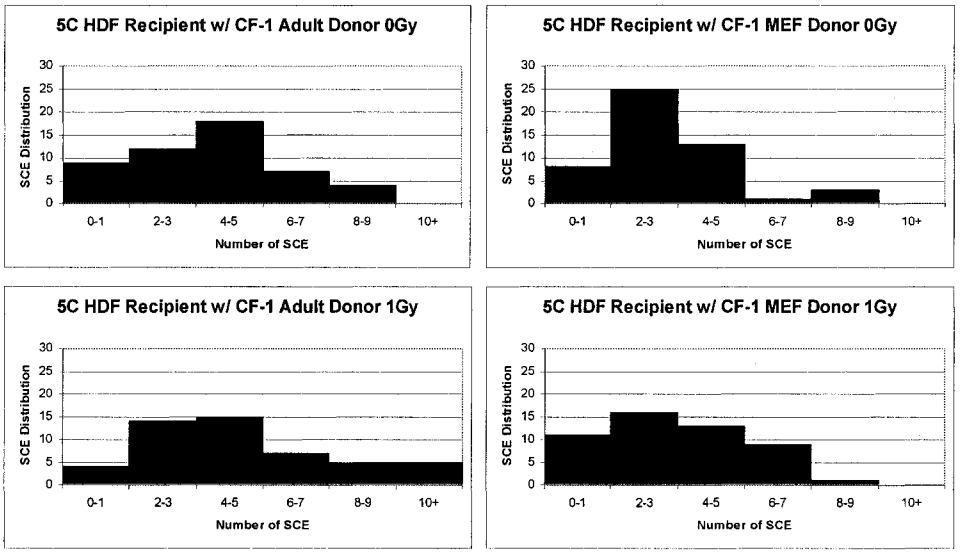

Table 1

BSE Summary of Adult vs MEF Cell Transfer					
Cell Line	**Background**	**Signal Generated**	**p value**	**metaphases scored**	**Figure**
Adult C57	C57BL/6	yes	0.0001	50	1A
MEF C57	C57BL/6	no	0.3776	50	1A
MEF 286	C57BL/6	no	0.2542	50	1A
Adult Artemis +/+	129Sv1/C57BL/6	yes	0.0032	50	2A
MEF Artemis +/+	129Sv1/C57BL/6	no	0.4648	50	2A
Adult Artemis -/-	129Sv1/C57BL/6	yes	0.0004	50	2C
MEF Artemis -/-	129Sv1/C57BL/6	no	0.8622	50	2C
Adult CF-1	outbred	yes	0.0018	75	3A
MEF CF-1	outbred	no	0.4708	50	3A

References

1. Collis, S. J., DeWeese, T. L., Jeggo, P. A. & Parker, A. R. (2005) The life and death of DNA-PK. *Oncogene* 24, 949-61.
2. Purkayastha, S., Milligan, J. R. & Bernhard, W. A. (2008) An investigation into the mechanisms of DNA strand breakage by direct ionization of variably hydrated plasmid DNA. *J Phys Chem B* 112, 4152.
3. Purkayastha, S., Milligan, J. R. & Bernhard, W. A. (2006) An investigation into the mechanisms of DNA strand breakage by direct ionization of variably hydrated plasmid DNA. *J Phys Chem B* 110, 26286-91.
4. Yokoya, A., Cunniffe, S. M. & O'Neill, P. (2002) Effect of hydration on the induction of strand breaks and base lesions in plasmid DNA films by gamma-radiation. *J Am Chem Soc* 124, 8859-66.
5. Iyer, R. & Lehnert, B. E. (2002) Alpha-particle-induced increases in the radioresistance of normal human bystander cells. *Radiat Res* 157, 3-7.
6. Kovalchuk, O. & Baulch, J. E. (2008) Epigenetic changes and nontargeted radiation effects--is there a link? *Environ Mol Mutagen* 49, 16-25.
7. Ponnaiya, B., Cornforth, M. N. & Ullrich, R. L. (1997) Radiation-induced chromosomal instability in BALB/c and C57BL/6 mice: the difference is as clear as black and white. *Radiat Res* 147, 121-5.
8. Mothersill, C. & Seymour, C. (1997) Medium from irradiated human epithelial cells but not human fibroblasts reduces the clonogenic survival of unirradiated cells. *Int J Radiat Biol* 71, 421-7.
9. Nagasawa, H. & Little, J. B. (1992) Induction of sister chromatid exchanges by extremely low doses of alpha-particles. *Cancer Res* 52, 6394-6.
10. Yang, H., Anzenberg, V. & Held, K. D. (2007) The time dependence of bystander responses induced by iron-ion radiation in normal human skin fibroblasts. *Radiat Res* 168, 292-8.
11. Grifalconi, M., Celotti, L. & Mognato, M. (2007) Bystander response in human lymphoblastoid TK6 cells. *Mutat Res* 625, 102-11.
12. Nagasawa, H., Peng, Y., Wilson, P. F., Lio, Y. C., Chen, D. J., Bedford, J. S. & Little, J. B. (2005) Role of homologous recombination in the alpha-particle-induced bystander effect for sister chromatid exchanges and chromosomal aberrations. *Radiat Res* 164, 141-7.
13. O'Neill-Mehlenbacher, A., Kilemade, M., Elliott, A., Mothersill, C. & Seymour, C. (2007) Comparison of direct and bystander effects induced by ionizing radiation in eight fish cell lines. *Int J Radiat Biol* 83, 593-602.
14. Azzam, E. I., de Toledo, S. M. & Little, J. B. (2001) Direct evidence for the participation of gap junction-mediated intercellular communication in the transmission of damage signals from alpha -particle irradiated to nonirradiated cells. *Proc Natl Acad Sci U S A* 98, 473-8.
15. Azzam, E. I., de Toledo, S. M., Gooding, T. & Little, J. B. (1998) Intercellular communication is involved in the bystander regulation of gene expression in human cells exposed to very low fluences of alpha particles. *Radiat Res* 150, 497-504.

16. Lehnert, B. E., Goodwin, E. H. & Deshpande, A. (1997) Extracellular factor(s) following exposure to alpha particles can cause sister chromatid exchanges in normal human cells. *Cancer Res* 57, 2164-71.
17. Mothersill, C. & Seymour, C. B. (1998) Cell-cell contact during gamma irradiation is not required to induce a bystander effect in normal human keratinocytes: evidence for release during irradiation of a signal controlling survival into the medium. *Radiat Res* 149, 256-62.
18. Kashino, G., Prise, K. M., Suzuki, K., Matsuda, N., Kodama, S., Suzuki, M., Nagata, K., Kinashi, Y., Masunaga, S., Ono, K. & Watanabe, M. (2007) Effective suppression of bystander effects by DMSO treatment of irradiated CHO cells. *J Radiat Res (Tokyo)* 48, 327-33.
19. Shao, C., Stewart, V., Folkard, M., Michael, B. D. & Prise, K. M. (2003) Nitric oxide-mediated signaling in the bystander response of individually targeted glioma cells. *Cancer Res* 63, 8437-42.
20. Shao, C., Folkard, M. & Prise, K. M. (2008) Role of TGF-beta1 and nitric oxide in the bystander response of irradiated glioma cells. *Oncogene* 27, 434-40.
21. Mothersill, C., Rea, D., Wright, E. G., Lorimore, S. A., Murphy, D., Seymour, C. B. & O'Malley, K. (2001) Individual variation in the production of a 'bystander signal' following irradiation of primary cultures of normal human urothelium. *Carcinogenesis* 22, 1465-71.
22. Nagar, S., Smith, L. E. & Morgan, W. F. (2003) Characterization of a novel epigenetic effect of ionizing radiation: the death-inducing effect. *Cancer Res* 63, 324-8.
23. Nagasawa, H., Wilson, P. F., Chen, D. J., Thompson, L. H., Bedford, J. S. & Little, J. B. (2008) Low doses of alpha particles do not induce sister chromatid exchanges in bystander Chinese hamster cells defective in homologous recombination. *DNA Repair (Amst)* 7, 515-22.
24. Li, S. K., Smith, D. K., Leung, W. Y., Cheung, A. M., Lam, E. W., Dimri, G. P. & Yao, K. M. (2008) FoxM1c counteracts oxidative stress-induced senescence and stimulates Bmi-1 expression. *J Biol Chem* 283, 16545-53.
25. Wolff, S. (1996) Aspects of the adaptive response to very low doses of radiation and other agents. *Mutat Res* 358, 135-42.
26. Ocbina, P. J. & Anderson, K. V. (2008) Intraflagellar transport, cilia, and mammalian Hedgehog signaling: Analysis in mouse embryonic fibroblasts. *Dev Dyn*.
27. He, X., Chen, M. G. & Ma, Q. (2008) Activation of Nrf2 in Defense against Cadmium-Induced Oxidative Stress. *Chem Res Toxicol*.
28. Masud, A., Mohapatra, A., Lakhani, S. A., Ferrandino, A., Hakem, R. & Flavell, R. A. (2007) Endoplasmic reticulum stress-induced death of mouse embryonic fibroblasts requires the intrinsic pathway of apoptosis. *J Biol Chem* 282, 14132-9.
29. Vengellur, A. & LaPres, J. J. (2004) The role of hypoxia inducible factor 1alpha in cobalt chloride induced cell death in mouse embryonic fibroblasts. *Toxicol Sci* 82, 638-46.

30. Shareef, M. M., Cui, N., Burikhanov, R., Gupta, S., Satishkumar, S., Shajahan, S., Mohiuddin, M., Rangnekar, V. M. & Ahmed, M. M. (2007) Role of tumor necrosis factor-alpha and TRAIL in high-dose radiation-induced bystander signaling in lung adenocarcinoma. *Cancer Res* 67, 11811-20.
31. Raaphorst, G. P., Li, L. F. & Yang, D. P. (2006) Evaluation of adaptive responses to cisplatin in normal and mutant cell lines with mutations in recombination repair pathways. *Anticancer Res* 26, 1183-7.
32. Banuelos, C. A., Banath, J. P., Macphail, S. H., Zhao, J., Eaves, C. A., O'Connor, M. D., Lansdorp, P. M. & Olive, P. L. (2008) Mouse but not human embryonic stem cells are deficient in rejoining of ionizing radiation-induced DNA double-strand breaks. *DNA Repair (Amst)*.
33. Smiraldo, P. G., Gruver, A. M., Osborn, J. C. & Pittman, D. L. (2005) Extensive chromosomal instability in Rad51d-deficient mouse cells. *Cancer Res* 65, 2089-96.
34. Rooney, S., Sekiguchi, J., Zhu, C., Cheng, H. L., Manis, J., Whitlow, S., DeVido, J., Foy, D., Chaudhuri, J., Lombard, D. & Alt, F. W. (2002) Leaky Scid phenotype associated with defective V(D)J coding end processing in Artemis-deficient mice. *Mol Cell* 10, 1379-90.
35. Perry, P. & Wolff, S. (1974) New Giemsa method for the differential staining of sister chromatids. *Nature* 251, 156-8.
36. Prise KM, Folkard M and Michael BD (2003) A review of the BSE and its implications for low-dose exposure, Radiation Protection Dosimetry 104, NO.4, 347-355
37. Rooney S, Alt FW, Sekiguchi J, Manis JP. 2005 Artemis-independent functions of DNA-dependent protein kinase in Ig heavy chain class switch recombination and development. Proc Natl Acad Sci U S A. Feb 15;102(7):2471-5. Epub 2005 Feb 7.

Chapter 4

The impact of the *Prkdc* polymorphism in the LEWES mouse strain

Abstract

Improper DNA repair of double-strand breaks (DSBs) can potentially lead to cellular transformation and tumorigenesis. Evidence suggests that even small mutations, such as point mutations, in DNA repair genes can affect an individual's predisposition to cancer. We have been using a mouse model to further explore the impact of single nucleotide polymorphisms (SNPs) in mammary carcinogenesis. The BALB/c mouse strain has been shown to be susceptible to radiation-induced mammary cancer and is deficient in DNA repair. Further studies demonstrate that two polymorphisms located in the coding regions of the non-homologous end-joining (NHEJ) gene, *Prkdc*, may be linked to the BALB/c phenotype. We now set out to determine the consequence of one of the BALB/c-like SNPs by using another mouse strain named LEWES. The LEWES strain was recently derived from wild mice and has only one BALB/c-like SNP. Utilizing and characterizing this strain provides insight into the impact of a single point mutation in cancer predisposition.

Introduction

Ionizing radiation (IR) acts as a carcinogen by depositing energy directly in DNA, or generating free radicals that targets DNA producing a multitude of genomic lesions including base damage, single-strand breaks (SSBs) and double-strand breaks (DSBs) (Munro, 1970; Ward, 1981; Cornforth, 1987). Of these, double-strand breaks (DSBs) are a hallmark lesion of IR and if improperly repaired, can result in deletions, amplifications and translocations of tumor suppressors and oncogenes. Therefore, efficient DNA repair is critical for maintaining the integrity and stability of the genome.

Mammalian cells rely on two pathways for DSB repair: homologous recombination (HR) and non-homologous end-joining (NHEJ) (Hoeijmakers, 2001). HR occurs in S/G2-phase and uses the sister chromatid as a template and is virtually error-free (Helleday, T., 2003). NHEJ occurs throughout the cell cycle and is responsible for the majority of IR-induced DSB repair in mammalian cells. Unlike HR, NHEJ does not require a homologous template for repair and is consequently more error prone and can produce small deletions (Hoeijmakers, 2001).

It is now appreciated that genes involved in these DNA repair pathways can play important roles in cancer predisposition. Mutations in the HR genes BRCA1 and BRCA2 are highly penetrance because of the extremely high breast cancer incidences observed (Venkitaraman, A, 2001; Wenham, R, 2003). However, these mutants occur at low frequencies in the human population, accounting for a small fraction of the total breast cancers diagnosed. The

remaining breast cancer occurrences are considered to be "spontaneous", with recent evidence suggesting a large portion of these cases (20-40%) are due to low penetrance, high frequency mutations (Scott D., 2004).

In many cases, these mutations do not become apparent until DNA repair is induced by some exogenous factor, i.e. IR exposure (accidental, medical). A recent epidemiologic study evaluated Radiation Technologists and revealed 3 SNPs in *Prkdc,* the gene encoding the NHEJ protein DNA-dependent protein kinase catalytic subunit (DNA-PKcs), that significantly correlated to individuals with breast cancer (Bhatti et al., 2008).

The relationships between SNPs in *Prkdc,* DNA-PKcs deficiency and breast carcinogenesis can also be modeled in the BALB/c mouse. Ullrich et al. have shown a significant induction of both lung and mammary adenocarcinomas after exposure to ^{137}Cs γ-irradiation (Ullrich, R., 1991). Cytogenetic analysis revealed elevated frequencies of chromatid-type aberrations in BALB/c (Ponnaiya, B., 1997). These abnormalities increased significantly 20 population doublings after exposure, demonstrating delayed instability.

Such high levels of chromatid aberrations may have been due to a deficiency for the cell to properly repair the initial insult produced by IR. Okayasu et al. investigated repair activity and repair time in BALB/c and discovered a deficiency of repair in the BALB/c strain (Okayasu, R., 2000). Western blot analysis revealed decreased expression of the DNA-PKcs, but not of Ku70/Ku80, in both SCID and BALB/c compared to C57BL/6. Kinase activity of DNA-PKcs was then determined and compared in BALB/c and other strains

(Okayasu, R., 2000). Results revealed a significant decrease in DNA-PKcs kinase activity in BALB/c; it is not certain whether the decrease is due to a defect in specific kinase activity of the enzyme or due to lower quantities of stable protein. Additional studies have demonstrated a role for DNA-PKcs in telomeric end-capping (Bailey et al., 2004; Bailey et al., 2001; Bailey et al., 1999). BALB/c has elevated levels of radiation-induced telomere-DSB fusions which can lead to genomic instability (Williams, manuscript in progress). Current research has also demonstrated that DNA-PKcs is necessary for cell communication via the bystander effect (BSE) (Hagelstrom et al., manuscript in press, 2008). We find that DNA-PKcs is required to generate a bystander signal, but is not needed to receive one.

Efforts then focused on the hypomorphic variant of DNA-PKcs in the BALB/c strain. Yu et al. discovered two SNPs located in the coding region of *Prkdc* that may be responsible for the BALB/c phenotype (Yu, Y., 2001). One SNP is located in exon 48, which is positioned between a leucine zipper domain and an autophosphorylation cluster. This SNP is in a highly conserved region and may impact DNA-protein or protein-protein interaction due to the relatively close vicinity of the leucine zipper. Another possibility is that it may affect the ability of DNA-PKcs to autophosphorylate, an event crucial for proper enzymatic activity (Block, W., 2004). The second SNP position is near the C-terminal domain in exon 81. This codon is not well conserved among species; however, it is located in the kinase domain and so may affect enzymatic activity.

The goal of this research is to determine the functional significance of the BALB/c SNP located in the kinase domain. We have obtained LEWES/EiJ mice, an inbred strain that was recently derived from wild trapped mice. This strain is of particular interest because it possesses only one of the BALB/c-like SNPs, specifically the one located in the kinase domain. We performed sequencing and genotyping to ensure that LEWES does in fact have the SNP and no other point mutations in the *Prkdc* coding region that could possibly affect our results. Real-time PCR revealed no difference in mRNA levels between LEWES, BALB/c and C57BL/6 (wild-type) compared to both C57BL/6 and BALB/c. We then set out to characterize the LEWES strain to determine if it is more BALB/c-like or C57BL/6-like in terms of protein expression (immunoblotting), DNA repair (γ-H2AX) and the BSE (SCE frequency). In addition to the characterization, haplotying was done to determine if LEWES shares common ancestry with BALB/c or if the point mutation in the kinase domain occurred spontaneously. These results give insight into how a natural occurrence can affect cancer predisposition in a population.

Our results show that the LEWES strain is intermediate compared to C57BL/6 and BALB/c in terms of protein expression, with DNA-PKcs levels more similar to BALB/c. We also demonstrate that DNA repair kinetics in LEWES is not as efficient compared to C57BL/6 but better than BALB/c. Furthermore, we show that LEWES could generate a bystander signal, similar to C57BL/6. These results suggest that the SNP in the kinase domain affect protein levels and, to an extent, DSB repair but is not needed to generate a bystander

response. It is also interesting that both DNA-PKcs levels and repair that the LEWES were intermediate, suggesting that another factor may be needed to generate the complete BALB/c phenotype. This may imply that both *Prkdc* SNPs are required to produce a radiosensitive phenotype similar to BALB/c. Another possibility may be that a modifying gene, not currently known to interact with DNA-PKcs, in the BALB/c background may influence its radiosensitivity.

Materials and Methods

Irradiations

Irradiations were performed using a sealed-source Mark I ^{137}Cs γ-ray irradiator (J.L. Shepherd and Associates). All irradiated samples were exposed to an acute dose of 1Gy low LET γ-radiation at a dose rate of 3.9Gy/min.

Mice and cell culture

LEWES, C57BL/6 and BALB/c female mice (2-3 months in age) were obtained from Jackson Laboratories (Stock# - 002798 Strain name - LEWES/EiJ, Stock# - 000664 Strain name - C57BL/6ByJ and Stock# - 000650 Strain name - BALB/cByJ). To isolate primary kidney fibroblasts, kidneys were minced and placed in α-MEM media containing collagenase (Worthington Type III; 200 units/ml) at 37°C for 3–5 h with gentle agitation. Disaggregated cells were washed six times in phosphate buffered saline (PBS) containing 0.5% fetal bovine serum (FBS) and cultured in complete α-MEM medium (15% FBS, penicillin/streptomycin). Media was changed after 3 days of incubation. Cells were kept in culture at 37°C with 5% CO_2 and passaged when confluent using trypsin to dissociate the cells and placed in fresh complete α-MEM media.

DNA/RNA/cDNA isolation and purification

DNA and RNA from primary mouse kidney fibroblasts were extracted and purified using Qiagen kits (Qiagen: DNeasy blood and tissue kit, #69506 and RNeasy kit #74104). The cDNA was isolated and purified using RNA and an

iScript cDNA synthesis kit (BioRad: iScript select cDNA synthesis kit, #170-8896).

DNA/RNA/cDNA isolation and purification

All PCR products were either purified by a PCR purification kit or a gel extraction kit (Qiagen: QIAquick PCR purification kit #28104 and QIAquick gel extraction kit, 28704).

Genotyping

The restriction fragment length polymorphism (RFLP) method was used to genotype all mouse strains. The first SNP located downstream of the leucine zipper abolishes a BsmB1 site. PCR primers (PKF-GCCTAAGGTAAGGTGCTGTA AND PKR-GCCATGATCCTTAGCAAGTG) were designed flanking the SNP location and the sequence amplified using *Taq* polymerase (Invitrogen; *Taq* DNA polymerase, Recombinant 10342-020). PCR product was then digested with BsmB1 and corresponding buffer (NEB; #R0580) at 55°C for 2 hours. The second SNP in the kinase domain creates a novel Hph1 site. Primers (81F-ATGTTCTTTGCCATGCAGT AND 81R-TTCTTCCCTCCCTTCTCAGTA) were used to amplify the region containing the SNP. The PCR product was digested with Hph1 and corresponding buffer (NEB; #R0158) at 37°C for 2 hours. Size was detected for both sets of digested product using either a 2% or 3% agarose gel.

Sequencing

The entire cDNA of the LEWES *Prkdc* gene was sequenced and compared to C57BL/6 and BALB/c sequences obtained from the Ensemble and NCBI databases (http://www.ensembl.org/index.html and http://www.ncbi.nlm.nih.gov/entrez/viewer.fcgi?db=nuccoreandid=124517705). A total of 19 PCR primer sets were designed using the Primer3 website (http://frodo.wi.mit.edu/cgi-bin/primer3/primer3_www.cgi). The amplified products were purified and sent to Davis sequencing (http://www.davissequencing.com/pricing.htm) for results.

Primer sequences were: PKSF-CTGGTTCTGTCCCTTTGCAT and PKSR-CTGCAGTAGCCAACACCGTA, PK1F-CGTACGGTGTTGGCTACTGC and PK1R-CACATAAAAACTTTAGGGCTTC, PK2F- CAGGCATTGCAGATTTCCTT and PK2R- TTCAGCCTGCTCTTATGCA, PK3F-TGGCAGAAGATGCAGAGTTG and PK3R- CCTCCTGCTCTCCAACAGTC, PK4F- GCTGTGACCAGATGGAGGA and PK4R-CCAGTGGCTCTTGGTTTCA, PK5F- GCCACTGGCAGAAATAGGT and PK5R- AGGGTCCACAATACCATCC, PK6F- CGCCCATGTACCAGCTTTA and PK6R- AGTAGACGAGGGTTGGCTG, PK7F-CTCAGCCAACCCTCGTCTA and PK7R- TACAGCTGGGGTCCAAAGA, PK8F- GTCTTTGGACCCCAGCTGT and PK8R-CGCTGTTCCCGACAAAGTA, PK9F- GTCGGGAACAGCGACATAT and PK9R- GGCCAGTGGTAGGTTTACG, PK10F-

ACCACTGGCCATTTTCAGAG and PK10R-GGCAGCAGAAAGAACAAAGC, PK11F- CTTCCCTCCTCTTGCTGAC and PK11R- CCCTTCTTGGGTTTGGGTA, PK12F-CTGGAGCCATGAAACCAGA and PK12R- GAAGCGGTTGAAATCTTGG, PK13F- TCCAAGATTTCAACCGCTT and PK13R-TCCTTAGGGGACCCAGAGA, PK14F- AAGCCATGAACAAGGAGCTG and PK14R- ACCCGTGATTACCGTCTCTG, PK15F-GCATTCTCTTGGGCACAAC and PK15R- AACCCAGTCCTTGAAGAGC, PK16F- CAAGTGCAGAAATGGAAGC and PK16R-ATGGCCTCGAATAACAATG, PK17F- TGGGAATGGTGGTTCTAAG and PK17R- ATGGCCACCATGAAATTGT, PK18F-AAGCGGGCCTTTGTAAAGAT and PK18R- GTTGGTTCACTGCCTCCAAT

Haplotyping

Haplotyping was done on the LEWES strain and compared to C57BL/6 and BALB/c. The mouse genome informatics database (http://www.informatics.jax.org/) was used to obtain a total of 11 different SNPs in C57BL/6 versus BALB/c that were downstream and upstream of the *Prkdc* gene. Primers were designed flanking these SNP loci using Primer3, and standard *Taq* PCR methods were used to amplify the SNPs. PCR products were purified and sent to Davis sequencing to type each SNP in the LEWES strain.

Primer sequences were: H1F-GCCAGAAGGATTCACCAAAA AND H1R-GGTGACCTGAAGGAGTCTGG, H2F-CAAGCCATCTCACCTTGGTT

AND H2R-TTCATAGCTATCGTCTGCTCCA, H3F-TTGGTTTGTTTGTTCGTTCG AND H3R-GGAAAATAGTGCCTTTTCAAGATG, H4F-ATTGAATTCTTGGCAAATCTCT AND H4R-GAGGAGCAGGGTTTGTTCTG, H5F-GTGGCAGTCCATCTTCCTCT AND H5R-CTGCCCCTTGAAGCTAATCA, H6F-TCAAGGGGCAGTCACACTCT AND H6R-CATGCCAGCTAGCACTGTGT, H7F-CCATGAGAATGCTGAGACCA AND H7R-GCTCATGAGAACATGGTGGA, H8F-ATCTGGGCCCTGGTATCTCT AND H8R-TCAACTTGAGCCTTGCATTG, H9F-TCCCAGGTGTACCCTGTTTC AND H9R-GAAAGGAGCGGCAGTGTTAG, H10F-TTTACCTCCCCCAGATCCTT AND H10R-CTCAGGCTGCTGTCTCAGTG, H11F-GGCTCTCCAGAACCTCACAG AND H11R-GAGGCTGAAGACGATGGAAG

Reverse Transcriptase/Quantitative real-time PCR

Quantitative real-time PCR was used to determine mRNA levels in C57BL/6, BALB/c and LEWES. RNA was isolated and converted into cDNA as described previously. Samples were added to a 96-well plate in triplicate containing a SYBR green mix (Thermo Scientific: QPCR SYBR Green Fluorescein mix; 100 Reactions AB-1219A Thermo Scientific No: AB-1219/A). Standard real-time protocol was done using the BioRad Icycler thermal cycler iQ5. Data was then retrieved and analyzed using Icycler-iQ software version 3.1,

and relative expression was compared between all three strains. *HPRT* (primer set: F-GCTGACCTGCTGGATTACAT and R-TTGGGGCTGTACTGCTTAAC) was used for the internal control. *Prkdc* primers (PRKDC4491F-GCCTGCAGTCTTTGGACCC and PRKDC4564R-TCCTCCAAAACCAAAGGCTAATT) were used for this set of experiments.

Immunoblotting (Western blots)

Mouse primary kidney fibroblasts were lysed using cold lysis buffer (50nM Tris, 150mM NaCl, 2mM EDTA, 2Mm EGTA, 25mM NAF and β-glycerolphosphate (pH 7.5). Freshly prepared detergent and proteinase inhibitors immediately before use (.2% triton X-100, .3% NP40, 0.1mM phenylmethylsulfonyl fluoride, 5ug/mL leupeptin and 5ug/mL aprotinin). Sixty ug of protein lysate was added to 4-15% gradient SDS-PAGE gel (BioRad: 161-1104EDU Tris-HCl Ready Gel Precast Gel, 4–15% linear gradient, 10-well, 30 µl). Electrophoresis was at 125V for 1-1.5 hours then transferred onto nitrocellulose membranes (Amersham Biosciences: Hybond ECL nitrocellulose membrane #RPN78D) in transfer buffer (4.5g Tris base, 21.6g glycine and 300mL to make 1.5L) for 20 hours at 4°C. The membranes were washed 3X's in 1X TBST buffer (25mM Tris, 125mM NaCl and .025% Tween) and incubated in blocking buffer (1X TBST with 5% dry milk) for 1 hour at room temperature. Primary antibody for DNA-PKcs (Neomarkers: DNA-PKcs Ab-4 cocktail mouse monoclonal, #MS-423-P) was added at a 1:500 dilution and incubated at room temperature for 1 hour. Membranes were washed in 1X TBST and secondary

antibody (Amersham: ECL Mouse IgG, HRP-Linked $F(ab')_2$ Fragment [from sheep], # NA9310) was added at a 1:1000 dilution and incubated for 1 hour at room temperature. Membranes were again washed with 1X TBST and incubated with an ECL detection kit (Amersham: ECL plus Western Blotting Detection Reagents, # RPN2132) for 2 minutes. Detection of signal was done using STORM (Molecular Dynamics: STORM 860 Fluor Imager system) and comparison of expression was done using Microsoft Image Quant version 5.1.

DNA DSB repair/γ-H2AX foci

Immunofluorescence was used to detect γ-H2AX foci in mouse primary kidney fibroblasts. Cells were placed in a 4-well chamber slide (Lab-Tech: chamber slide w/ cover, #154526) at approximately a density of 15,000 cells per chamber. They grew for 24 hours and then were synchronized in the G1 phase of the cell cycle using leucine-deprived media (Kato, T, 2007) (provided by Dr. Hatsumi Nagasawa) for another 36 hours. Slides were then fixed in 4% formaldehyde (in PBS) for 6 minutes and washed in PBS. Permeablization buffer (0.2% Triton X-100 in PBS) was added for 6 minutes at room temperature and then blocking buffer (5% dry milk in PBS) was added for 30 minutes at room temperature. Primary antibody (Upstate: p-H2AX Ser139, #05-636) was added at a 1:500 dilution and incubated at room temperature for 1 hour. Slides were washed then secondary antibody (Invitrogen: Mouse IgG Alexafluor 488, #99E2-1) was added at a 1:200 dilution and incubated for 1 hour at room temperature. Slides were washed well with PBS and chambers were removed. DAPI was

added to stain nuclei and mount the slide. At least 50 interphase cells were scored and experiments repeated for a minimum total of 100 cells scored per sample. The averages were calculated and SEM was used for statistical relevance/error bars. The γ-H2AX foci images were analyzed and captured using a Zeiss Axioskop2 plus microscope equipped with a Photometrics Coolsnap ES2 camera and Metavue 7.1 software.

Bystander Experiments

We have developed a straight-forward cell transfer assay to differentiate between the generation and the reception of radiation-induced bystander signals. Donor mouse cells were either sham irradiated or exposed to 1Gy of low LET γ-radiation, trypsinized, rinsed and added to normal human recipient cells at a 1:100 dilution. The co-culture grew for two population doublings, allowing the thymidine analogue 5'-bromodeoxyuridine (BrdU) to incorporate into the DNA. Cells were then harvested (as previously described) to measure sister chromatid exchange (SCE) frequencies using fluorescence-plus-giemsa (FPG; Perry and Wolfe, 1974). After standard cytogenetic preparation, slides were stained with Hoechst dye 33258 (Fisher: Hoechst 33528, #AC22989-1000), treated with 2X SSC at 60°C, rinsed and stained with Giemsa (5% for 10 minutes). Differential (harlequin) staining of the chromatid results; single-substituted strands will be dark and double-substituted strands will be light. A minimum of 25 metaphases were scored and repeated for a total of 50 cells scored. Images were analyzed and

captured using a Zeiss Axioskop2 Plus microscope equipped with a Photometrics Coolsnap ES2 camera and Metavue 7.1 software.

Results

The aim of this study was to determine the effects of the BALB/c-like *Prkdc* SNP located in the kinase domain on radiosensitivity. A number of characterization experiments were done using the LEWES mouse strain to determine the impact of the SNP in the kinase domain. Primary mouse kidney fibroblasts were isolated from C57BL/6ByJ, BALB/cByJ, SCID and LEWES/EiJ female mice. Genomic DNA was extracted and purified from the cells and used for PCR RFLP genotyping. PCR products were purified and digested with either BsmB1 or Hph1 (for the SNP downstream of the leucine zipper or for the SNP in the kinase domain, respectively). The first BALB/c SNP abolishes a BsmB1 site; consequently, DNA from C57BL/6 was digested but BALB/c was not (Fig.1). Digestion of LEWES DNA with BsmB1 yielded similar fragments as seen in C57BL/6. DNA was also cut when BsmB1 was added. The second SNP in BALB/c creates a novel Hph1 site which yields an additional fragment following digestion. As expected, only two fragments were generated when Hph1 was added to C57BL/6; whereas BALB/c yielded three fragments when digested (Fig.1). Similar to BALB/c, LEWES has an additional fragment when cleaved by Hph1. The results indicated that LEWES contains the BALB/c-like SNP in the kinase domain but has the common nucleotide downstream of the leucine zipper. Confirmation of these results was obtained by sequencing the PCR products of all three strains.

The entire coding region of the LEWES *Prkdc* was sequenced to ensure that there were no additional mutations that may affect our results. A total of 19

PCR primer sets were designed to amplify overlapping portions of the *Prkdc* cDNA (Fig.2A). PCR products were then purified, sequenced and compared to the C57BL/6 *Prkdc* cDNA sequence. Our data showed no differences in *Prkdc* sequence between LEWES and C57BL/6 with the exception of the SNP in the kinase domain (Fig.2B).

LEWES was also haplotyped to determine if LEWES shared common ancestry with either C57BL/6 or BALB/c. This was accomplished by selecting a total of 11 additional SNP loci flanking the *Prkdc* gene and polymorphic between the strains from the mouse genome informatics database (http://www.informatics.jax.org/) confirmed all SNPs were different between C57BL/6 and BALB/c. Primers were designed for PCR amplification of regions containing the SNP loci in LEWES. Products were purified, sequenced and compared to both C57BL/6 and BALB/c (Fig.3). A total of 9 SNPs (including the one in the kinase domain) are BALB/c-like, and a total of 4 SNPs are similar to C57BL/6 (including the one downstream of the leucine zipper).

DNA-PKcs protein levels have been shown to be lower in BALB/c than C57BL/6 (Okayasu, 2000); therefore, we decided to compare protein levels of these strains to LEWES. Primary kidney fibroblasts from all three strains were used for immunoblotting and DNA-PKcs signal was quantified using Image Quant software. Results revealed DNA-PKcs levels in LEWES were intermediate between C57BL/6 and BALB/c. Quantitative real time PCR on these strains showed no difference in mRNA levels, suggesting a post-translational event is responsible for reduced DNA-PKcs protein expression. Numerical values on the

DNA-PKcs to actin ratios varied, but the trends remained the same throughout the repeated experiments. On average, the PK: actin value was .90 for C57BL/6, BALB/c was .18 and LEWES was .22.

Previous work has demonstrated that BALB/c is deficient in DNA DSB repair following exposure to low LET γ-radiation (Okayasu, 2000). For this reason, we used the γ-H2AX (Kato, 2006) foci assay to evaluate DNA repair kinetics in LEWES compared to C57BL/6 and BALB/c. Primary kidney fibroblasts from C57BL/6, BALB/c, LEWES and SCID (mice that have a truncated mutation in DNA-PKcs) strains were plated onto chamber slides and synchronized using isoleucine-deprived media. Cells were then irradiated with 1Gy γ-radiation and allowed to repair for 15 minutes, 2 hours or 4 hours. All strains had similar background levels of γ-H2AX foci and showed a similar increase at the 15 minute time interval, indicating that there was no difference in the frequency of DSBs among these strains. As expected, reduced levels of repair were observed in both SCID and BALB/c, with SCID showing a greater deficiency. C57BL/6 demonstrated the greatest amount of repair, followed by LEWES. This data suggests an intermediate response in the LEWES strain.

The ability of LEWES fibroblasts to generate a bystander signal was assessed. We designed a cell transfer approach that utilizes sister chromatid exchange (SCE) frequencies as a marker of the IR-induced bystander effect (BSE), and facilitates discrimination between generation versus receipt of bystander signals. A small number of LEWES donor cells (either 0 or 1Gy) were added to a non-irradiated human cell population (recipient cells). Immediately

following IR exposure (1 Gy ^{137}Cs γ-rays), LEWES donor cells were pelleted and rinsed in PBS to remove any remaining media. The cells were then added at a 1:100 dilution to non-irradiated recipient human dermal fibroblasts (5C HDF). The co-culture was collected following two rounds of replication in the presence of BrdU and scored for SCEs in human cells. Our previous work demonstrated that BALB/c kidney fibroblasts (deficient in DNA-PKcs) were not able to generate an IR-induced bystander response when added to normal human fibroblasts. However, a significant increase in SCE frequency was observed in human cells when irradiated C57BL/6 mouse donor cells (normal DNA-PKcs) were co-cultured, reflective of a bystander response (Hagelstrom, 2008, in press). We used the same approach to determine if LEWES was capable of generating a bystander response (Fig6A). A significant elevation in SCE frequency was seen in the human recipient cells co-cultured with irradiated donor LEWES cells compared to the control unirradiated samples (Figure 6B). The 5C HDF displayed a frequency of 4.22 SCE/ metaphase when unirradiated LEWES donor cells were added and 5.70 SCE/ metaphase when irradiated LEWES donor cells were added. This implies that LEWES strain can generate a bystander response in human cells similar to that observed with C57BL/6.

Discussion

The association between *Prkdc* and susceptibility to IR-induced carcinogenesis has been reported in both humans and mice. One such study suggests a link between DNA-PKcs kinase activity and individuals with lung cancer (Auckley, 2001). Another recent report observed a link between radiation technologists and polymorphisms in *Prkdc* in patients with breast cancer (Bhatti, 2008). This would suggest that point mutations in DNA repair genes, such as *Prkdc*, can potentially have an impact on cancer predisposition in the human population. SNPs in DNA repair genes can also be observed in mice, making the mouse an ideal model to study polymorphisms in DNA repair genes and cancer predisposition. The BALB/c strain is susceptible to spontaneous and IR-induced lung and mammary adenocarcinomas (Ullrich, 1991). This strain also has a hypomorphic variant of DNA-PKcs that is linked to two polymorphisms in the coding sequence of the *Prkdc* gene (Yu, 2001). Currently, our lab is focusing on the significance of the SNPs and what impact they have on the BALB/c phenotype. These studies will give insight as to how point mutations in DNA repair genes can influence carcinogenesis and support the importance of screening individuals to assess cancer risk.

The LEWES strain was utilized to evaluate the impact of the BALB/c-SNP located in the *Prkdc* kinase domain, the presence of which was confirmed by genotyping and sequencing. It was imperative to ensure that there were no additional changes in the cDNA of *Prkdc* that could affect our characterization studies; sequencing confirmed that LEWES has identical *Prkdc* sequence to

C57BL/6 with the exception of the kinase domain SNP. We also sequenced SNP loci surrounding *Prkdc* to determine if LEWES shares a similar lineage with either C57BL/6 or BALB/c. Results were interesting but offered no straightforward answer. The region upstream of LEWES *Prkdc* has one C57BL/6-like SNP while the remaining 7 SNPs were BALB/c-like. Only one BALB/c-like SNP and 2 C57BL/6 SNPs are downstream of the gene. These mixed results could indicate that LEWES does not share a common lineage with either C57BL/6 or BALB/c. Another possibility would be that LEWES is related to both strains and that a recombination event occurred in *Prkdc*. Either case is intriguing in that the kinase domain SNP occurred independently on two different backgrounds and was potentially selected for in nature. This observation may be of potential importance when considering relevance to the human population.

We selected a number of different radiobiological end-points to characterize the LEWES mouse: DNA-PKcs protein levels, *Prkdc* mRNA expression, DNA DBS repair kinetics and the BSE. DNA-PKcs protein expression in LEWES was quantified and compared to C57BL/6 and BALB/c. Protein expression in LEWES is intermediate between C57BL/6 and BALB/c; in fact, protein levels were closer to BALB/c. These data imply that the kinase domain SNP is partly responsible for the reduced DNA-PKcs levels in BALB/c. Quantitative real-time PCR data show no differences in mRNA expression between all three mouse strains, suggesting the decrease in DNA-PKcs protein is due to a post-translational event.

Utilizing γ-H2AX foci as a marker is a simple and well accepted method to measure DSB repair (Kato T, 2007). We used an acute dose of 1Gy γ-radiation and allowed cells to repair for 15 minutes, 2 hours and 4 hours. At the 4 hour post-irradiation time point, 65% of DSBs were repaired in C57BL/6, 56% in LEWES, 43% in BALB/c and 24% in SCID. LEWES displays better repair capacity than BALB/c but is not as efficient as C57BL/6, demonstrating another intermediate response. These data shows that perhaps both BALB/c-like SNPs are needed for the lack of repair seen in BALB/c. Alternatively, it may also indicate that another unknown allele interacts with DNA-PKcs for optimal activity that is hindered by the kinase domain SNP. Definitive resolution of these possibilities requires further study.

The bystander effect was examined in LEWES using SCE frequency as an end-point. We have previously shown that mice lacking DNA-PKcs were not able to generate a bystander effect in normal human fibroblasts (manuscript in press, Oncogene, 2008). LEWES kidney fibroblasts were irradiated and added to 5C normal human dermal fibroblasts (5C). The 5Cs were harvested after 2 population doublings and scored for SCEs. Normal levels of SCEs were observed in 5Cs cultured with non-irradiated LEWES cells; however, a significant elevation in SCE frequency was detected following culture with irradiated LEWES cells. This indicates that the *Prkdc* kinase domain SNP does not affect the capacity to generate a bystander signal.

The LEWES strain was only recently derived from wild mice, yet it possesses the same *Prkdc* SNP in the kinase domain as BALB/c. It is entirely

possible that these SNPs occurred independently in two different populations rather than once in a common ancestor. This makes LEWES an ideal strain to analyze the impact of the kinase domain SNP in IR-induced radiosensitivity and mammary carcinogenesis. Our results show that LEWES has intermediate DNA-PKcs levels and intermediate DSB repair capacity between C57BL/6 and BALB/c. In addition, LEWES is capable of generating a bystander response, similar to C57BL/6, which has the common allele. These results support the concept that each BALB/c *Prkdc* SNP plays a unique role, and so has different consequences. In addition, BALB/c may also have a modifying gene that, with the hypomorphic DNA-PKcs, influences the IR-sensitive phenotype. It appears that both SNPs are necessary for the complete BALB/c phenotype to be expressed, as we observed an intermediate level of protein expression and DSB repair in LEWES.

These studies have provided insight into consequences of the BALB/c *Prkdc* kinase domain SNP, but not much is known about the BALB/c-like SNP located downstream of the leucine zipper. Future studies will focus on generating knock-in mice that contain one or both of the BALB/c-like SNPs, definitively defining the significance and roles of each SNP. Our goal is to gain greater mechanistic perspective as to how IR-induced mammary carcinogenesis occurs in BALB/c mice. Better comprehension of this mouse model and the consequences of its *Prkdc* SNPs enlighten the importance of SNPs in the genome and how they may influence genetic predisposition to cancer.

Figures

Figure 1: RFLP genotyping

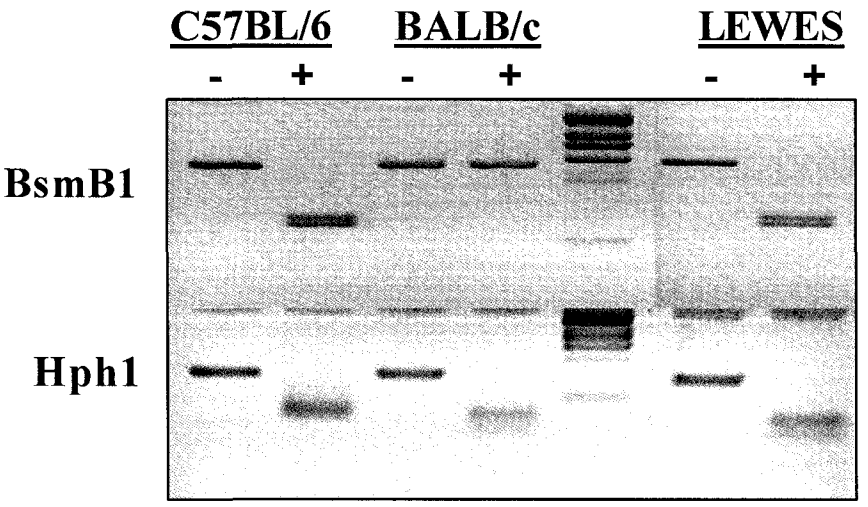

Figure 2: LEWES cDNA sequencing

A.

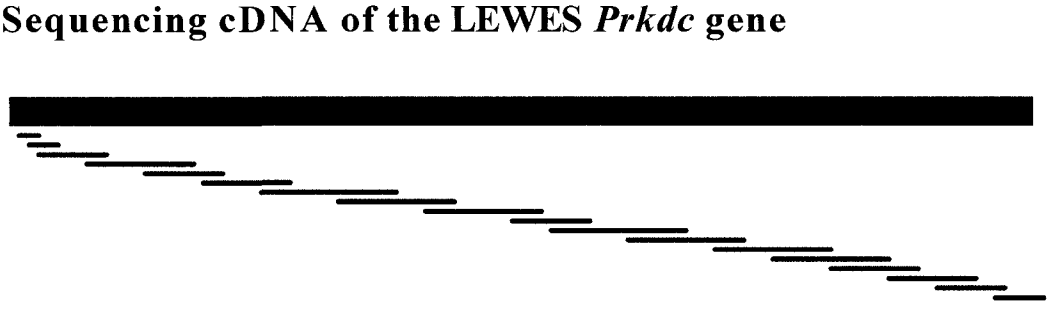

B.

Figure 3: Haplotyping

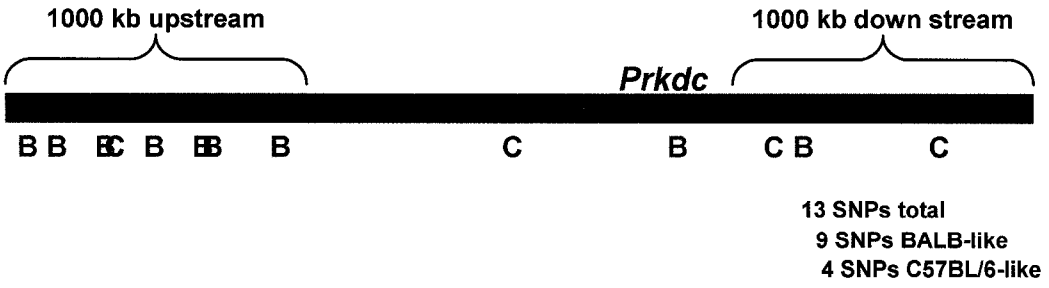

Figure 4: Protein expression

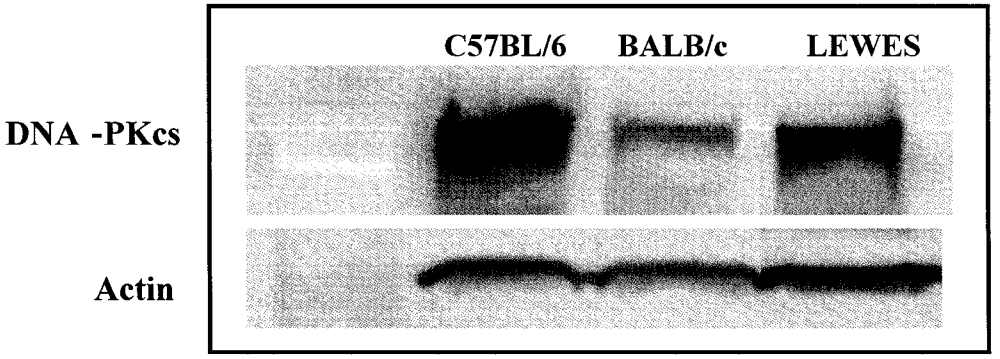

Figure 5: DNA DBS repair

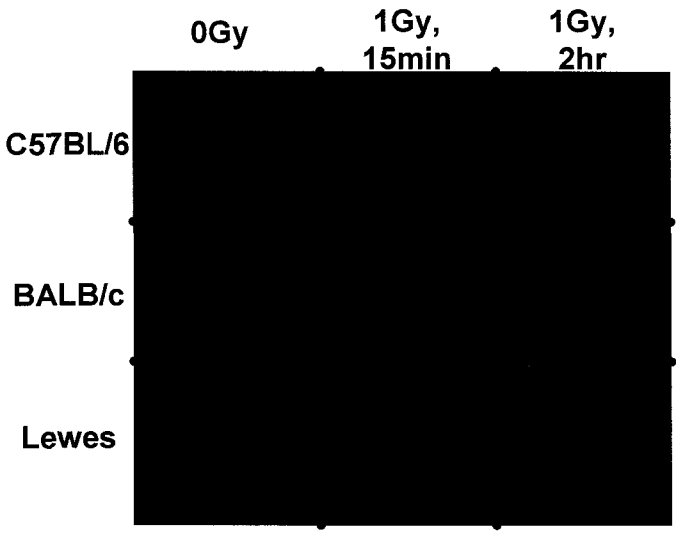

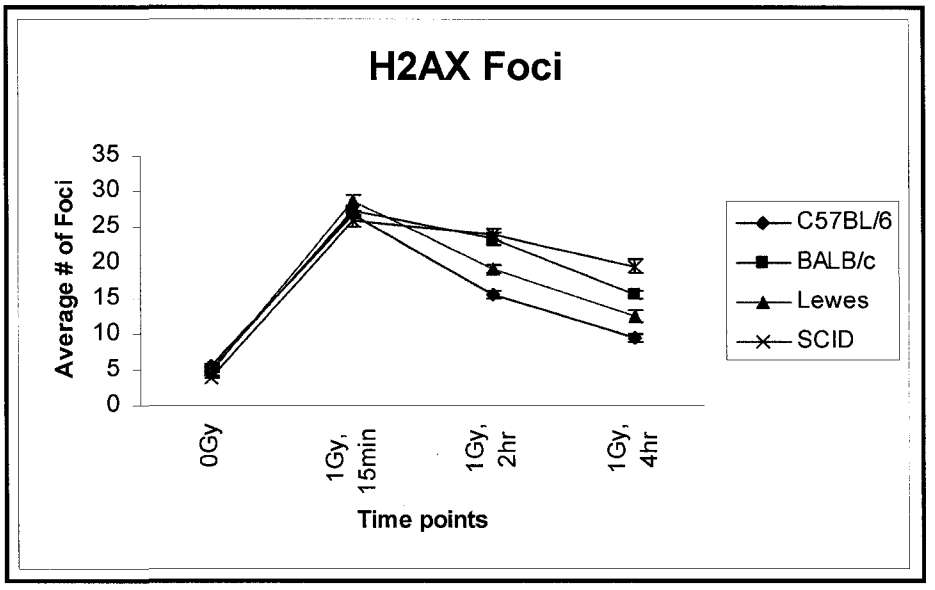

Figure 6:

A.

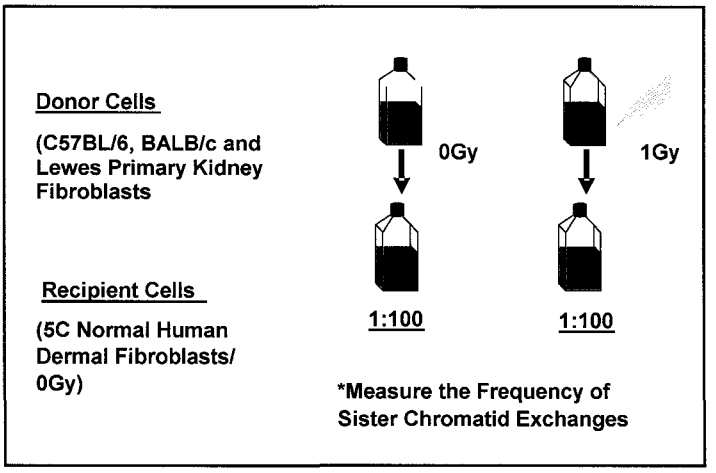
Donor Cells
(C57BL/6, BALB/c and Lewes Primary Kidney Fibroblasts
Recipient Cells
(5C Normal Human Dermal Fibroblasts/ 0Gy)
0Gy
1Gy
1:100
1:100
*Measure the Frequency of Sister Chromatid Exchanges

B.

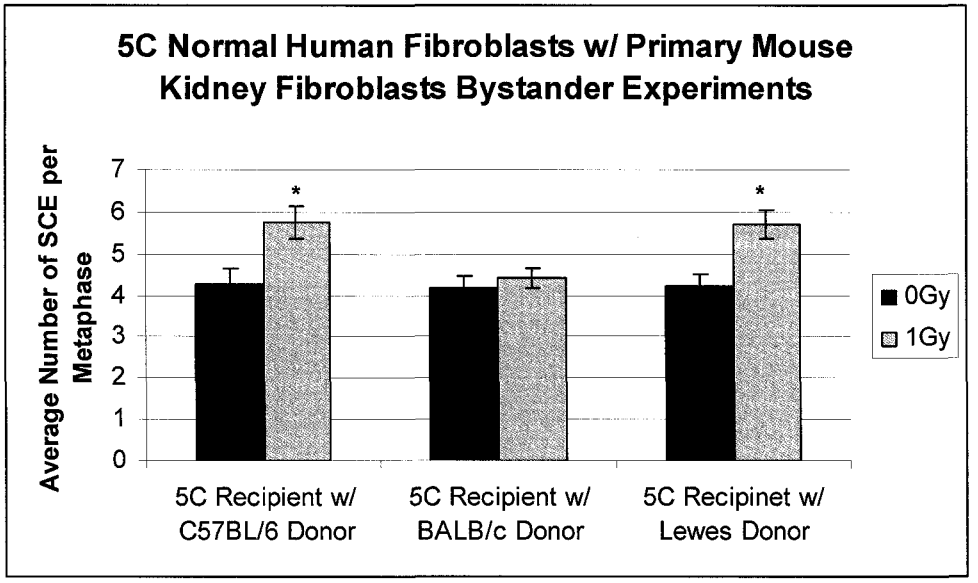
5C Normal Human Fibroblasts w/ Primary Mouse Kidney Fibroblasts Bystander Experiments
Average Number of SCE per Metaphase
0
1
2
3
4
5
6
7
*
*
0Gy
1Gy
5C Recipient w/ C57BL/6 Donor
5C Recipient w/ BALB/c Donor
5C Recipinet w/ Lewes Donor

Figure legends

1. Genotyping using the PCR RFLP method. PCR products from both SNP loci were purified and digested with BsmB1 (for the SNP downstream of the leucine zipper) or Hph1 (for the SNP in the kinase domain). The first SNP aboloshes a BsmB1 site, so the BALB/c fragment was not digested. Both C57BL/6 and LEWES have the common allele and were cleaved with BsmB1. The second SNP creates a novel Hph1 site. Only one cut occurred in C57BL/6 DNA, but BALB/c and LEWES DNA yielded an extra digested fragment. This gel demonstrates that LEWES has the BALB/c allele in the kinase domain but not the SNP found downstraem of the leucine zipper.

2. A. A schematic showing how the primers were designed and chosen for LEWES *Prkdc* cDNA sequencing.

B. A schematic showing either the common nucleotide or SNPs at the designated loci in all 3 strains.

3. Haplotyping results show that LEWES has both C57BL/6 and BALB/c SNPs upstream and downstream of the Prkdc gene. This would suggest that LEWES does not definitively share common ancestry with either strain. Another possibility is that it shares common lineage with both and that there was recombination and a separate sponateous SNP event that occurred in *Prkdc* over time.

4. Immunoblotting demonstrates that LEWES DNA-PKcs protein expression is intermediate between C57BL/6 and BALB/c. Multiple blots were performed and compared to the loading control actin. Quantitative comparison was done using Image Quant.

5. Immunofluorescence was done to examine DSB repair. Primary mouse kidney fibroblasts were synchronized using isoleucine-deprived media and the exposed to 1Gy γ-rays and allowed to repair for 15 minutes, 2hours and 4 hours. Results show that C57BL/6 was the most efficient in DNA repair, followed by LEWES. Both BALB/c and SCID were defiecent in repair, with SCID showing less repair. These results show that LEWES DSB repair is intermediate compared to C57BL/6 and BALB/c.

6. Bystander experiments were performed to determine if LEWES was more similar to C57BL/6 or BALB/c in generating a bystander signal. Control and irradiated donor mouse cells were added to normal human dermal 5C cells. SCEs were measured as an end-point for the bystander effect. Both C57BL/6 and LEWES were capable of generating a bystander effect, but BALB/c was not.

References

1. Antoniou, AC and DF Easton. Models of genetic susceptibility, Oncogene, 250, 5898-5905, 2006

2. Auckley DH, Crowell RE, Heaphy ER, Stidley CA, Lechner JF, Gilliland FD and Belinsky SA; Reduced DNA-dependent protein kinase activity is associated with lung cancer, Carcinogenesis, 22, NO 5, 723-727, 2001

3. Baeyens, A.; Thierens, H.; Claes, K.; Poppe, B.; Messiaen, L.; Ridder, L. and Vral, A. Chromosomal radiosensitivity in breast cancer patients with a known or putative genetic predisposition, British Journal of Cancer, 87, 1379-1385, 2002

4. Bailey SM, Goodwin EH and Cornforth MN; Strand-specific fluorescence *in situ* hybridization: the CO-FISH family, Cytogenet Genome Res, 107, 2004, 14-17

5. Bailey SM, Brenneman MA, Halbrook J, Nickoloff JA, Ullrich RL and Goodwin EH. (2004). *DNA Repair (Amst)*, 3, 225-33.

6. Bailey SM, Cornforth MN, Kurimasa A, Chen DJ and Goodwin EH. (2001). *Science*, 293, 2462-5.

7. Bailey SM, Meyne J, Chen DJ, Kurimasa A, Li GC, Lehnert BE and Goodwin EH. (1999). *Proc Natl Acad Sci U S A*, 96, 14899-904

8. Bhatti P, Stuewing JP, Alexander BH, Hauptmann M, Bowen L, et al.; Polymorphisms in DNA repair genes, ionizing radiation exposure and risk of breast cancer in US radiologic technologists, Int. J. Cancer, 122, 177-182, 2008

9. Boice, J. Radiation and breast carcinogenesis, Medical and Pediatric Oncology, 36, 508-513, 2001

10. Collis, S.; DeWeese, T.; Jeggo, P. and Parker, A. The life and death of DNA-PKcs (review), Oncogene, 1-13, 2004

11. Cornforth MN, Bedford JS; A quantitative comparison of potentially lethal damage repair and rejoining of interphase chromosome breaks in low passage normal human fibroblasts; Radiat Res, 111, 385-405, 1987

12. Hagelstrom RT, Askin KF, Williams AJ, Ramaiah L, Desaintes C, Ullrich RL and Bailey SM; DNA-PKcs and ATM influence generation of ionizing radiation-induced bystander signals

13. Hartley, K.; Gell, D.; Smith, G.; Zhang, H.; Divecha, N.; Connelly, M; Admon, A.; Lees-Miller, S.; Anderson, C. and Jackson, S. DNA-dependent

protein kinase catalytic subunit: a relative of PI3-kinase and the ATM gene product, Cell, 82, 849-856, September 8, 1995

14. Helleday, T.; Pathways for mitotic HR in mammalian cells, Mutation Research, 532, 103-115, 2003.

15. Hoeijmakers, J. Genome maintenance mechanisms for preventing cancer, Nature, 411, 366-374, May 17, 2001

16. Kato TA; Nagasawa H., Weil MM, Little JB, Bedford JS; Levels of gamma-H2AX Foci after low-dose-rate irradiation reveal a DNA DSB rejoining defect in cells from human ATM heterozygotes, Radiat Res. 2006 Sep;166(3):443-53

17. Lengauer, C et al. Genetic instabilities in human cancers, Nature, 396, 643-648, 1998

18. Morgan; Genomic instability induced by ionizing radiation, 146, 247-258

19. Munro TR; The relative radiosensitivity of the nucleus and cytoplasm of the Chinese hamster fibroblasts; Radiat Res, 42, 451-470, 1970.

20. Okayasu R, Suetomi K, Yu Y, Silver A, Bedford JS, Cox R and Ullrich RL; A deficiency in DNA repair and DNA-PKcs expression in the radiosensitive BALB/c mouse, Cancer Research, 60, 4342-4345, 2000

21. Scott, D Chromosomal radiosensitivity and low penetrance predisposition to cancer, Cytogenetics Genome Research, 104, 365-370, 2004

22. Smider, V and Chu, G. The end-joining reaction in V(D)J recombination, Immunology, 9 187-197, 1997

23. Smith, G.; and Jackson, S. The DNA-dependent protein kinase (Review), Genes and Development, 13, 916-934, 199

24. Smith, T.; Miller, M.; Lohman, K.; Case, L. and Hu, J. DNA damage and breast cancer risk, 24, No.5, 883-889, 2003

25. Ullrich, R.L. Cellular and Molecular changes in mammary epithelium following irradiation, Radiation Research, 128, S136-S140, 1991

26. Ullrich RL, Bowles ND, Satterfield LC and Davis CM; Strain-dependent susceptibility to radiation-induced mammary cancer is a result of differences in epithelial cell sensitivity to transformation, Radiat Res, 146, 353-355, 1996

27. Venkitaraman, A. Functions of BRCA1 and BRCA2 in the biological response to DNA damage, Journal of Cell Science, 114, 3591-3598, 2001

28. Ward JF; DNA damage produced by ionizing radiation in mammalian cells, Prog Nucleic Acis Res Mol Biol, 35, 95-125, 1988

29. Wenham, R.; Schildkraut, J.; McLean, K.; Calingaert, B.; Bentley, R.; Marks, J. and Berchuck, A. Polymorphisms in BRCA1 and BRCA2 and risk of epithelial ovarian cancer, Clinical Cancer Research, 9, 4396-4403, 2003

30. Yu Y, Okyasu R, Weil MM, Silver A, McCarthy M, Zabriskie R, Long S, Cox R and Ullrich RL; Elevated breast cancer risk in irradiated BALB/c mice associates with unique functional polymorphisms of the *Prkdc* gene, Cancer Research, 61, 1820-1824, 2001

Chapter 5

The Knock-in mouse project/Constructing targeting vectors

Introduction

Sequence variations at single bases can occur throughout the genome via DNA replication, DNA repair, endogenous insults (free radicals) and exogenous insults (chemicals, radiation) (http://www.ncbi.nlm.nih.gov/). The majority of such single nucleotide polymorphisms (SNPs) are thought to be inconsequential; however, some point mutations may influence an individual's predisposition to a variety of diseases. The relationship between breast cancer and point mutations in DNA repair genes is a prime example in which research has demonstrated links between SNPs and genetic predisposition (Fu, Y., 2003; Pepe, M. & Janes, H., 2008; Hsieh, S., 2007; Bartsch, H., 2007).

Numerous reports have described polymorphisms in the base excision repair (BER) gene, XRCC1, that correlate to breast cancer risk (Duell, E ., 2001). Other studies have examined an association between SNPs in the nucleotide excision repair (NER) gene, ERCC2 and breast cancer incidence (Bernard-Gallon, D., 2008). A recent study has shown that the non-homologous end-joining (NHEJ) gene *Prkdc* also can impact breast cancer risk in individuals (Bhatti, 2008).

Prkdc encodes the protein DNA-dependent protein kinase catalytic subunit (DNA-PKcs), a key component of DNA double-strand break (DSB) repair, V(D)J recombination, telomere maintenance and the bystander effect (Yu, Y., 2001; Finnie, N., 1995; Dai, Y., 2003; Ma, Y., 2002; Bailey, S., 2004; Hagelstrom, R., [manuscript in press, Oncogene]). Mouse models have shown that deficiency in DNA-PKcs can lead to suppressed immune responses and sensitivity to ionizing

radiation-induced carcinogenesis (Danska, J., 1996; Adams, L., 1987; Ullrich, R., 1996).

The BALB/c strain has a hypomorphic variant of DNA-PKcs. BALB/c has decreased DNA-PKcs expression, reduced kinase activity, deficient DNA DSB repair, and lack in cell-to-cell communication via the bystander effect (Okayasu, R., 2000; Hagelstrom, R., [manuscript in press]) and improper telomere maintenance (Williams, E., [manuscript submitted]). Yu et al. discovered two SNPs located in the coding region of *Prkdc* that may be responsible for the BALB/c phenotype (Yu, Y., 2001). One SNP is located in exon 48, which is positioned between a leucine zipper domain and an autophosphorylation cluster. This SNP is in a highly conserved region and may impact DNA-protein or protein-protein interaction due to the relatively close vicinity of the leucine zipper. Another possibility is that it may affect the ability of DNA-PKcs to autophosphorylate, an event crucial for proper enzymatic activity (Block, W., 2004). The second SNP position is near the C-terminal domain in exon 81. This codon is not conserved among species; however, it is located in the kinase domain and may affect enzymatic activity.

These SNPs in $Prkdc^{BALB/c}$ are linked to the BALB/c radiosensitive phenotype; however, it is not known which SNP is responsible for the BALB/c radiosensitive phenotype. This was previously examined utilizing the LEWES/EiJ (LEWES) mouse strain, which was derived from wild mice and has only the kinase domain SNP (Askin, K., [manuscript in progress]). Characterization of LEWES revealed intermediate results between BALB/c and

C57BL/6, which has the common variant of *Prkdc*, in DNA-PKcs levels and DNA repair, but no differences were observed in the bystander effect compared to C57BL/6.

These studies give insight into the impact two point mutations can have on genetic predisposition to radiation-induced mammary cancer in BALB/c; however, they do not definitively give an explanation as to which SNP is responsible for the BALB/c phenotype, or if they are both needed or if they are needed at all. Other factors could potentially play a role such as genetic background; therefore, we are now focusing on generating knock-in mice (Fig.1). This technique is extremely effective in giving definitive results as to the impact a single base change can make in a mouse system. This process involves generating a targeting vector designed to contain a specific base change. The vector is then transfected into mouse ES cells and individual ES cell colonies resulting from the transfection are assayed for the appropriate insertion. Once positive colonies are selected and tested, the targeted ES cells are injected into mouse blastocysts which are then implanted into pseudo-pregnant mice. The chimeric progeny are genotyped to identify those that carry the desired sequence. Male progeny with the change are then backcrossed to female mice from the 129 strain from which ES cells originated. The progeny are be genotyped to test for the conversion then bred to achieve homozygosity at the SNP loci.

The 129 mouse strain variant 129S1/Sv-+^{p}+$^{Tyr\text{-}c}$*Kitl*$^{Sl\text{-}J/+}$ (129S1) were genetically contaminated (breeding error) with BALB/c and have both polymorphisms. Another benefit is that two separate ES cell lines were derived

from the 129S1 strain. This is advantageous because we will be able to use these ES cells to create knock-in mice that will convert these SNPs back to the common sequence variant and determine if this could "rescue" the BALB-like phenotype in the 129S1 strain. Our goal is to generate two groups of knock-in mice, one strain containing only the kinase domain SNP in exon 81 and one strain having the SNP in exon 48. These mice will provide insight into which of these SNPs in the *Prkdc* DNA repair gene does in fact impact cancer susceptibility in the BALB/c mouse strain. Such knowledge is crucial and can be translated to the human population because it justifies the need for developing efficient, reliable SNP screening systems for individuals that would determine genetic predisposition to certain cancers.

Figure 1

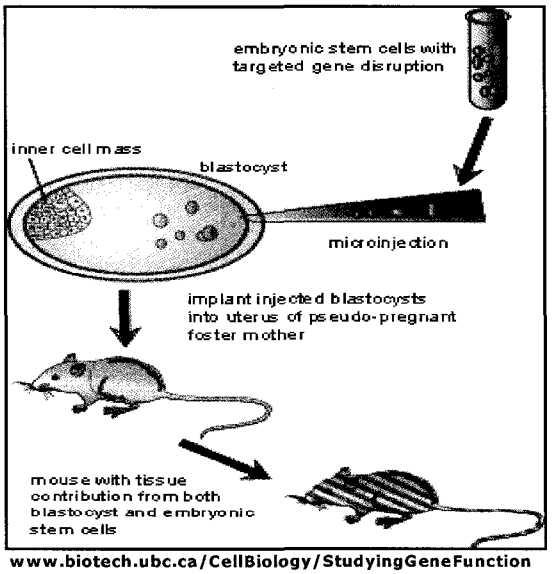

Figure 1: Blastocysts injection. Once a vector has been incorporated correctly into the genome of the embryonic stem cells, the cells are expanded in culture and injected into 3.5 day old mouse blastocysts. The blastocysts are injected into the uterus of a pregnant female and the embryos are allowed to come to term. Mice with brown coat color are selected and bred to make pure knockout mice.
http://www.bioteach.ubc.ca/CellBiology/StudyingGeneFunction/

Methods & Materials

Mice and cell culture

C57BL/6, BALB/c and 129S1 female mice (2-3 months in age) were obtained from Jackson Laboratories (Stock# - 000090 Strain name – 129S1/Sv-$+^{p}+^{Tyr\text{-}c}Kitl^{Sl\text{-}J}$/+, Stock# - 000664 Strain name - C57BL/6ByJ and Stock# - 000650 Strain name - BALB/cByJ). Primary kidney fibroblasts were isolated using standard protocols. Kidneys were minced and placed in α-MEM media containing collagenase (Worthington Type III; 200 units/ml) at 37°C for 3–5 h with gentle agitation. Disaggregated cells were washed six times in phosphate buffered saline (PBS) containing 0.5% fetal bovine serum (FBS) and cultured in complete α-MEM medium (15% FBS, penicillin/streptomycin). Media was changed after 3 days of incubation. Cells were kept in culture at 37°C with 5% CO_2 and passaged when confluent, are trypsinized to dissociate the cells and placed in fresh complete α-MEM media.

DNA/RNA/cDNA isolation & purification

DNA and RNA from primary mouse kidney fibroblasts were extracted and purified using Qiagen kits (Qiagen: DNeasy blood & tissue kit, #69506 & RNeasy kit #74104). The cDNA was isolated and purified using RNA and an iScript cDNA synthesis kit (BioRad: iScript select cDNA synthesis kit, #170-8896). All PCR products were either purified by a PCR purification kit or a gel extraction kit (Qiagen: QIAquick PCR purification kit #28104 or QIAquick gel extraction kit, 28704).

Genotyping

The restriction fragment length polymorphism (RFLP) method was used to genotype all mouse strains. The first SNP located downstream of the leucine zipper abolishes a BsmB1 site. PCR primers (PKF-GCCTAAGGTAAGGTGCTGTA & PKR-GCCATGATCCTTAGCAAGTG) were designed flanking the SNP location and amplified using *Taq* polymerase (Invitrogen; *Taq* DNA polymerase, Recombinant 10342-020). PCR conditions were: stage 1-1 cycle at 94°C for 4 minutes; stage 2- 30 cycles with 94°C for 30 seconds, 55°C for 30 seconds, 72°C for 30 seconds; stage 3- 1 cycle at 72°C for 7 minutes, then held at 4°C.

The purified PCR product was then digested with BsmB1 and corresponding buffer (NEB; #R0580) at 55°C for 2 hours. The second SNP in the kinase domain creates a novel Hph1 site. Primers (81F-ATGTTCTTTGCCATGCAGT & 81R-TTCTTCCCTCCCTTCTCAGTA) were used to amplify the region containing the SNP. The PCR product was digested with Hph1 and corresponding buffer (NEB; #R0158) at 37°C for 2 hours. Size was detected for both sets of digested product using a 3% agarose gel.

Real-time PCR

Real time PCR was done on C57BL/6, BALB/c and 129S1 to ensure that *Prkdc* mRNA levels were the same. RNA was isolated and converted into cDNA as described previously. Samples were added to a 96-well plate in triplicate containing a SYBR green mix (Thermo Scientific: QPCR SYBR Green

Fluorescein mix; 100 Reactions AB-1219A

Thermo Scientific No: AB-1219/A). Standard real-time protocol was done using the BioRad Icycler thermal cycler iQ5. Data was then retrieved and analyzed using

Icycler-iQ software version 3.1, and relative expression was compared between all three strains. *HPRT* (primer set: F-GCTGACCTGCTGGATTACAT & R-TTGGGGCTGTACTGCTTAAC) was used for the internal control. DNA-PKcs primers (PRKDC4491F-GCCTGCAGTCTTTGGACCC & PRKDC4564R-TCCTCCAAAACCAAAGGCTAATT were used for this set of experiments.

Immunoblotting (Western blots)

Mouse primary kidney fibroblasts were lysed using cold lysate buffer (50nM Tris, 150mM NaCl, 2mM EDTA, 2Mm EGTA, 25mM NAF and β-glycerolphosphate (pH 7.5). Freshly prepared detergent and proteinase inhibitors were added immediately before each use (.2% triton X-100, .3% NP40, 0.1mM phenylmethylsulfonyl fluoride, 5ug/mL leupeptin and 5ug/mL aprotinin). Sixty ug of protein lysate was added to 4-15% gradient SDS-PAGE gel (BioRad: 161-1104EDU Tris-HCl Ready Gel Precast Gel, 4–15% linear gradient, 10-well, 30 µl). Gels were electrophoresed at 125V for 1-1.5 hours then transferred onto nitrocellulose membranes (Amersham Biosciences: Hybond ECL nitrocellulose membrane #RPN78D) in transfer buffer (4.5g Tris base, 21.6g glycine and 300mL to make 1.5L) for 20 hours at 4°C. The membranes were washed 3X's in 1X TBST buffer (25mM Tris, 125mM NaCl and .025% Tween) and incubated in

blocking buffer (1X TBST with 5% dry milk) for 1 hour at room temperature. Primary antibody for DNA-PKcs (Neomarkers: DNA-PKcs Ab-4 cocktail mouse monoclonal, #MS-423-P) was added at a 1:500 dilution and incubated at room temperature for 1 hour. Membranes were washed in 1X TBST and secondary antibody (Amersham: ECL Mouse IgG, HRP-Linked $F(ab')_2$ Fragment [from sheep], # NA9310) was added at a 1:1000 dilution and incubated for 1 hour at room temperature. Membranes were again washed with 1X TBST and incubated with an ECL detection kit (Amersham: ECL plus Western Blotting Detection Reagents, # RPN2132) for 2 minutes. Detection of signal was done using the horseradish peroxidase (HRP) conjugate and the STORM (Molecular Dynamics: STORM 860 Fluor Imager system) system. Comparison of expression was done using Microsoft Image Quant version 5.1.

Bacterial Transformation

Bacterial transformation was carried out using DH5α competent cells and a heat shock protocol (Invitrogen: Subcloning Efficiency Competent Cells, #18265-017). Competent cells were thawed on ice, and then mixed with plasmid (not exceeding 10ng). The mix was incubated on ice for 0.5-1 hour, then placed in a 40°C water bath for 30 seconds and then immediately placed on ice for 10 minutes followed by addition of 1mL Luria-Bertani (LB: tryptone, yeast extract and NaCl) media and an incubation at 37° for 1 hour with shaking. Bacteria were then plated on LB agar plates containing ampicillin (20ug/mL) and incubated overnight at 37°C.

Plasmid extraction from bacterial cells

Individual colonies were selected from agar plates and grown in LB media containing ampicillin (20ug/mL) at 37°C for 12-16 hours. Plasmid DNA was extracted and purified using either Qiagen Miniprep (#27106) or Qiagen Midiprep (#12143) kits. DNA concentration was obtained using a Nanodrop spectrometer (NanoDrop Technologies, Inc.: ND-1000 Spectrophotometer).

BAC DNA

Bacterial artificial chromosome (BAC) DNA was selected using the Ensembl Genome database (http://www.ensembl.org/index.html). Clone DNA (bMQ292i03 for first and bMQ297c10 for the second SNP) was obtained through the Wellcome Trust Sanger Institute (www.sanger.ac.uk).

Molecular Cloning

A number of enzymes and corresponding buffers were used in creating both targeting vectors. Restriction endonucleases used were EcoR1, Not1, Pac1, BamH1, HindIII, Sal1, BsmB1, Ahd1, Acc651 and Pst1 (New England BioLabs.) All incubations were carried out and then heat inactivated according to the manufacture's recommended protocol. Digested product was then purified as previously described.

Cloning enzymes i.e. ligase, shrimp alkaline phosphatase (SAP), calf intestinal phosphatase (CIP), T4-polynucleotide kinase (T4-PNK) and PolI Klenow fragment (New England BioLabs) were utilized. All reactions were done

using recommended protocols, followed by heat inactivation and DNA purification.

pACN Vector

The targeting cassette chosen for this project is referred to as pACN (Bunting, M., 1999).

Long-range PCR

The high-fidelity DNA polymerase *PfuUltra* (Stratagene: #600382) was used to create the *Prkdc* homologous "left and right arms" for the targeting vectors. PCR conditions were: stage 1-1 cycle at 95°C for 2 minutes; stage 2- 30 cycles with 95°C for 35 seconds, 62°C for 40 seconds, 72°C for 4:00; stage 3- 1 cycle at 72°C for 5 minutes, then held at 4°C. PCR product was then purified and ran on a .8% agarose gel to confirm the product sizes were those expected from published sequences. Primers were designed that surround the SNP regions. Restriction site sequence was added onto the 5' ends of the primers so that the PCR product could be cloned into the targeting vectors. Primer sequences were: 48LASal1F-TCTTTGTCGACtggaaaatctgggtgtcctc, 48LASal1R-TCTTTGTCGACgacggtcagaactgcacaga, 48RAPac1F-CTCTTTTAATTAAtcatgttcttccgagtgctg, 48RAPac1R-CTCTTTTAATTAAaaggaattgagcacccaca, 81LASal1F-AACGCGTCGACtcctcaggagataaaaggacca, 81LASal1R-AACGCGTCGACgaaccatggtctaaagccactc, 81RANot1F-

CATGAGGTTGCGGCCGCtgttggaatcccaaagaagat, and 81RANot1R-CATGAGGTTGCGGCCGCcccacgttgtgttttcactatg.

DNA Sequencing

A portion of completed targeting vectors were sequenced by Davis Sequencing (http://www.davissequencing.com/pricing.htm) to confirm correct insertions and orientations of cloned portions. Primers used were: RAF-1: GTTTTCCCAGTCACGACGTT, RAF-2: TAAAACGACGGCCAGTGAA, RAR-1: AGGGGATCGGCAATAAAAAG, RAR-2: GTGTTGGGTCGTTTGTTCG, LAF-1: GAGGTCTCTGTGAGGCTGGT, LAF-2: GCCCATGGAGATCCATAAC, LAR-1: AATCAGGTAGGCATGCTGCT, LAR-2: CTCAGGGAAGGTCCTTGAC, 81LA-1: CGCGAGCTCGAGATCTAGAT, 81LA-2: TATAAGCTTTCGCGAGCTCG, 81RA-1: CGAATTGGAGCTCGAGATCT, 81RA-2: CTATAGGGCGAATTGGAGCTC, TK-1: GACCATGATTACGCCAAGCT, TK-2: ACCATGATTACGCCAAGCTC

Isolation of DNA from clones

Genomic DNA was isolated from CJ7 embryonic stem (ES) cells derived from the 129S1 strain. Transfected ES colonies containing the desired targeting vector were grown in 24-well plates. Wells were rinsed with 1mL of PBS followed by addition of 300uL digestion buffer (100mMTris-HCl, pH 8.3;

200mM NaCl; 5mM EDTA, 20uM SDS and 1uL of 10mg/mL proteinase K per 100uL of buffer). The digestion was incubated at 55°C for 3-5 hours in a humid chamber. The reaction was deactivated by 15 minute 80°C incubation. The standard sodium acetate/ethanol procedure was used to precipitate the DNA, which was then re-suspended in water.

Results

There was a possibility that a sub-strain of the 129/SvJ mouse strain was genetically contaminated with BALB/c. We tested the "contaminated" 129S1/SvJ (129S1) substrain and the ES cell lines (CJ7 & W9.5) derived from 129S1 to determine if it has the two BALB/c SNPs in *Prkdc*. Genomic DNA from kidney tissues of the C57BL/6, BALB/c, 129S1 were extracted and purified, and DNA from the 129S1 ES cell lines (CJ7 and W9.5) were commercially obtained (Jackson Laboratories) and used for RFLP genotyping. PCR was done to amplify regions in *Prkdc* that contained the SNPs. The products were purified and digested with either BsmB1 or Hph1 (for the SNP downstream of the leucine zipper or for the SNP in the kinase domain, respectively). The first BALB/c SNP abolishes a BsmB1 site; consequently, DNA from C57BL/6 was digested but BALB/c was not (Fig.1). There was no digestion with BsmB1 on 129S1, CJ7 or W9.5 samples, similar to BALB/c. The second SNP in BALB/c creates a novel Hph1 site which yields an additional fragment following digestion. As expected, only two fragments were generated when Hph1 was added to C57BL/6; whereas BALB/c yielded three fragments when digested (Fig.2). Like BALB/c, the digests from 129S1, CJ7 and W9.5 had an additional fragment when processed by Hph1. The data illustrated that 129S1 and its corresponding stem cell lines have both BALB/c-like SNPs in the 129S1 *Prkdc* gene. Confirmation of these results was done by sequencing PCR products of all samples.

Figure 2

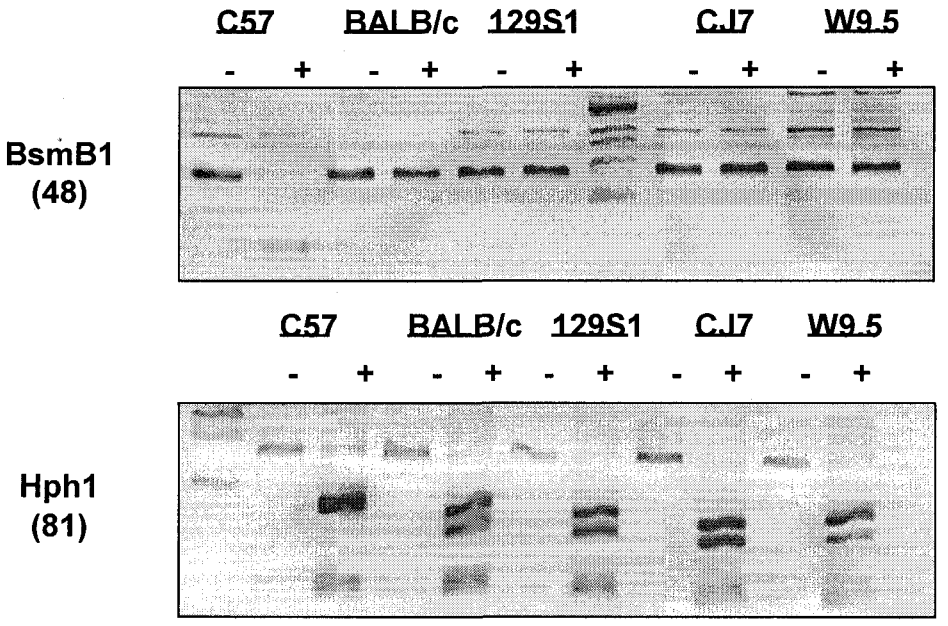

Figure 2: Genotyping. The C57BL/6 strain contains the common alleles at the SNP loci. BALB/c, 129S1 and its derived ES cell lines (CJ7 & W9.5) all have the BALB/c-like SNPs. The SNP in exon 48 abolishes a BsmB1 site. The second SNP in exon 81 creates a new Hph1 site which yields an additional digested fragment.

The *Prkdc* product, DNA-PKcs protein expression has been shown to be deficient in BALB/c compared to C57BL/6 mice (Okayasu, 2000); therefore, we decided to compare protein expression of these strains to 129S1 which carries the BALB/c allele of *Prkdc*. Primary kidney fibroblasts from all three strains were used for immunoblotting and quantified using Image Quant software. Results revealed diminished DNA-PKcs expression in 129S1, similar to BALB/c (Fig.3). Quantitative real time PCR on these strains showed no difference in mRNA expression (data not shown), suggesting a post-translational event.

Figure 3

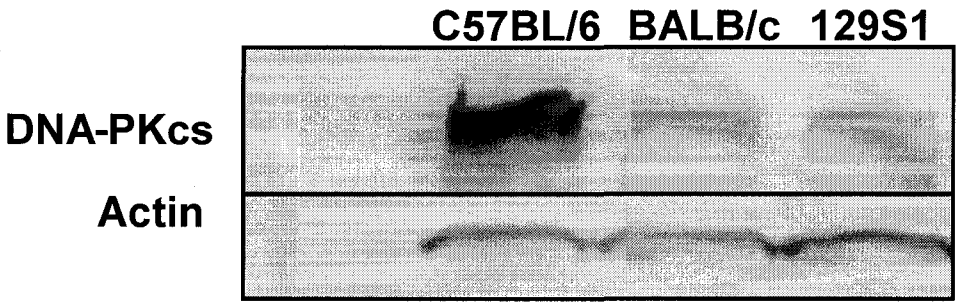

Figure 3: Protein quantification. Previous research has shown a deficiency in DNA-PKcs expression in the BALB/c strain. Immunoblotting here shows that the 129S1 strain also has a deficiency in protein expression. All samples were subjected to real-time PCR, and results illustrated that mRNA levels are the same throughout the different strains, suggesting a post-translational mechanism.

The experimental approach for generating the knock-in mice was to create one strain with the BALB-like kinase SNP while converting the SNP downstream of the leucine zipper back to the common allele. The other strain of knock-in mice will have the common allele in the kinase domain and the BALB/c-like SNP downstream of the leucine zipper. We have established that 129S1 has both SNPs; therefore, we needed genomic DNA wild-type at both loci. BAC DNA derived from the *Prkdc* gene of the 129S7 sub-strain was utilized for this purpose and was obtained from the Wellcome Sanger Institute. Genomic DNA from the BAC clones (BACi03 for the SNP downstream of the leucine zipper & BACc10 for the kinase SNP) was genotyped to confirm that it had the common allele at the

SNP loci (Fig.4). Results show that the BAC clones were similar to C57BL/6 and has the common allele at both positions.

Figure 4

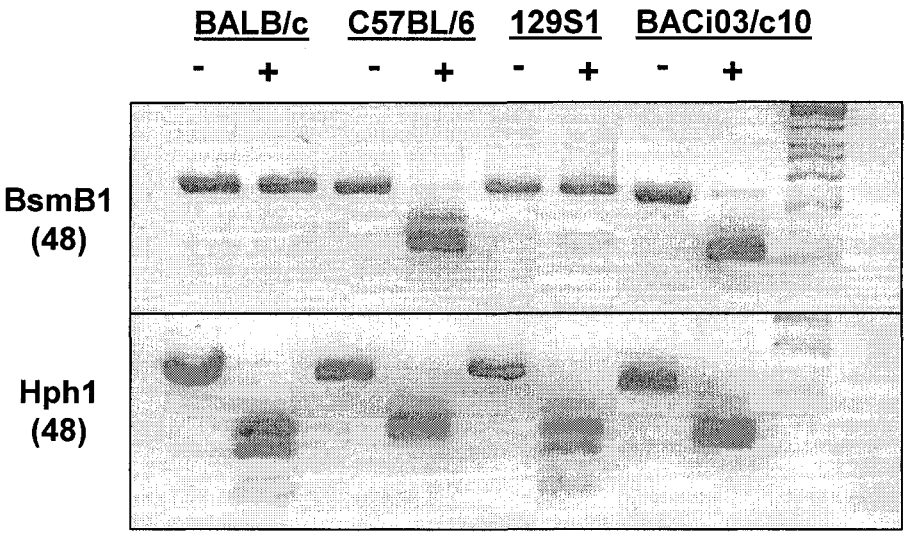

Figure 4: Genotyping BAC DNA. PCR products from the mouse strains and BAC DNA were genotyped. RFLP results show that the BAC DNA has the common nucleotides at the loci, similar to C57BL/6. The BAC was then chosen for the template in long-range PCR that created the "targeting portion" of the vectors.

The pACN targeting vector (Bunting; 1999) was selected for constructing the targeting vectors (Fig.5). The neomycin phosphotransferase (Neo) gene was previously inserted for a positive selection marker. During G418 (an analogue of neomycin) drug selection, the Neo gene expresses the phosphotransferase which then adds a phosphate group to the antibiotic, rendering it incapable of inhibiting protein synthesis in the cell. This means that transfected mouse ES cells containing the vector will survive in the presence of the drug G418. The Neo

gene is driven by a polII promoter which is designed to be constitutively active thus having a continuous expression of the Neo gene. The vector has an ampicillin-resistant gene that was used for plasmid selection during the molecular cloning process. A Cre recombinase/loxP system was also previously added to pACN. With this approach, the recombinase is expressed, which then cleaves and recombines at loxP sequence sites. In pACN, the Cre system is governed by the tissue-specific tACE (murine angiotensin-converting enzyme) promoter. Originally, the biological function of this promoter was used to initiate transcription only during spermatogenesis; here, this promoter is being exploited for a different purpose in the pACN cassette. It has been designed so that during spermatogenesis in chimeric mice, the tACE promoter will become active and express the Cre recombinase. The enzyme will then cleave and recombine sequences at the loxP sites flanking the "selection" portion of pACN which deletes the cassette located in between. What will be left is a small potion of loxP sequence in a targeted intron and the desired base pair change in the coding portion of *Prkdc*.

Figure 5

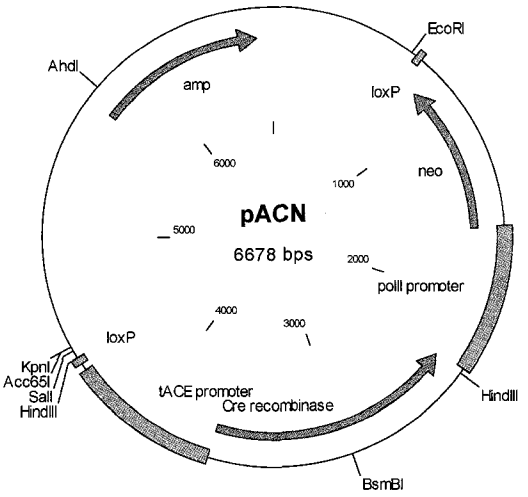

Figure 5: pACN. A schematic of the targeting vector utilized for the knock-in project. The vector contains a Neo gene for positive selection in ES cell transfection and an ampicillin gene for bacterial selection. The "selecting portion" of the vector (with the exception of the ampicillin gene) is located in between two loxP sites, which will be cleaved and recombined when the Cre-recombinase gene is expressed. The tACE promoter is tissue specific and is only active in the testis during spermatogenesis.

The first manipulation of pACN was to create a cloning site in place of the original EcoRI site near a loxP segment. Oligonucleotides were designed to knock-out the EcoRI site and replace it with NotI, PacI and SfiI sites (Fig.6).

Figure 6

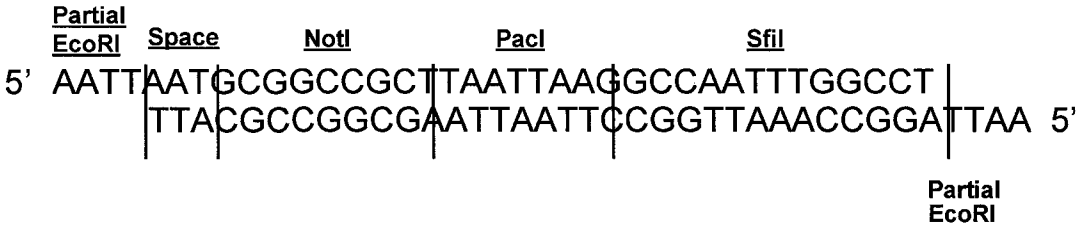

Figure 6: EcoRI knock-out oligonucleotides. Oligonucleotides were designed to insert at a digested EcoRI site because of the incomplete EcoRI sequence overhang. The rare-cutting enzymes NotI, PacI and SfiI replaced the original EcoRI site and were utilized for further cloning events.

The pACN vector was digested with EcoRI, and then purified. The linearized vector was de-phosphorylated with shrimp alkaline phosphatase (SAP) and again purified to rid any impurities from the reaction. The oligonucleotides were denatured by heat and allowed to anneal at room temperature and then phosphorylated by T4-polynucleotide kinase (T4-PNK). The insert was purified then added to the linearized, de-phosphorylated pACN at a 5:1 **(insert: vector)** ratio. The mixture was then ligated following standard protocol and transformed into bacteria. Bacterial colonies were selected, grown and plasmid extracted. Once plasmid was isolated and purified, then EcoRI and NotI digests were performed to determine if the cloning was successful. Results showed a colony resembling the predicted diagnostics. The original pACN will cleave once at the EcoRI site, but not the NotI site. The manipulated pACN, now named pACN.1 will digest with NotI, but not EcoRI because the EcoRI site was replaced with the new multiple cloning sites including NotI (Fig.7).

Figure 7

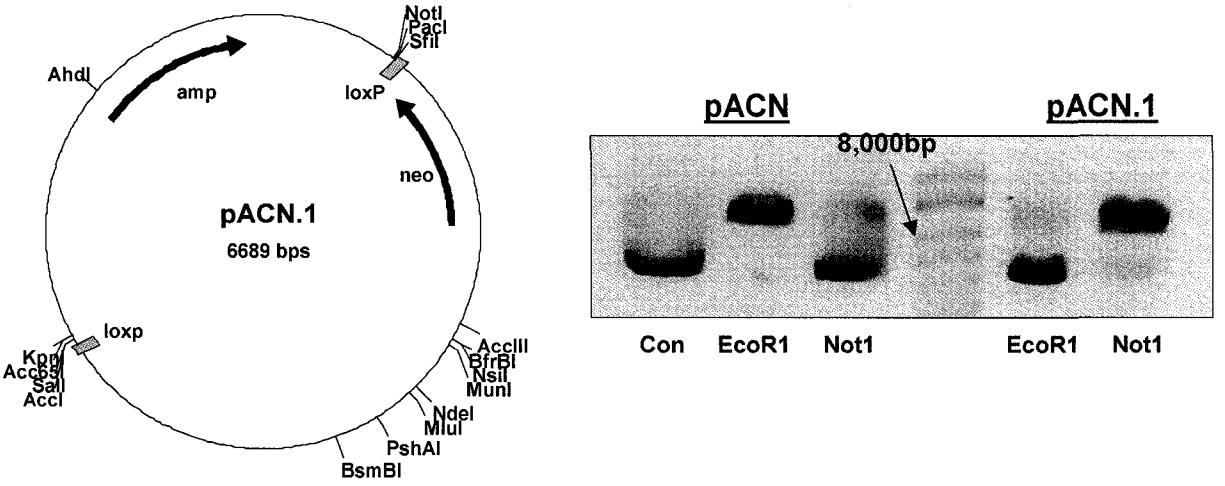

Figure 7: pACN.1. The addition of the oligonucleotides insert abolished an EcoRI site and replaced it with NotI, PacI and SfiI sites. Digests on the original pACN showed a digested fragment with the addition of EcoRI, but not NotI. The pACN.1 plasmid digested with NotI, but not with EcoRI implicating that the insert was successfully incorporated. Results were confirmed through sequencing.

The pACN vector is capable of positive selection via the Neo and ampicillin genes, but it has nothing for negative selection. We had chosen to use the herpes simplex thymidine kinase gene (Mt1-HSVtkpA or TK) for this task. In this system, randomly integrated vector into the mouse genome will express TK, which kills cells treated with ganciclovir or 2'-fluoro-2'-deoxy-1-β-D-arabinofuranosyl-5-iodo-uracil (FIAU). If the desired homologous recombination occurred during integration, then the TK gene is not incorporated into the genome, so these cells survive negative selection with FIAU.

We have acquired from Dr. Brian Parr (University of Colorado Cancer Center) the MCI-TK plasmid that contains a TK gene. The gene was extracted from the MCI plasmid using BamHI and HindIII and gel purified (Fig.8).

Figure 8

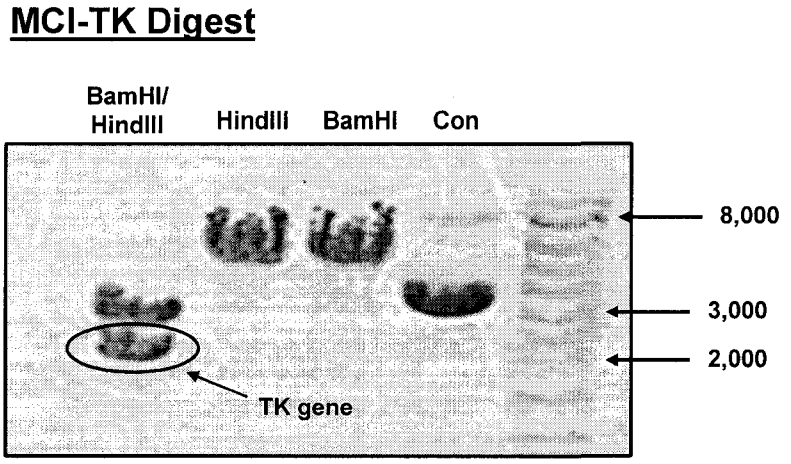

Figure 8: The TK gene. TK was extracted from the MCI plasmid using a HindIII/BamHI double digest. The TK gene itself is approximately 2,400bp. The TK gene was then separated on an agarose gel and purified for further cloning.

The pACN.1 plasmid was digested with Acc651 and column purified. Both the pACN.1 vector and the TK insert were blunt-ended using the standard Klenow fill-in reaction. The vector was de-phosphorylated using SAP and column purified. The insert was then added to the Acc651-digested pACN.1 at a 3:1 ratio and ligated using standard protocols. The ligation mix was transformed into bacteria and colonies selected for plasmid extraction. Plasmids were then digested with EcoRI and NotI to test for correct insertion and orientation. The pACN.1 vector no longer has an EcoRI site (as described previously) but, with

addition of the TK gene, the newly formed plasmid has a single EcoRI site. Double digestion with NotI and EcoRI yields a 3237bp product which shows correct insertion and also gives the orientation of the TK gene (Fig.9). Samples from the now named pACN.1TK were sequenced for confirmation of insertion and orientation.

Figure 9

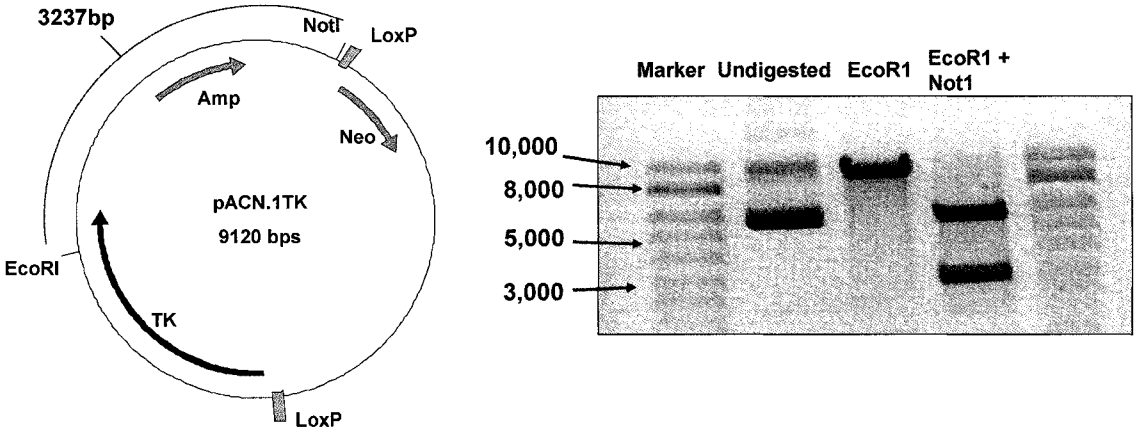

Figure 9: pACN.1TK. The TK gene was inserted into the pACN.1 vector and tested using an EcoRI/NotI double digest. Not only does this digest show insertion, but also orientation due to the location of the EcoRI site.

The final step in creating the vector is to insert the "targeting" segment, portions of DNA homologous to the *Prkdc* gene. We have performed long-range PCR using the BAC DNA (previously mentioned) as our template to create the right (RA) and left (LA) "arms" that are homologous to segments of Prkdc; with

one arm containing the desired point mutation. The primers designed for the PCR had restriction digest sequences (NotI or PacI for the right arm and SalI for the left arm) added for cloning purposes. From here, pACN.1TK will be used to generate two different vectors; pACN.1TK.48 for the SNP downstream of the leucine zipper in exon-48 & pACN.1TK.81 for the SNP in the kinase domain in exon-81.

The LA for the pACN.1TK.48 vector had SalI restriction sites added to the ends of the PCR product. The pACN.1TK vector was linearized with SalI, purified and de-phosphorylated with calf intestinal phosphatase (CIP) following standard protocols. The LA insert was digested with SalI, column purified and added to the digested plasmid at a 4:1 ratio. The ligation mix was purified and transformed into bacteria. Selected colonies were grown and plasmid extracted to determine if any contained the correct insert. SalI and HindIII were used to test DNA from the selected colonies, and we observed some colonies with potentially correct inserts. Further diagnostics revealed one colony (called pACN.1TK.48LA) having both correct insertion and orientation of the LA. Digestion with SalI will show that the LA was inserted. As mentioned earlier, the insert has SalI sites on both sides and was incorporated into the plasmid at a SalI site, thus creating two SalI sites flanking the 2600bp insert (Fig.10). Orientation is important because both the LA and RA must be cloned in the same direction so that it can successfully match the targeted region of *Prkdc*. BsmBI digestion was utilized to determine orientation of the LA insert. The desired orientation has the BsmBI site of the LA near the loxP site and yields a 1573bp product (Fig.10)

The RA for the pACN.1TK.48LA vector had PacI restriction sites added to the ends of the PCR product. PacI-linearized plasmid was purified and de-phosphorylated using CIP, then again purified. The RA was digested with PacI, purified and added to the linearized pACN.1TK48LA at a 3:1 ratio. The ligation products were purified and transformed into bacteria. Selected colonies were grown and plasmid extracted. Purified DNA from the colonies was then digested with PacI, EcoRI and PstI to detect insertions. The RA was inserted into a PacI site, creating two sites in the vector, and when digested, yielded a fragment the size of the insert that is 3757bp (Fig.10). EcoRI was also used to determine if the RA was correctly inserted. The RA has two EcoRI sites in addition to the EcoRI site in the TK gene. The insertion of the RA gives a 2362bp, 9067bp and 4011bp product; however, both EcoRI sites are similar distances from their ends of the RA and could not be used for determining correct orientation. The PstI enzyme was then selected for establishing the direction. Correct insertion yielded six fragments from the PstI digestion: 3277bp, 2298bp, 4453bp, 840bp, 237bp (too small to see on this particular gel) and 4335bp (Fig.10). The completed pACN.1TK.48 vector was tested with a number of digest enzymes including HindIII, SalI, PacI, PstI, EcoRI, BsmBI and NotI to ensure that all of the cloning steps to the original pACN plasmid yielded the proper insertions and orientations. Confirmation also was done by sequencing.

Figure 10

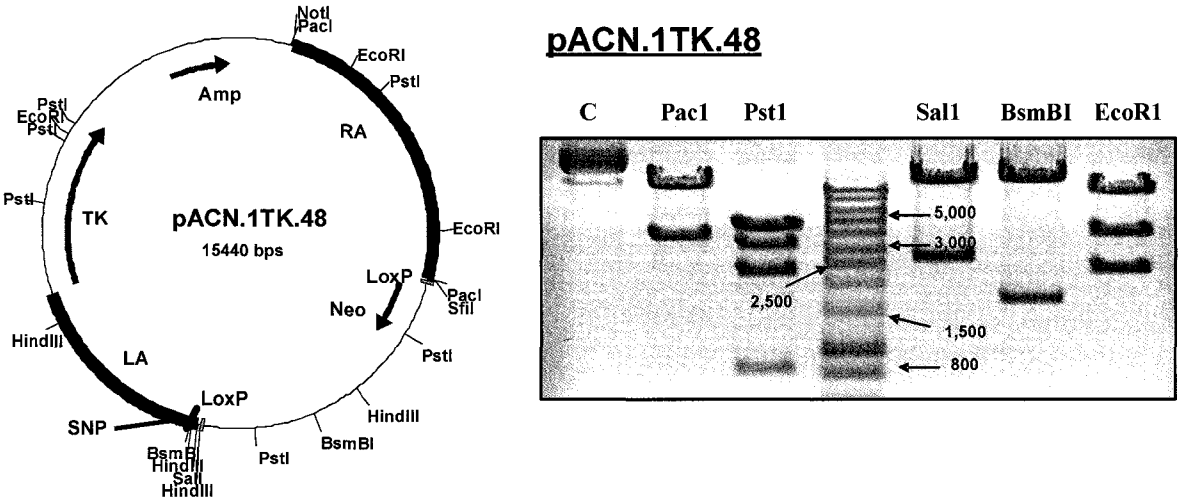

Figure 10: pACN.1TK.48. A schematic illustrating the design of the targeting vector for the SNP located downstream of the leucine zipper. RA and LA were design to be homologous to the region on *Prkdc* that contains the SNP in exon 48. Multiple digests were used to determine insertion and orientation. Confirmation was done by sequencing the cloning regions of the vector.

The second targeting vector was designed for the BALB/c-like SNP found in the kinase domain. PCR primers were designed so that NotI sites were added to the RA and SalI sites were added to the LA. The pACN.1TK vector was first linearized using NotI and de-phosphorylated using CIP. The purified product was ligated to the NotI digested RA at a 2:1 ratio. The ligated product was then purified and transformed into bacteria. Colonies were selected and grown, and plasmid extracted. Plasmid DNA from these colonies was digested using NotI to test for insertion. The RA insert will create an additional site to the plasmid now designated pACN.1TK.81RA adding a 3036bp fragment (Fig.11A). PacI was used to test insert orientation. The desired direction contains a PacI site near

another PacI site that flanks the region of insertion yielding a 237bp fragment (Fig.11A).

The LA was then inserted into the pACN.1TK.81RA vector. The plasmid was digested with SalI, de-phosphorylated using CIP, and then purified. The LA was also digested with SalI, then purified and ligated to the vector at a 3:1 ratio. Using a standard procedure, the ligation mix was column purified and used to transform bacteria. Colonies were selected, and grown, and plasmid extracted and purified. DNA was digested with SalI to determine if any selected colonies had the insert. Incorporation of the LA would create an additional SalI site that would generate a 3389bp fragment (Fig.11A). HindIII was used to determine orientation of the LA insert in the vector. Correct orientation yielded a 2073bp and 2441bp product when digested with HindIII (Fig.11A).

To complete the vector, we removed one of the NotI sites so that the remaining site could be used to linearize the plasmid for transfection. We took advantage of the two PacI sites previously used to determine the orientation of the RA. These sites were only 273bp apart, but one of the NotI sites was between them. After PacI digestion, the vector was re-ligated together without the small PacI-digested fragment, removing the extra NotI site (Fig.11B). The completed pACN.1TK.81 vector was sequenced to ensure that all cloning procedures were successful and that proper orientation was achieved for the vector arms.

Figure 11

A.

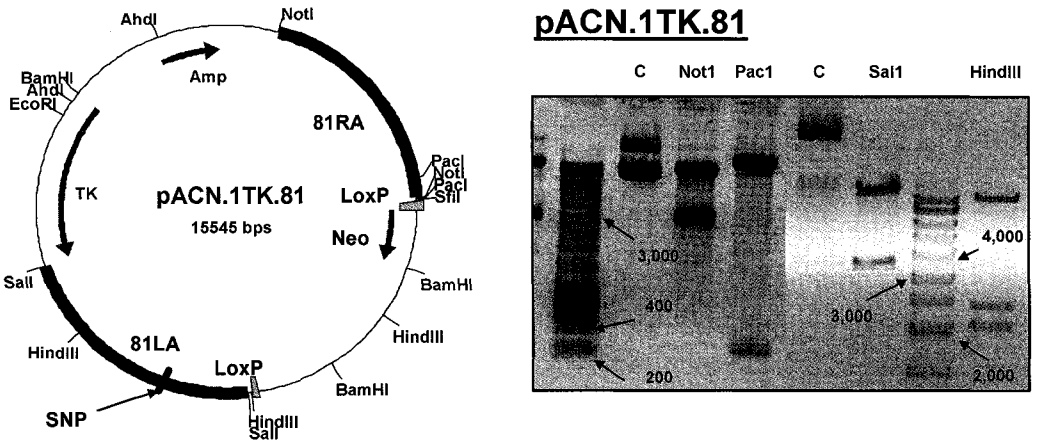

B.

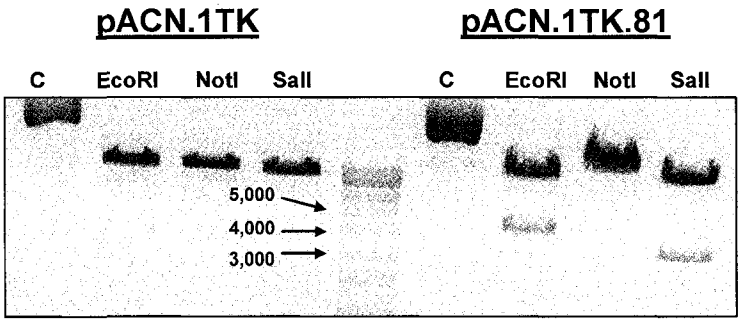

Figure 10: pACN.1TK.81. A schematic illustrating the design of the targeting vector designed for the SNP located in the kinase domain of DNA-PKcs. RA and LA were design to be homologous to the region on *Prkdc* that contains the SNP in exon 81. **A.** Multiple digests were used to determine insertion and orientation. Confirmation was done by sequencing the cloning regions of the vector. **B.** The vector was completed by removing the second NotI site so that it will be used to plasmid linearization. The pACN.1TK was used as a control.

Future Directions

Both the pACN.1TK.48 and pACN.1TK.81 targeting vectors were grown on a large scale (1ug/mL), purified and sent to the Transgenic Core Facilities at the University of Colorado Cancer Center (Denver, CO) for mouse ES cell transfection. Colonies were selected using the Neo/FIAU drug selection and grown in 24-well tissue culture plates. Genomic DNA was isolated from these colonies and column purified. Currently, there are stocks samples from a number of transfections stored and ready for screening.

There are two methods that will be utilized for ES screening: long-range PCR and southern blot analysis. Once positive ES colonies are selected and tested, cells will be injected into mouse blastocysts which will then be transferred into pseudo-pregnant mice. The chimeric progeny will be genotyped to identify pups that contain the desired mutation, expectedly in heterozygote form. Male progeny with the change will be backcrossed to female 129S1 mice. The progeny will be genotyped to test for the conversion then interbred to achieve homozygosity at the SNP loci.

These two different knock-in mice strains will have one of the BALB/c-like SNPs converted back to the common alleles. Once the mice are made, they will be characterized to determine if the base change is sufficient to rescue the BALB/c phenotype. Protein expression, DNA repair, telomere maintenance, kinase activity and the BSE will be assessed and compared to BALB/c and C57BL/6. Further studies will measure radiation-induced ductal dysplasias and

tumor development in these strains. These novel findings will give insight as to which SNP if any, or both, is responsible for the BALB/c radiosensitivity.

References

1. Adams, L.; Ethier, S. and Ullrich, R.L. Survival of mammary epithelial cells from virgin female BALB/c mice following in vivo irradiation, Radiation Research, 100, 264-272, 1984

2. Adams, L.; Ethier, S. and Ullrich, R.L. Enhanced in vitro proliferation and in vivo tumorigenic potential of mammary epithelium from BALB/c mice exposed in vivo to radiation, Cancer Research, 47, 4425-4431, August 15, 1987

3. Bailey, S.; Meyne, J.; Chen, D.; Kurimasa, A.; Li, G.; Lehnert, B. and Goodwin, E. DNA-double-stand break repair proteins are required to cap the ends of mammalian chromosomes, PNAS, 96, No. 26, 14899-14904, December 21, 1999

4. Bailey, S.; Brenneman, M.; Halbrook, J.; Nickoloff, J; Ullrich, R. and Goodwin, E. The kinase activity of DNA-PK is required to protect mammalian telomeres, DNA Repair, 3, 225-233, 2004

5. Bartsch, H.; Dally, H., Popanda, O., Risch, A. and Schmezer, P. Genetic profiles for cancer susceptibility and therapy response, Recent Results Caner Research, 174, 19-36, 2007

6. Bernard-Gallon, D; Bosviel R., Delort, L., Fontana, L. Chamoux, A., Rabiau, N., Satih, S. and Bignon, Y. DNA repair hene ERCC2 polymorphisms and associations with breast cancer and ovarian cancer risk, Mol Cancer, 2:36, 2008

7. Block, W.; Yu, Y.; Merkle, D.; Gifford, J.; Ding, Q.; Meek, K. and Lees-Miller, S. Autophosphorylation-dependent protein kinase catalytic subunit regulates ligation of DNA ends, Nucleic Acids Research, 32, No. 14, 4351-4357, 2004

8. Bunting, Michaeline; Bernstein, Kenneth E.; Greer, Joy M.; Capecchi, Mario R. and Thomas, Kirk R. Genes and Development, 13, 1524-1528, 1999

9. Chen, B.; Chan, D.; Kobayashi, J.; Burma, S. Yano, K.; Botvinick, E.; Qin, J. and Chen, D. Cell cycle dependence of DNA-PK phosphorylation in response to DNA double strand breaks, The American Society for Biochemistry and Molecular Biology, Jan. 26, 2005

10. Duell, E.; Millikan, R.; Pittman, G.; Winkel, S.; Lunn, R.; Tse, C.; Easton, A.; Mohrenweiser, H.; Newman, B. and Bell, D. Polymorphisms in the DNA repair gene XRCC1 And breast cancer, Cancer Epidemiology, Biomarkers and Prevention, 10, 217-222, March 2001

11. Faulkin, L.; Mitchell, D.; Cardiff, R.; Rosenblatt, L. and Goldman, M. Effects of X irradiation on the growth of normal and hyperplastic mouse mammary gland transplants, Radiation Research, 94, 390-403, 1983

12. Finnie, N.; Gottlieb, T., Blunt, T., Jeggo, P. and Jackson, S. DNA-PKcs activity is absent in xrs-cells: implications for site-specific recombination and DNA DSB repair, PNAS, 92, 320-324, 1995

13. Friedberg, E. and Meira, L. Database of mouse strains carrying targeted mutations in genes affecting biological responses to DNA damage, DNA Repair 3, 1617-1638, 2004

14. Fu, Y.; Yu, J.; Cheng, T.; Lou, A.; Hsu, G.; Wu, C.; Chen, S.; Wu, H.; Wu, P. and Shen, C. Breast cancer risk associated with genotypic polymorphism of the nonhomologous end joining genes: a multigenic study on cancer susceptibility, Cancer Research, 63, 2440-2446, May 15, 2003

15. Gilley, D.; Tanaka, H.; Hande, M.; Kurimasa, A.; Li, G.; Oshimura, M and Chen, D. DNA-PKcs is critical for telomere capping, PNAS, 98, No. 26, 15084-15088, December 18, 2001

16. Gofman, J. Confirmation that ionizing radiation can induce genomic instability, ONLINE, www.ratical.com/radiation/CNR/GenomicInst.html, 1998

17. Hsieh, S.; Lintell, N., Hunter, K. Germline polymorphisms are potential metastasis risk and prognosis markers in breast cancer, Breast Dis, 26,157-162, 2007

18. Jackson Laboratory; JAX notes, No. 481, February 2001

19. Kurimasa, A.; Kumano, S.; Boubnov, N.; Story, M.; Tung, C. Peterson, S. and Chen, D. Requirement for the kinase activity of human DNA-dependent protein kinase catalytic subunit in DNA strand break rejoining, Molecular and Cellular Biology, 3877-3884, May 1999

20. Kuschel, B.; Auranen, A.; McBride, S.; Novik, K.; Antoniou, A.; Lipscombe, J.; Day, N.; Easton, D.; Ponder, B.; Pharoah, P.and Dunning, A. Variants in DNA double-strand break repair genes and breast cancer susceptibility, Human Molecular Genetics, 11, No.12, 1399-1407, 2002

21. Okayasu, R.; Suetomi, K.; Yu, Y.; Silver, A.; Bedford, J, Cox, R. and Ullrich, R.L. A deficiency in DNA repair and DNA-PKcs expression in the radiosensitive BALB/c mouse, Cancer Research, 60, 4342-4345, August 15, 2000

22. Pepe, M & Janes, H. Gauging the performance of SNPs, biomarkers and clinical factors for predicting risk of breast cancer, 100, Issue 14, 978-979, 2008

23. Picciotto, M. and Wickman, K. Using knockout and transgenic mice to study neurophysiology and behavior, Physiologic Reviews, 78, No. 4, 1131-1143, October, 1998

24. Ponnaiya, B.; Cornforth, M.N. and Ullrich, R.L. Radiation-induced chromosomal instabililty is as clear as black and white, Radiation Research, 147, 121-125, 1997

25. Roderick, T.; Langley, S. and Leiter, E. Some unusual genetic characteristics of BALB/c and evidence for genetic variation among BALB/c substrains, Current Topics in Microbiology and Immunology, 122, 1985

26. Ma, Y.; Pannicke, U., Schwarz, K. and Lieber, M.. Hairpin opening and overhang processing by an Artemis/DNA-PKcs complex in NHEJ and V(D)J recombination, Cell, 108, 781-794, 2002

27. Ronckers, C.; Erdmann, C. and Land, C. Radiation and breast cancer: a review of current evidence, Breast Cancer Research, 7, 21-32, 2004

28. Schar, P. Spontaneous DNA damage, genome instability and cancer-when DNA replication escapes control, Cell, 104, 329-332, February 9, 2001

29. Smith, G.; and Jackson, S. The DNA-dependent protein kinase (Review), Genes and Development, 13, 916-934, 1999

30. Smith, T.; Levine, E.; Perrier, N.; Miller, M.; Freimanis, R.; Lohman, K.; Case, L.; Xu, J.; Mohrenweiser, H. and Hu, J. DNA-repair genetic polymorphisms and breast cancer risk, Cancer Epidemiology, Biomarkers and Prevention, 12, 1200-1204, November, 2003

31. Storer, J.; Mitchell, T. and Fry, R. Extrapolation of the relative risk of radiogenic neoplasms across mouse strains and to man, Radiation Research, 114, 331-353, 1988

32. Ullrich, R.L. Cellular and Molecular changes in mammary epithelium following irradiation, Radiation Research, 128, S136-S140, 1991

33. Ullrich, R.L.; Bowles, N.; Satterfield, L. and Davis, C. Strain-dependent susceptibility to radiation-induced mammary cancer is a result of differences in epithelial cells sensitivity to transformation, Radiation Research, 146, 353-355, 1996

34. Ullrich R.L. and Ponnaiya, B. Radiation-induced instability and its relation to radiation carcinogenesis, INT. J. RADIAT. BIOL, 74, No. 6, 747-754, 1998

35. Walinski, H. Studying gene function: creating knockout mice; constructing a knockout mouse, ONLINE, www.bioteach.ubc.ca/CellBiology/StudyingGeneFunction/, May 2, 2005

36. Wenham, R.; Schildkraut, J.; McLean, K.; Calingaert, B.; Bentley, R.; Marks, J. and Berchuck, A. Polymorphisms in BRCA1 and BRCA2 and risk of epithelial ovarian cancer, Clinical Cancer Research, 9, 4396-4403, 2003

37. Yu, Y.; Okayasu, R.; Weil, M.; Silver, A.; McCarthy, M. Zabriskie, R.; Long, S.; Cox, R. and Ullrich, R.L. Elevated breast cancer risk in irradiated BALB/c mice associates with unique functional polymorphisms of the Prkdc gene, Cancer Research, 61, 1820-1824, March 1, 2001

Chapter 6

Discussion

It is becoming clear that the progression from IR exposure to cancer is complex and involves a multitude of separate events. A number of pathways involved intertwine to create events necessary for cellular transformation. These events are difficult to identify and study because of the complexity and the long-latency period between IR exposure and tumorigenesis. Therefore, mouse models are used to better understand the underlying mechanisms involved in the carcinogenic process. It has been shown that the BALB/c mouse strain is sensitive to acute IR effects (Kallman, 1962; Storer, 1988) as well as susceptible to IR-induced mammary carcinogenesis (Ullrich, 1991). Subsequent studies demonstrated that this susceptibility is linked to IR-induced GI which was hypothesized to be an early event that aides in initiation (Ethier, 1982; Ethier, 1984; Selvanayagam, 1995; Ponnayia, 1999). This sensitivity was linked to a hypomorphic variant of DNA-PKcs which is a result of two SNPs located in *Prkdc*, the gene that encodes DNA-PKcs (Yu, 2001). The first SNP is located downstream of a leucine zipper domain in a highly conserved region, while the second SNP is located in the kinase domain. The BALB/c SNPs are believed to be responsible for its deficient protein levels, decreased kinase activity, decreased DSB repair capabilities, sensitivity to GI and deficient telomere end-capping (Okayasu, 2000; Bailey and Williams, manuscript in progress).

Research to date in BALB/c has focused on targeted effects of IR-induced damage. Recent studies demonstrating the BSE phenomenon led us to examine the impact of DNA-PKcs deficiencies on this non-targeted effect. Based on

observations in BALB/c with respect to alterations in DSB repair, we hypothesized dysfunctional DNA repair may also affect the BSE. To test this, we extended these investigations to examining potential connections between DNA damage repair and the BSE by using a novel cell transfer assay. This entailed using irradiated and non-irradiated donor cells added at low cell densities to recipient unirradiated cells, and then measuring bystander responses using SCE frequencies. Using this approach, we found that DNA-PKcs is required to generate a BSE signal, but not to receive such signals (Chapter 2). Similar results were also observed with ATM in that it is necessary to generate a bystander response, but not required for receiving signals. Our findings reveal a link between the BSE and DNA repair proteins and consequently open new lines for further investigation.

In the course of these studies, we noted differences in MEFs compared to mouse adult fibroblasts. These initial observations led to a series of studies investigating the BSE in adult mouse cells versus MEFs (Chapter 3). Results demonstrated that irradiated mouse adult donor cells were able to induce a bystander response when irradiated donor cells were added to normal human fibroblast recipient cells. However, the MEFs counterparts, regardless of their genetic background, were not capable of inducing a bystander response; i.e. no elevations in SCE levels were observed. These results suggest that there are differences in mouse adult fibroblasts compared to MEFs that have yet to be identified. Of possible interest in this regard is a recent study demonstrating that mouse embryonic stem cells express less DNA-PKcs than MEFs (Banuelos,

2008). It may be reasonable to hypothesize that there are lower levels of DNA-PKcs expression in MEF versus adult fibroblasts, which we have shown to be necessary for the generation of a bystander signal, providing a possible explanation for our observation of the lack of a BSE in MEFs. MEFs are obviously not the same as ES cells, but MEFs do exhibit some chromatin epigenetic marks similar to ES cells, suggesting incomplete commitment to differentiated lineage (personal correspondence, Schemanti J). Our results highlight the need to better characterize MEFs and so warrant further study to define mechanisms. Extending the BSE to additional end-points, like mutagenesis and micronuclei would confirm our initial findings and extend these to end-points directly associated with radiation injury. It is also important to establish DNA-PKcs protein levels in MEFs versus mouse adult fibroblasts to determine if decreased levels of DNA-PKcs are responsible for the lack of a BSE. Another important approach would be microarray analysis for a genome-wide examination of MEFs versus mouse adult fibroblasts. Results of such studies would be extremely informative and provide possible insight into mechanistic explanations for our findings.

With the background of previous studies and observations made in the present findings, we sought to examine the functional significance of the *Prkdc*$^{BALB/c}$ SNPs. The first SNP is in a highly conserved region, suggesting it is at an essential locus. In addition, the SNP is surrounded by autophosphorylation clusters that have been established to be critical for DNA-PKcs function. It is therefore reasonable to speculate that this SNP may affect autophosphorylation

which may disrupt protein activity. The second SNP in the kinase domain may be responsible for deficient kinase activity, hindering protein function. However, it is found in a less conserved region in the gene and so its significance could be questioned. On the other hand, support for kinase activity being involved in key functions of DNA-PKcs comes from studies with Bailey et al. using a specific kinase inhibitor. Such functional changes are not necessarily required to affect the phenotypic changes observed however. Because of the decreased levels of DNA-PKcs in BALB/c, it is possible that these SNPs simply affect protein stability. It is also possible that both SNPs cooperate in producing the BALB/c phenotype.

There are two approaches to study the functional significance of each BALB/c SNP: 1.) The use of inbred mouse strains that have the SNPs naturally; 2.) And/or the use of knock-in mice. The first approach is at least partially feasible using the LEWES mouse strain. This strain was recently derived from wild mice and contains the BALB/c SNP in the kinase domain but has the common allele downstream of the leucine zipper. Because LEWES has only the SNP located in the kinase domain, it provides an opportunity to determine the impact of this polymorphism on DNA-PKcs function. Once we confirmed that LEWES contained only the one polymorphism (the BALB/c-like SNP in the kinase domain) and no additional SNPs in the coding region of *Prkdc*, we began characterizing the strain. DNA-PKcs protein expression was first examined and results revealed that Lewes had intermediate levels compared to C57BL/6 and BALB/c. In fact, the DNA-PKcs protein levels were closer to BALB/c than

C57BL/6. This implies that the SNP in the kinase domain is partially, and perhaps predominately, responsible for the decreased levels of DNA-PKcs observed in BALB/c. The SNP may affect DNA-PKcs conformation, making the protein unstable and hence rapidly degraded.

Using the γ-H2AX foci assay, we measured DBS repair in LEWES compared to C57BL/6, BALB/c and SCID (null for DNA-PKcs). Our results again showed that LEWES was intermediate in repair kinetics between C57BL/6 (full repair) and BALB/c (incomplete repair). This data implies that the kinase domain SNP may be at least partly involved with DSB repair.

We have previously shown that DNA-PKcs is needed for the generation of a bystander signal as measured by SCE frequencies (Hagelstrom et al., Oncogene 2008, in press). Based on this and our results described above, we hypothesized that LEWES would have a deficiency in the BSE. Unexpectedly, we found LEWES was fully capable of generating a bystander response, similar to C57BL/6. Our results suggest that the intercellular signaling role of DNA-PKcs is not dependent on the SNP found in the kinase domain, DNA-PKcs protein levels or DSB repair (Chapter 4).

As described previously by Yu et al., it has been shown that the BALB/c variation of DNA-PKcs is genetically associated with increased IR-induced GI and potentially mammary cancer. Our work has provided evidence of a novel role for DNA-PKcs as a component in the BSE, which has also been linked to GI (Reviewed in Goldberg, 2002; Prise, 2003). The possible link between the BSE

and IR-induced GI raises interesting questions with respect to the role played by the BSE in BALB/c sensitivity to IR-induced cancer.

To date, there are many contradictory reports regarding whether or not the BSE is harmful or beneficial, but most of these studies have been done *in vitro* (Prise, 2003; Morgan, 2003). If the BSE exists *in vivo*, then it is reasonable to assume that the BSE may provide a protective mechanism developed to respond to infection and inflammation. Coincidentally, the effects of IR can also induce the same bystander response. A key protective mechanism may be related to BSE-induced apoptosis (Prise, 1998; Morgan, 2003). Therefore it has been speculated that, in an *in vivo* system, the BSE is beneficial and protective against the propagation of IR-induced damage by the removal of these cells. Conversely, the lack of the BSE and the inability to remove IR-induced damaged cells and surrounding cells via apoptosis may contribute to the propagation of GI.

Our studies have allowed us to hypothesize that BALB/c susceptibility to IR-induced GI is not linked to defects in DNA repair but rather defects in telomere maintenance and the lack of a BSE. Recently, it has been shown that, in fact, BALB/c is susceptible to IR-induced telomere-DSB fusions (Williams et al., manuscript in progress). This study demonstrated a delayed increase in telomere-DSB fusions in the progeny of unirradiated cells, suggesting a link between GI and telomere dysfunction. It was postulated that these telomere-DSB fusions may be a sensitive marker for ongoing GI or it may, in fact, be the underling mechanism for IR-induced GI. During replication an interstitial telomere signal derived from a telomere-DSB fusion may stall replication and cause further

breaks and gaps in the chromosome, potentially inducing GI observed in BALB/c. Other studies have shown that BALB/c is less prone to IR-induced apoptosis (Mori, 1998). Reduced levels of apoptosis observed in BALB/c may allow for the survival/propagation of IR-induced damaged cells and consequently GI.

With this reasoning, we hypothesize that the lack of a BSE in BALB/c may be contributing to its IR-induced GI (Summarized in Fig.1). To test this, the LEWES model may be useful. Studies characterizing IR-induced apoptosis and delayed cytogenetic instability would be an important first step in testing this hypothesis. Additional studies examining sensitivity to telomere-DSB fusions in the progeny of irradiated cells would also be important. As we have shown, LEWES is capable of generating a BSE response but has decreased levels of DNA-PKcs and DSB repair. If LEWES has similar levels of apoptosis to C57BL/6 and lacks elevated levels of IR-induced delayed GI or telomere fusions as seen in BALB/c, then we can speculate that decreased DNA-PKcs levels and deficient repair are not responsible for the BALB/c phenotype. Our studies reveal that LEWES displays a BSE while BALB/c does not, suggesting an association between the BSE and IR-induced GI. These investigations will provide a better understanding into the relevance of the BSE *in vivo* and its potential role as a protective mechanism against IR exposure.

Such studies provide a basis to expand several lines of research that can test this hypothesis by examining other mouse strains that are deficient in bystander signaling, apoptosis and DNA-repair. In this regard, two congenic mouse strain recently developed could be an important approach. The first

congenic strain has the BALB/c background and the C57BL/6 *Prkdc* (common) allele (named C.B6). The second congenic strain has the C57BL/6 background and the BALB/c *Prkdc* (variant) allele (named B6.C). We have observed that B6.C has decreased DNA-PKcs protein levels, deficient DSB repair (data not shown) and lacks a BSE (Chapter 2). Examining the delayed telomere-DSB fusions, apoptosis and delayed GI in these congenic mice strains would allow our hypothesis to be tested directly. Another approach would be the use of specific inhibitors of apoptosis or the use of apoptosis-resistant or BSE-resistant knock-out mice. Potential findings from such studies may lead to the identification of subpopulations of humans that are sensitive to IR-induced cancer.

Figure 1

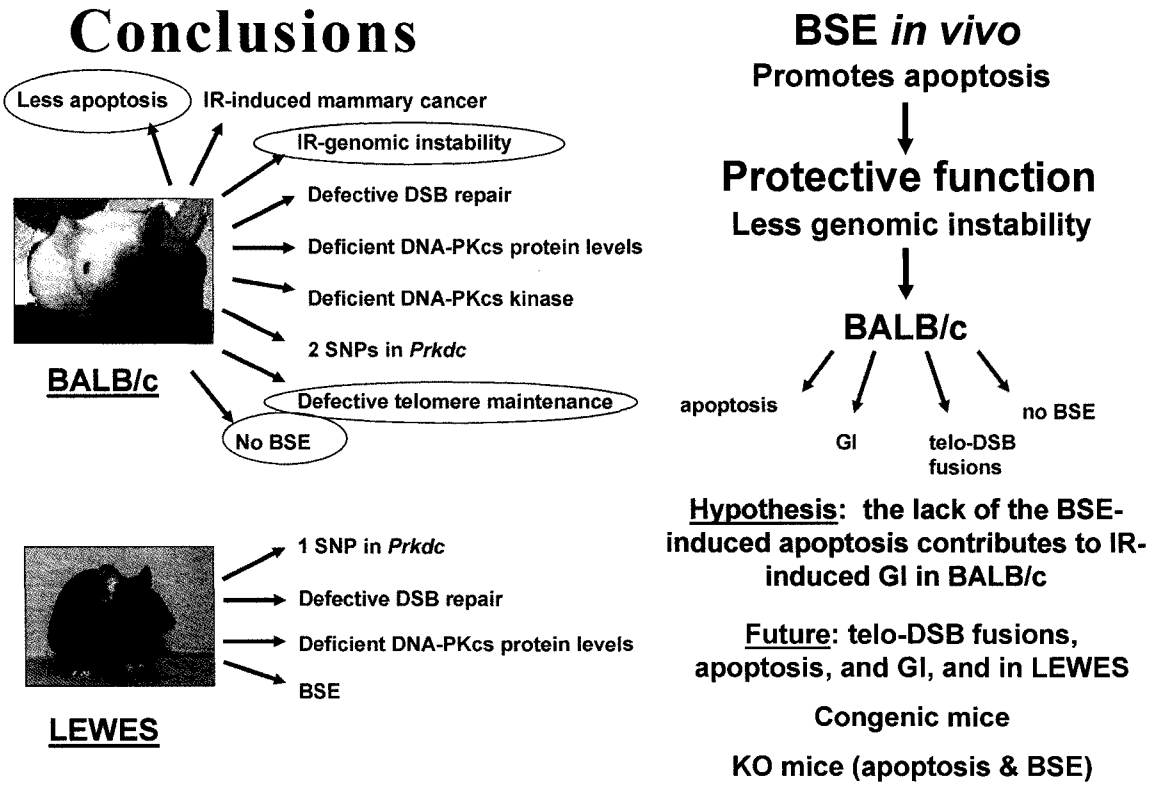
Conclusions
Less apoptosis
IR-induced mammary cancer
IR-genomic instability
Defective DSB repair
Deficient DNA-PKcs protein levels
Deficient DNA-PKcs kinase
2 SNPs in Prkdc
Defective telomere maintenance
No BSE
BALB/c
1 SNP in Prkdc
Defective DSB repair
Deficient DNA-PKcs protein levels
BSE
LEWES
BSE in vivo
Promotes apoptosis
Protective function
Less genomic instability
BALB/c
apoptosis
GI
telo-DSB fusions
no BSE
Hypothesis: the lack of the BSE-induced apoptosis contributes to IR-induced GI in BALB/c
Future: telo-DSB fusions, apoptosis, and GI, and in LEWES
Congenic mice
KO mice (apoptosis & BSE)

References

1. Bailey SM, Goodwin; DNA and telomeres: beginnings and endings. Cytogenet Genome Res. 2004;104(1-4):109-15.
2. Bailey SM, Cornforth MN, Kurimasa A, Chen DJ and Goodwin EH . Strand-specific fluorescence in situ hybridization: the CO-FISH family (2004) Cytogenet Genome Res 2004;107:14-17
3. Bailey SM, Brenneman MA, Halbrook J, Nickoloff JA, Ullrich RL and Goodwin EH. (2004). *DNA Repair (Amst)*, 3, 225-33.
4. Bailey SM, Cornforth MN, Kurimasa A, Chen DJ and Goodwin EH. (2001). *Science*, 293, 2462-5.
5. Bailey SM, Meyne J, Chen DJ, Kurimasa A, Li GC, Lehnert BE and Goodwin EH. (1999). *Proc Natl Acad Sci U S A*, 96, 14899-904
6. Banuelos, C. A., Banath, J. P., Macphail, S. H., Zhao, J., Eaves, C. A., O'Connor, M. D., Lansdorp, P. M. & Olive, P. L. (2008) Mouse but not human embryonic stem cells are deficient in rejoining of ionizing radiation-induced DNA double-strand breaks. *DNA Repair (Amst)*.
7. Ethier SP, Ullrich RL. Detection of ductal dysplasia in mammary outgrowths derived from carcinogen-treated virgin female BALB/c mice. Cancer Res. 1982 May;42(5):1753-60.
8. Ethier SP, Adams LM, Ullrich RL. Morphological and histological characteristics of mammary dysplasias occurring in cell dissociation-derived murine mammary outgrowths. Cancer Res. 1984 Oct;44(10):4517-22.
9. Goldberg, Z and Lehnert B; Radiation-induced effects in unirradiated cells: a review and implications in cancer, International Journal of Oncology, 21, 2002, 337-349
10. Kato TA; Nagasawa H., Weil MM, Little JB, Bedford JS; Levels of gamma-H2AX Foci after low-dose-rate irradiation reveal a DNA DSB rejoining defect in cells from human ATM heterozygotes, Radiat Res. 2006 Sep;166(3):443-53
11. Kallman, RF; The effect of dose rate on mode of acute radiation death of C57BL/6 and BALB/c mice. Radiat Res., 16, 1962, 796-810
12. Mori N, van Wezel T, van der Valk M, Yamate J, Sakuma S, Okumoto M, Demant P. Genetics of susceptibility to radiation-induced apoptosis in colon: two loci on chromosomes 9 and 16. Mamm Genome. 1998 May;9(5):377-80
13. Morgan WF. Is there a common mechanism underlying genomic instability, bystander effects and other nontargeted effects of exposure to ionizing radiation? Oncogene. 2003 Oct 13;22(45):7094-9. Review.
14. Okayasu, R.; Suetomi, K.; Yu, Y.; Silver, A.; Bedford, J, Cox, R. and Ullrich, R.L. A deficiency in DNA repair and DNA-PKcs expression in the radiosensitive BALB/c mouse, Cancer Research, 60, 4342-4345, August 15, 2000
15. Ponnaiya, B.; Cornforth, M.N. and Ullrich, R.L. Radiation-induced chromosomal instabililty is as clear as black and white, Radiation Research, 147, 121-125, 1997

16. Prise KM, Belyakov OV, Folkard M, Michael BD. Studies of bystander effects in human fibroblasts using a charged particle microbeam. Int J Radiat Biol. 1998 Dec;74(6):793-8.
17. Prise KM, Folkard M, Michael BD; A review of the bystander effect and ots implications for low-dose exposure, Radiation Protection Dosimerty, 104, NO 4, 2003, 347-355.
18. Selvanayagam CS, Davis CM, Cornforth MN, Ullrich RLCancer Res. Latent expression of p53 mutations and radiation-induced mammary cancer.1995 Aug 1;55(15):3310-7.
19. Storer JB, Mitchell TJ, Fry RJ. Extrapolation of the relative risk of radiogenic neoplasms across mouse strains and to man. Radiat Res. 1988 May;114(2):331-53. Erratum in: Radiat Res 1989 Feb;117(2):362.
20. Ullrich, R.L. Cellular and Molecular changes in mammary epithelium following irradiation, Radiation Research, 128, S136-S140, 1991
21. Ullrich R.L. and Ponnaiya, B. Radiation-induced instability and its relation to radiation carcinogenesis, INT. J. RADIAT. BIOL, 74, No. 6, 747-754, 1998
22. Yu, Y.; Okayasu, R.; Weil, M.; Silver, A.; McCarthy, M. Zabriskie, R.; Long, S.; Cox, R. and Ullrich, R.L. Elevated breast cancer risk in irradiated BALB/c mice associates with unique functional polymorphisms of the Prkdc gene, Cancer Research, 61, 1820-1824, March 1, 2001

Appendix

List of Abbreviations

5C HDF	5C human dermal fibroblasts
ACS	American Cancer Society
Arg	arginine
Art	Artemis
ATM	ataxia telangectasia mutant
B6.C	C57BL/6 background with BALB/c DNA-PKcs allele
BAC	bacterial artificial chromosome
BLM	Bloom's protein
BRCA1/2	breast cancer associated 1/2
BrdU	bromodeoxyuridine
BSE	bystander effect
C.B6	BALB/c background with C57BL/6 DNA-PKcs allele
cDNA	coding DNA
ChIP	chromatin immuno-precipitation
CHO	Chinese hamster ovary
CIP	calf intestinal phosphatase
Cs	cesium
Cys	cysteine
D-loop	displacement-loop
DAPI	4',6-diamidino-2-phenylindole
DNA	deoxyribonucleic acid
DNA-PK	DNA-dependent protein kinase
DNA-PKcs	DNA-dependent protein kinase catalytic subunit
DSB	double strand breaks
ECL	enhanced or enzymatic chemiluminescence
EDTA	ethylenediaminetetraacetic acid
EGTA	ethylene glycol tetraacetic acid
ERCC2	excision repair cross-complementing group 2
ERK	extracellular signal-regulated kinases
ES	embryonic stem
FBS	fetal bovine serum
FIAU	1-(2-deoxy-2-fluoro-1-D-arabinofuranosyl)-5-iodouracil
FPG	fluorescence plus giemsa
GI	genomic instability
Gy	gray
H2AX	histone H2A
HR	homologous recombination
HRP	horseradish peroxidase
IKK	IκB kinase

IR	ionizing radiation
JNK	c-Jun N-terminal kinases
KCl	potassium chloride
Ku70/80	X-ray repair complementing 6/5 (XRCC6 and XRCC5)
LA	left arm
LB	Luria-Bertani broth
LET	linear energy transfer
LOH	loss of heterozygosity
MEF	mouse embryonic fibroblasts
MEK	MAP kinase or ERK kinase
Met	methionine
MEM	minimum essential medium
mRNA	messenger RNA
MRN	Mre11-Rad50-Nbs1
NaCl	sodium chloride
NaF	sodium fluoride
NCI	National Cancer Institute
Neo	neomycin
NER	nucleotide excision repair
NF-kB	nuclear factor-kappa B
NOS	nitric oxide species
PBS	phosphate buffered saline
PCR	polymerase chain reaction
PI3 kinase	phosphoinositide 3-kinases
PIKK	phosphatidylinositol 3-kinase-related kinase
PNK	polynucleotide kinase
NHEJ	non-homologous end-joining
RA	right arm
RAG1/2	recombination activating gene 1/2
RFLP	restriction fragment length polymorphism
RNA	ribonucleic acid
ROS	reactive oxygen species
RPA	replication protein A
SAP	shrimp alkaline phosphatase
SAPK	stress activated protein kinase
SCE	sister chromatid exchange
SCID	severe compromised immuno-deficiency
SDS-PAGE	sodium dodecyl sulfate polyacrylamide gel electrophoresis
SEM	standard error of the mean
SNP	single nucleotide polymorphism
SSB	single strand break
tACE	murine angiotensin-converting enzyme
Taq	*Thermus aquaticus*
TK	thymadine kinase

V(D)J recombination	variable diverse joining recombination
Val	valine
WRN	Werner's protein
XRCC2	X-ray repair complementing defective repair in CHO 2
XRCC3	X-ray repair complementing defective repair in CHO 3
XRCC4	X-ray repair complementing defective repair in CHO 4
XRCC5	X-ray repair complementing defective repair in CHO 5 /Ku80
XRCC6	X-ray repair complementing defective repair in CHO 6/Ku70